

NASA CR-54673



GPO PRICE \$ _____

CFSTI PRICE(S) \$ _____

Hard copy (HC) 5.00Microfiche (MF) 1.00

FACILITY FORM 602

N66 24381

(ACCESS NUMBER)

(PAGES)

CR-54673

(NASA CR OR TMX OR AD NUMBER)

(THRU)

(CODE)

(CATEGORY)

ff 653 July 65

DEVELOPMENT OF LINEAR-STRIP ION THRUSTORS FOR ATTITUDE CONTROL

Prepared by

J. Robert Anderson • Robert Kuberek • Stephen A. Thompson

Prepared for

NATIONAL AERONAUTICS and SPACE ADMINISTRATION

CONTRACT NO. NAS 3-4117

HUGHES

HUGHES AIRCRAFT COMPANY

RESEARCH LABORATORIES3011 MALIBU CANYON ROAD
MALIBU, CALIFORNIA

NASA CR 54673

SUMMARY REPORT

DEVELOPMENT OF LINEAR-STRIP ION THRUSTORS
FOR ATTITUDE CONTROL

prepared for

NATIONAL AERONAUTICS & SPACE ADMINISTRATION

prepared by

J. Robert Anderson, Robert Kuberek, and Stephen A. Thompson

of the

Ion Propulsion Department

G. R. Brewer, Manager
G. A. Work, Ass't. Manager

13 January 1966

CONTRACT NAS 3-4117

Project Manager
NASA-Lewis Research Center
Spacecraft Technology Division
D. M. Shellhammer

HUGHES RESEARCH LABORATORIES
Malibu, California

TABLE OF CONTENTS

	LIST OF ILLUSTRATIONS	v
	ABSTRACT	xi
I.	INTRODUCTION AND SUMMARY	1
II.	DESIGN CONSIDERATIONS	9
	A. Ion Thrustor	9
	B. Cesium Feed Systems	13
III.	LOW-MASS IONIZER AND HEATER DEVELOPMENT . .	23
	A. Low-Mass Ionizers	23
	B. Ionizer Heaters	28
IV.	THRUSTOR DESIGN VERIFICATION	43
	A. Thermal Tests	43
	B. Electrical Tests	48
V.	LONG-DURATION CYCLIC THERMAL TESTS	61
VI.	STEADY-STATE LIFE TESTS	67
	A. Introduction	67
	B. Test Results	67
	C. Residual Gas Environment	88
	D. Post-Test Analysis	92
	E. Summary	118
VII.	AUTOMATIC LIFE TEST CONSOLE	121
	A. The Primary Power Supply Unit	121
	B. Power Conditioning and Control Unit	121

VIII.	RELIABILITY AND QUALITY ASSURANCE	129
IX.	RECOMMENDATIONS AND CONCLUSIONS	135
X.	CONTRIBUTORS	139
	REFERENCES	141
	LIST OF ABBREVIATIONS	143
	DISTRIBUTION LIST	145

LIST OF ILLUSTRATIONS

Fig. I-1.	Photograph of the Hughes Linear Ion Thrustor . . .	3
Fig. I-2.	Cross-sectional drawings of two low-mass ionizer design	6
Fig. II-1.	Isometric and cross-sectional drawings of the Hughes Linear Ion Thrustor	10
Fig. II-2.	Photograph of complete low-mass ionizer assembly ready for mounting to focus electrode . . .	11
Fig. II-3.	Three gram capacity flight-type cesium feed system originally developed for the SERT-I Program	15
Fig. II-4.	Cross section of 250 g laboratory feed system . . .	16
Fig. II-5.	Photograph of 250 g laboratory feed system less heat shields	17
Fig. II-6.	Piercing mechanisms for cesium feed system. . . .	19
Fig. III-1.	Cross-sectional drawings of two low-mass ionizer design	24
Fig. III-2.	Photograph of low mass ionizer (LMI-F) cross section	25
Fig. III-3.	Cross section (50x) of tungsten rod sintered to porous tungsten with Sylvania M-55 tungsten powder	27
Fig. III-4.	Photomicrograph (1600x) showing the structure of the porous ionizer and filler material	29
Fig. III-5.	Low-mass ionizer (LMI-E), showing heater tubes, manifold plates, support straps and feed tube all electron beam welded to the porous emitter	30
Fig. III-6.	Parts comprising the basic elements of a low-mass ionizer	31
Fig. III-7.	Low-mass ionizer parts in an intermediate state of assembly	32
Fig. III-8.	Photograph of two low-mass ionizer heaters	35

Fig. III-9.	Heater resistance versus input power for doped and undoped alumina-coated tungsten filament	37
Fig. III-10.	Photomicrograph (100x) showing the structure of the filler material in a sintered heater lead connection	39
Fig. IV-1.	Steady-state thermal characteristics of the LB thruster	45
Fig. IV-2.	Equilibrium temperatures measured during repeated thermal cycling of the LB thruster	46
Fig. IV-3.	Heatup characteristics of the LB thruster with an 8 cm long Model F low-mass ionizer	47
Fig. IV-4.	Heatup characteristics for the LB thruster with an 8 cm long Model E low-mass ionizer	49
Fig. IV-5.	Heatup characteristics for the LC thruster with a 5 cm long Model E low-mass ionizer	50
Fig. IV-6.	Time profile of beam and accel currents during 16 hour period of design verification	52
Fig. IV-7.	Current-voltage characteristics measured on thruster LB-1	53
Fig. IV-8.	Ion emission and accel current characteristics as a function of ionizer temperature for thruster LB-1	54
Fig. IV-9.	Ionizer current density versus temperature for thruster LC-1	56
Fig. IV-10.	Current-voltage characteristics for thruster LC-1	58
Fig. IV-11.	Power-to-thrust characteristics of thruster LC-1	59
Fig. V-1.	Model LB thrusters mounted in evacuated sealed bottles for long-duration cyclic thermal life tests	62
Fig. V-2.	Block diagram of cycling test circuit	63

Fig. V-3.	Voltage and current waveforms for cyclic tests . . .	64
Fig. VI-1.	Performance history chart for steady-state life test of thruster LB-4	69
Fig. VI-2.	15x photograph of surface of accel electrode after 226 hour life test in LB-4	70
Fig. VI-3.	50 x photograph of copper section of accel electrode after 226 hour life test at 7 mA/cm^2 in thruster LB-4	71
Fig. VI-4.	Performance history chart for 2000 hour life test of thruster LB-7	75
Fig. VI-5.	Ionizer current density versus temperature during 2000 hour test of thruster LB-7	76
Fig. VI-6.	Perveance characteristics of thruster LB-7	77
Fig. VI-7.	Power-to-thrust ratio versus specific impulse for thruster LB-7 as compared to empirical calculation	79
Fig. VI-8.	Electron back emission from accel electrode to the positive electrodes during test of LB-7	80
Fig. VI-9.	Time profile of major engine parameters during 610 hour life test of thruster LD-2	82
Fig. VI-10.	Perveance data measured on thruster LD-2 during 610 hour life test	84
Fig. VI-11.	Ionizer current density versus temperature characteristics measured on ion thruster LD-2 during 610 hour life test	85
Fig. VI-12.	Dependence of accel current on accel temperature during life test of thruster LD-2	86
Fig. VI-13.	Accel temperature as a function of ionizer temperature during life test of thruster LD-2	87
Fig. VI-14.	Power-thrust characteristics of thruster LD-2	89
Fig. VI-15.	Neutralizer current-voltage characteristics for thruster LD-2	90

Fig. VI-16.	Closeup photograph of portion of accel electrode aperture after 1000 hours of cesium life test	95
Fig. VI-17.	Ion thruster LB-7 upon removal from vacuum chamber following successful completion of 2000 hour steady-state life test.	96
Fig. VI-18.	Major subassemblies of thruster LB-7 after 2000 hour life test	97
Fig. VI-19.	Closeup photograph of pitted areas on downstream side of accel electrode after 2000 hour steady-state life test	98
Fig. VI-20.	Photomicrographs of (a) the neutralizer filament (0.002 in diameter) and (b) the dummy filament after 2000 hours in the cesium environment of thruster LB-7	100
Fig. VI-21.	Photograph of portion of ionizer surface from engine LB-7	101
Fig. VI-22.	Positive and negative charged particle trajectories in the Model 70 accelerator system for $3/4$ of full space charge	103
Fig. VI-23.	Photomicrograph of LB-7 ionizer section showing shallow erosion groove along ion emitting surface	105
Fig. VI-24.	Interior of vacuum test chamber after 1000 hour period of LB-7 life test.	107
Fig. VI-25.	(a) Photograph of downstream side of the accel electrode from thruster LD-2 (b) Photograph of upstream side of the accel electrode from thruster LD-2	109
Fig. VI-26.	(a) Photograph of cross section adjacent to the accel aperture of thruster LD-2 (b) Photograph of cross section in most eroded region of accel of thruster LD-2	110
Fig. VI-27.	Bubble test pattern from the ionizer of thruster LD-2 after life test	111

Fig. VI-28.	Solenoid valve plunger after 984 cycles and 1000 hours in cesium at 280°C	115
Fig. VI-29.	Metallurgical sections of valve spool after 1000 hours in cesium	116
Fig. VI-30.	Photomicrograph of light erosion in valve spool after 1000 hours in cesium	117
Fig. VII-1.	Photograph of the Automatic Life Test Console	122
Fig. VII-2.	Photograph of the control unit portion of the Automatic Life Test Console	125

ABSTRACT

Single-strip cesium-contact ion thrusters covering the thrust range from 0.1 to 1.0 millipound have been developed. Extensive life testing with a number of thrusters has demonstrated that this thruster design potentially has the long life required for satellite control missions for both station keeping and attitude control functions. All life tests have simulated real system operational conditions in the sense that power conditioning consisted of units designed and qualified for the SERT-I flight test and in the sense that control and logic circuits were included to permit fully automatic, unattended testing.

Lifetime of the ion thruster was demonstrated by several steady-state life tests which accumulated over 3000 hours of total thrust time including a successful 2000 hour test at an average thrust level of 0.56 millipound. Diagnosis of observed accelerator electrode erosion gives a projected lifetime of two years as limited by charge exchange ion bombardment. In addition, neutralizers were operated during these steady-state life tests. Specific emission of the filament-type neutralizers was 50 mA/W before start of the test and no deterioration was observed after 2000 hours.

Since attitude control requires pulse operation of ion thrusters, four thrusters were temperature cycled from 40,500 to 85,000 times each with no deterioration of ionizer heater characteristics. A novel feature of this linear strip thruster design is the use of a very low mass ionizer which can be heated from less than 100°C to 1100°C within 15 sec with a warmup energy of only 0.5 W-hr. The low-mass ionizer was fabricated almost entirely from tungsten materials and was assembled with the aid of electron beam welding techniques. Several new technology developments were instrumental in the successful development of a rugged and reliable heater designed specifically to overcome the unique problem of temperature cycling an ion thruster with minimum warmup energy.

I. INTRODUCTION AND SUMMARY

The purpose of this program was to develop a linear-strip cesium-contact ion thruster having a nominal thrust level of 0.3 millipound. The principal technical task involved design of the thruster for long life and demonstration of this capability by performing a steady-state life test of 2000 hour duration. A secondary objective was to attain good reliability with regard to thermal cycling the thruster many tens of thousands of times. This was to be demonstrated by a number of cyclic thermal tests to at least 10,000 cycles on two thrusters and 50,000 on additional units. A possible application of such a thruster having both cyclic and steady state operational capability is for attitude control and station keeping of a synchronous satellite.

The particular major contractual tasks which were performed in order to prove the thruster design were: (1) design verification of thermal and electrical performance, (2) long duration cyclic thermal tests, and (3) steady-state life tests.

During the course of successfully attaining these contractual objectives, a number of additional problems were examined. Among these necessary correlary efforts, one of the most significant new technology contributions was the development of a low-mass ionizer which could be cycled to temperature (1100°C) in a time period of 20 sec or less in a reliable and repeatable fashion. In particular, this required the design of a novel ionizer heater and development of unique fabrication techniques to provide repeatable operational capability for temperature cycling. Electron beam welding techniques were perfected during fabrication of a number of low mass ionizers. Consequently, the ionizer does not have any contaminating materials, such as braze solders, and is fabricated completely from solid tungsten and porous tungsten materials.

In order to successfully conduct long-duration steady-state tests at minimum cost to NASA, an Automatic Life Test Console was designed and fabricated using SERT-I power conditioning supplies as the basic driving elements. Several control loops were closed, (e.g., beam current to cesium vaporizer heater) in order to permit unattended operation during steady-state life tests. This feature proved immensely valuable during the course of the contract as it permitted both steady and reliable operation of the ion thruster and also released a number of project personnel for other technical efforts on the contract. This automatic console was instrumental in the successful completion of a 2000 hour steady-state life test at an average thrust level of 0.56 millipound.

During the course of the life tests, considerable data were accumulated on the residual gas environment present in the test chamber. These data are important in helping to provide limits on the tolerable partial pressures of gases that may be present during life testing of cesium-contact ion thrusters.

The optimum thruster design for generating 0.3 millipound thrust level has been approached by scaling the thruster (see Fig. I-1) to a shorter length and demonstrating long term operational capability at ionizer current densities of 7 to 8 mA/cm². An important point which was observed is that thrusters can be scaled to give the same electrical performance but attention must be given to scaling thermal conduction and radiation losses in a corresponding manner in order to maintain or improve the power-to-thrust ratio.

Finally, a long-lived neutralizer was developed and tested during the 2000 hour life test. This neutralizer is a simple device consisting only of a carburized, thoriated-tungsten filament. Specific electron emission of this neutralizer before and after the life tests was 35 to 50 mA/W for saturated temperature-limited emission

M 3706

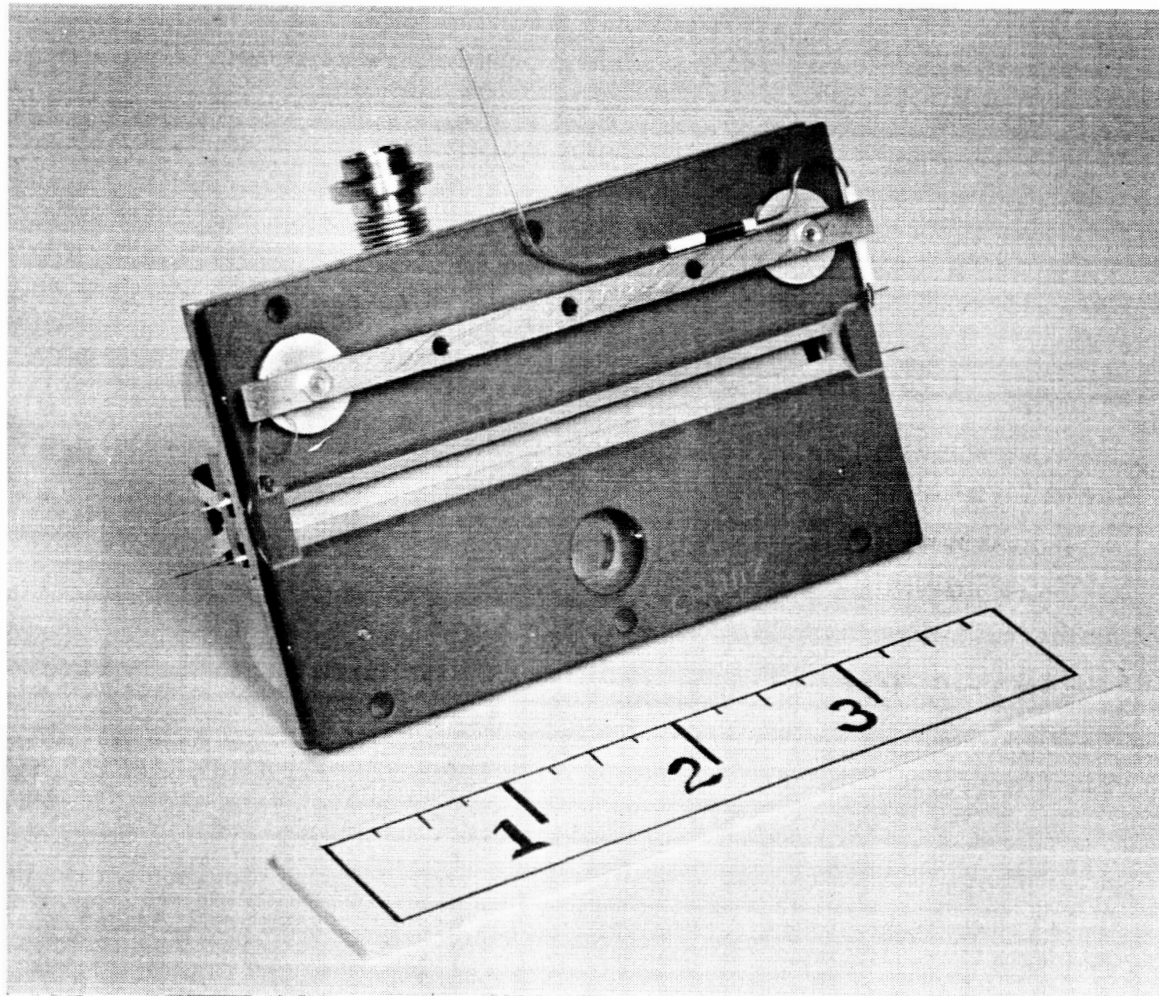


Fig. I-1. Photograph of the Hughes Linear Ion Thruster.

A chart summarizing all the thrusters fabricated and tested during this program is presented in Table I-1. All ionizers were manufactured from Philips Metalonics, Mod E, 75% dense porous tungsten except where noted. All thrusters utilized the Hughes Model 70 Ion Accelerator System and varied only in linear length of the ionizer:

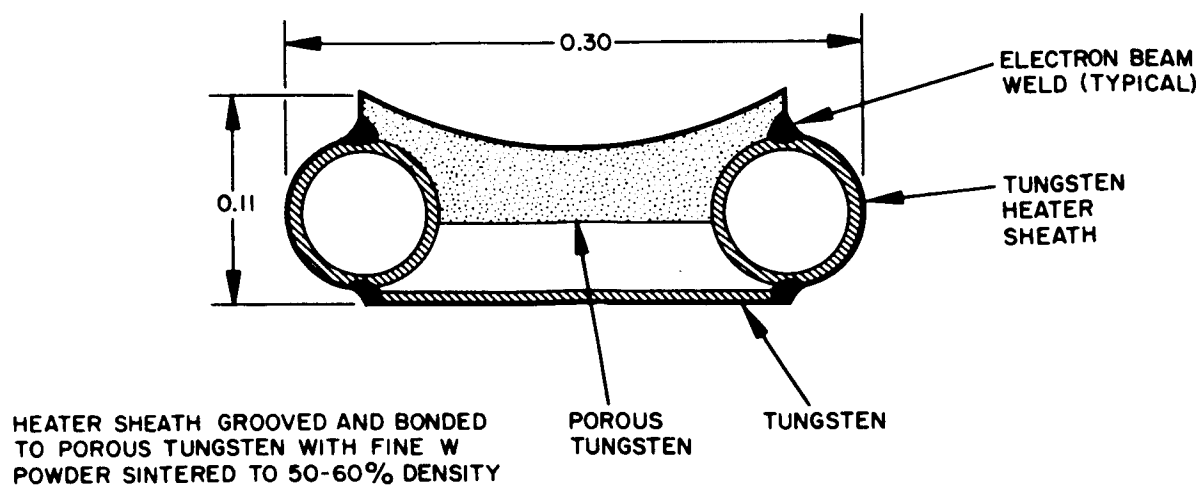
<u>Model</u>	<u>Ionizer Length</u>
LB	8 cm
LC	5 cm
LD	4.6 cm

Cross sectional drawings which differentiate between the low-mass ionizer designs are shown in Fig I-2. The three heater designs are described in Table I-2.

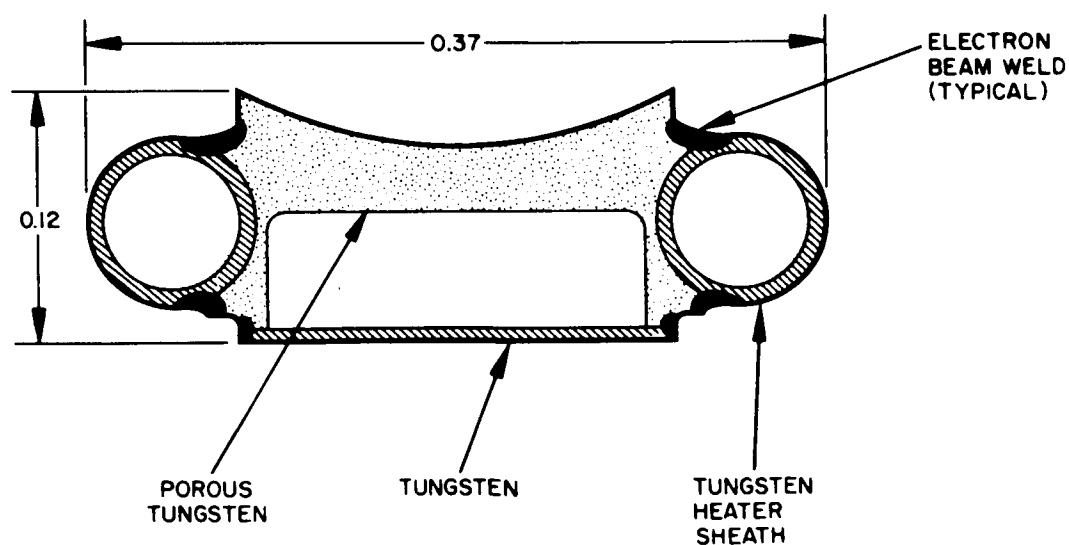
As shown in the subsequent sections of this report, it is now demonstrated that we have developed a linear-strip cesium-contact ion thruster covering the thrust range from 0.1 to 1.0 millipound with operational life time capability in the steady-state mode in excess of 10,000 hours and thermal cyclic capability of over 100,000 cycles with warmup times of 20 sec or less and warmup energy as low as 0.5 W-hr. Because of this advance in the state of the art, it is believed that this ion thruster now can be considered as a serious contender for inclusion in satellite control systems for both station keeping and attitude control.

TABLE I-1
ION THRUSTOR PERFORMANCE SUMMARY

Serial No.	Low-Mass Ionizer	Heater	Test Results
LB-1	F	D-8	Thermal and electrical design verification; 33 hours at 7 mA/cm ² .
LB-2	F	F-1	Thermal design verification.
LB-3	E	D-8	Heatup ionizer to 1100°C in 12 sec; warm-up energy = 0.53 W-hr.
LB-4	F	D-8	226 hour life test at 7 mA/cm ² .
LB-5	F	D-8	17,000 temperature cycles to 1200°C; 33,000 ~ to 1100°C.
LB-6	F	F-1	27,068 temperature cycles to 1200°C; 13,425 ~ to 1100°C.
LB-7	F	F-1	2000 hour steady-state life test at 6.5 mA/cm ² . Thrust = 0.56 mlbf.
LB-8	F	F-1	85,035 temperature cycles to 1100°C.
LB-9	E	F-2	64,119 temperature cycles to 1100°C.
LB-10	E (4.8 μ spheres)	F-1	Thermal improvement tests.
LB-11	E	F-2	Backup unit available for test.
LC-1	E	F-1	36 hours at 7 mA/cm ² plus 1636 temperature cycles; warmup energy = 0.43 W-hr. for 11 sec heat up.
LC-2	E	F-1	Electrical performance test.
LC-3	F	F-1	Performance tested and delivered to NASA-LeRC.
LD-1	F (3.8 μ spheres)	F-1	Thermal design verification.
LD-2	F (3.92 μ spheres)	F-1	610 hour steady state test at 7 mA/cm ² . Thrust = 0.3 mlbf. Minimum P/T = 196 W/mlb observed at 5000 sec for J = 9.2 mA/cm ² .
LD-3	F	F-1	Backup unit available for test.



(a) DESIGN E



(b) DESIGN F

Fig. I-2. Cross-sectional drawings of two low-mass ionizer design.

TABLE I-2
LINEAR-STRIP IONIZER HEATERS

Heater Model	Wire		Coil		Coating	Ceramic Tubing
	Material	Diam.	Diam.	tpi		
D-8	W	0.018 in.	0.055 in.	44	0.003 in. Al_2O_3 , Cr_2O_3 doped	None
F-1	97W-3Re	0.010 in.	0.033 in.	55	0.002 in. Al_2O_3 , Cr_2O_3 doped	0.036 I.D. x 0.060 O.D. alumina-slotted
F-2	97W-3Re	0.012 in.	0.043 in.	50	0.003 in. Al_2O_3 , Cr_2O_3 doped	0.050 I.D. x 0.073 O.D. alumina-slotted

II. DESIGN CONSIDERATIONS

A. Ion Thrustor

The linear single-strip cesium-contact ion thrustor to be described herein is an improved version of the unit employed in the early laboratory demonstration satellite control system developed under Contract NAS 3-2510.¹ The design philosophy employed was one of simplicity and ruggedness combined with conservative operating parameters so as to maximize reliability and lifetime without serious de-rating of the over-all thrustor performance. The thrustor was designed around the proven Hughes Model 70 Ion Optical System.

Isometric and cross-sectional drawings of the design that has evolved are shown in Fig. II-1. Several features of this thrustor design are novel. The ionizer assembly has been designed specifically for very low mass and low heat capacity so as to permit rapid warmup of the ionizer to its operating temperature. In this low-mass ionizer the heaters are encased within a tubular tungsten sheath, positioned in intimate contact with the porous tungsten ionizer on both sides of the emitter. The ionizer assembly is all tungsten, with the various elements electron beam welded to each other. The use of electron beam welding eliminates any contaminating braze materials. The ionizer heater itself consists of a tightly wound tungsten helix which is coated with aluminum oxide and placed within a protective ceramic sleeve. The ceramic sleeve is slotted to permit direct radiative transfer from the heater coil to the porous tungsten emitter. The heater subassembly simply slides through the tungsten sheath and is easily replaceable. Development of a reliable heater involved application of new technology and is discussed in detail in Section III. A completed ionizer assembly is shown in the photograph of Fig. II-2. For high efficiency in steady state operation, the ionizer is well heat shielded. In addition, thermal conduction losses are held to a minimum by the use of small cross-sectional area, relatively low thermal conductivity and refractory materials with long thermal conduction paths to the mounting brackets.

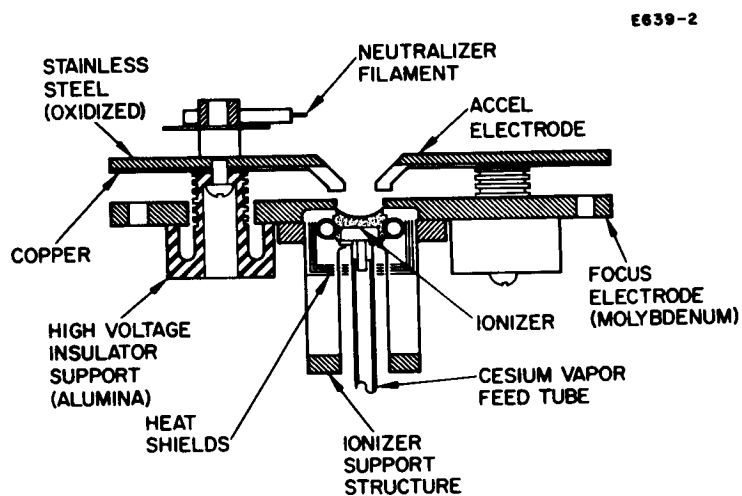
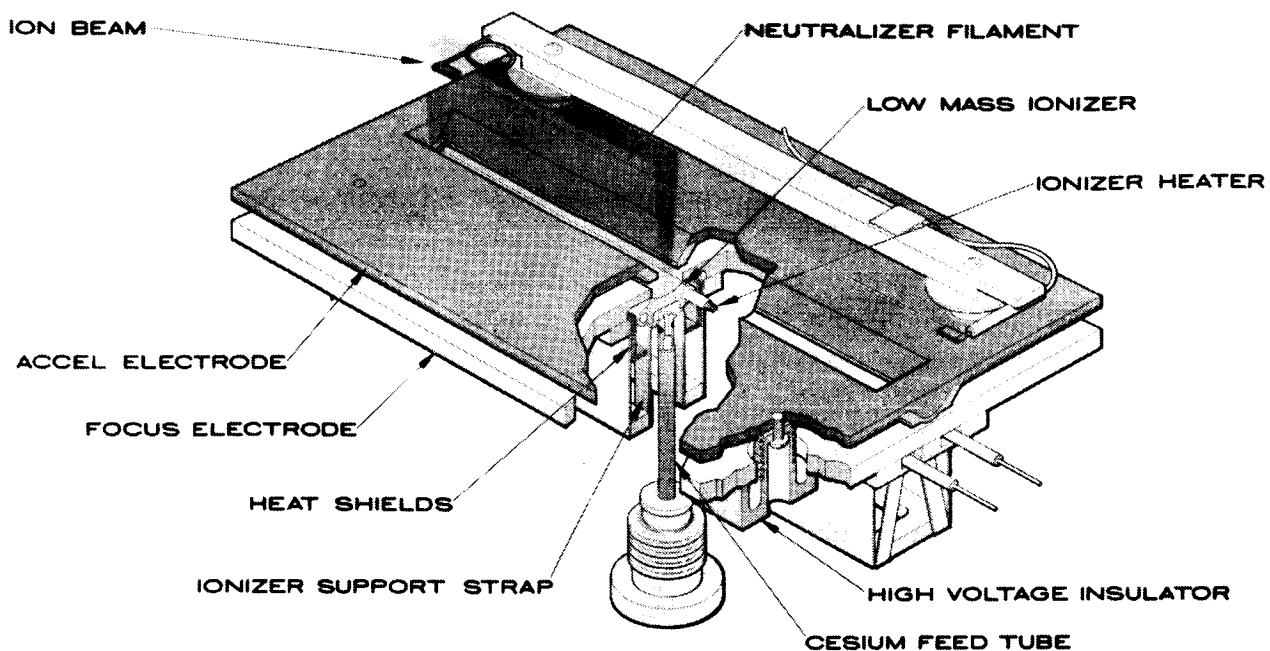


Fig. II-1. Isometric and cross-sectional drawings of the Hughes Linear Ion Thrustor.

M 3516

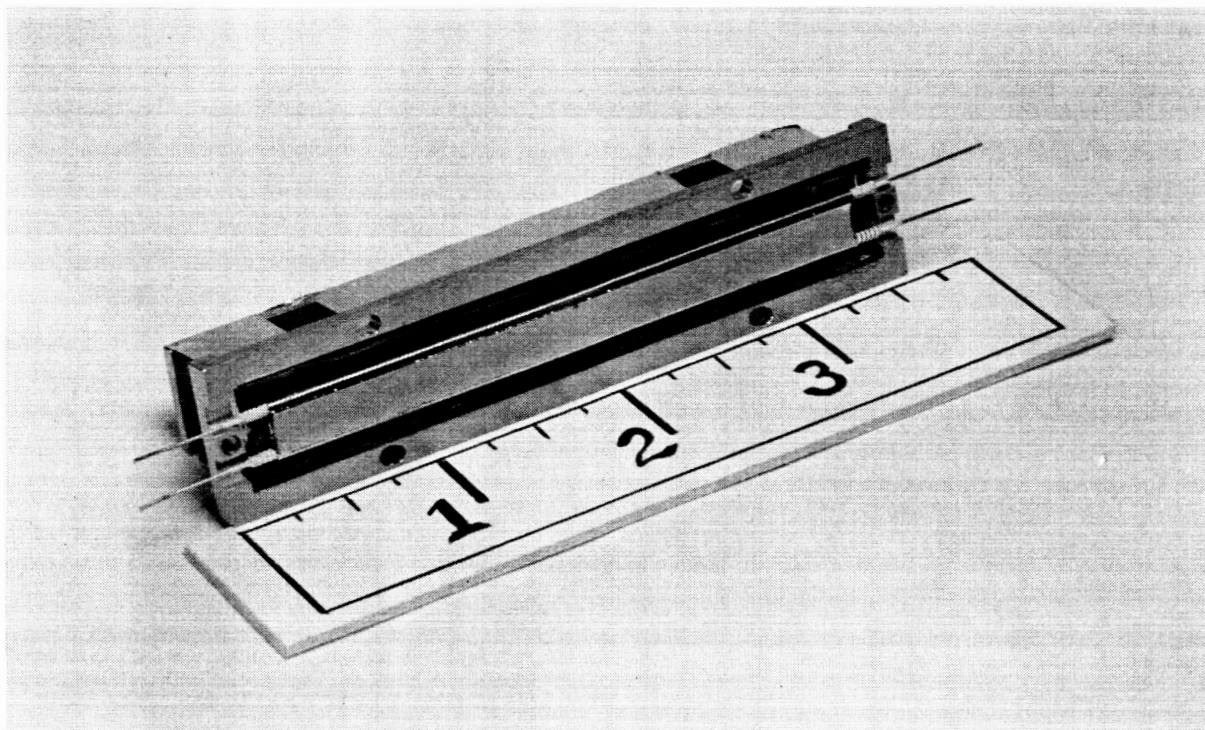


Fig. II-2. Photograph of complete low-mass ionizer assembly ready for mounting to focus electrode. (Scale in inches)

The over-all weight of the ionizer assembly, less the mounting brackets and heat shields, is only 1.5 g/cm. of linear length. Thus the 8 cm long ionizer which has been tested extensively has a mass of only 12 g and results in very rapid heatup to 1100°C with low warmup energy. Performance data on this thermal cyclic mode are presented in Section IV-A.

The accel electrode is designed as a bimetallic element of the thruster. Sheet material of stainless steel and copper are brazed together and then machined to provide the correct boundary shapes for the ion optical structure. Those surfaces of the accel electrode which are susceptible to ion bombardment are made of copper. The remaining surface of the accel electrode which radiates to free space consists of oxidized stainless steel so as to maximize the emittance and maintain a low accel temperature during operation of the thruster. Since the accel temperature can be held to less than 200°C (in a non-sputtering environment), this results in a minimum amount of thermionic back emission of electrons from the cesiated copper surface to the positive high voltage electrodes.

The high voltage standoff insulators are an integral part of the mechanical assembly and provide the correct spacing between the accel, focus electrode, and neutralizer. These high voltage insulators are convoluted and reentrant so as to minimize leakage currents and corona discharges. Cup-type shields over the insulators are not employed and have been found unnecessary in tests of the order of 1000 hour duration.

Another novel feature of the thruster design is the use of a carburized, thoriated-tungsten filament for generation of the neutralizing electrons. This neutralizer design has proved to be quite rugged and reliable and has operated with no deterioration in electron emission characteristics for a period of 2000 hours in the presence of a cesium ion beam. Filament lifetimes of over 10,000 hours are predicted at a temperature of 1950°K and a specific emission of 35 mA/W.

The major electrical design parameters for the 8 cm linear-strip thruster in steady state operation are listed in Table II-1.

TABLE II-1
8 cm THRUSTOR ELECTRICAL PARAMETERS
(Nominal Design Values)

Thrust	0.5 mlbf
Specific Impulse	5000 sec
Beam Current	32 mA
Beam Voltage	1.7 kV
Ionizer Current Density	7.0 mA/cm ²
Power-Thrust Ratio	225 W/mlbf
Weight	0.5 lb

For the case of the 5 cm thruster, the thrust level was scaled to approximately 0.3 mlbf and the beam current was correspondingly reduced. The power-to-thrust ratio remains approximately the same. The performance figures in Table II-1 have all been obtained in a number of thrusters which have been tested extensively.

B. Cesium Feed Systems

Cesium feed system work on this program was limited to the minimum effort required to support the thruster test program. For this purpose, two different cesium feed systems were provided: a 3 g capacity unit, designed and developed under the SERT-I program, and a new 250 g capacity laboratory unit. Both units were fabricated in sufficient quantities to support the thruster tests and were satisfactory for their intended use.

The 3 g capacity unit, shown in Fig. II-3, is a flight-type unit with a capillary reservoir which is insensitive to the attitude in which it is mounted. A solenoid flow-control valve, hermetic seal, piercing mechanism, and heaters are part of this feed system. All of the necessary hardware, except the capillary reservoirs, was carried over from previous programs, thus providing a cesium feed system tailored to the requirements of short duration thruster tests at minimal cost to this program.

Longer duration thruster tests called for a cesium feed system with a capacity of up to 250 g. To satisfy this requirement, a new feed system, shown in Figs. II-4 and II-5 was designed and fabricated. The principal design constraints applied to this feed system were capacity, ease of handling and filling, and economy of manufacturing. Secondary considerations were given to the development of high temperature solenoid coils, potting techniques, and to repackaging the previously developed electromechanical piercing mechanism. Four of these systems were fabricated and used for long duration thruster tests. The success of these tests demonstrated that the new feed system met its design objectives.

This feed system consisted of a cylindrical 250 g capacity reservoir, a reservoir heater, a manifold, a manifold heater, a hermetic seal and piercing mechanism, and a removable solenoid valve with a minimum of thermal insulation. No provisions for zero-gravity operation were included. The work required to reload this feed system was less than half the effort required to reload the flight-type feed system developed under Contract NAS 2-3510. Comparable savings in manufacturing and assembly costs were realized.

The reservoir, reservoir heater, manifold, and manifold heater were permanently assembled by copper brazing. The end plate incorporating the filling port, was tungsten-inert-gas (TIG) welded to the brazed assembly. The hermetic seal consisting of a stainless steel ring supporting a 0.001 in. thick stainless steel diaphragm that was copper brazed to the ring was used to close the reservoir outlet port. This diaphragm assembly was sealed to the reservoir with a soft oxygen-free high-conductivity (OFHC) copper gasket and retained in place

M 2912

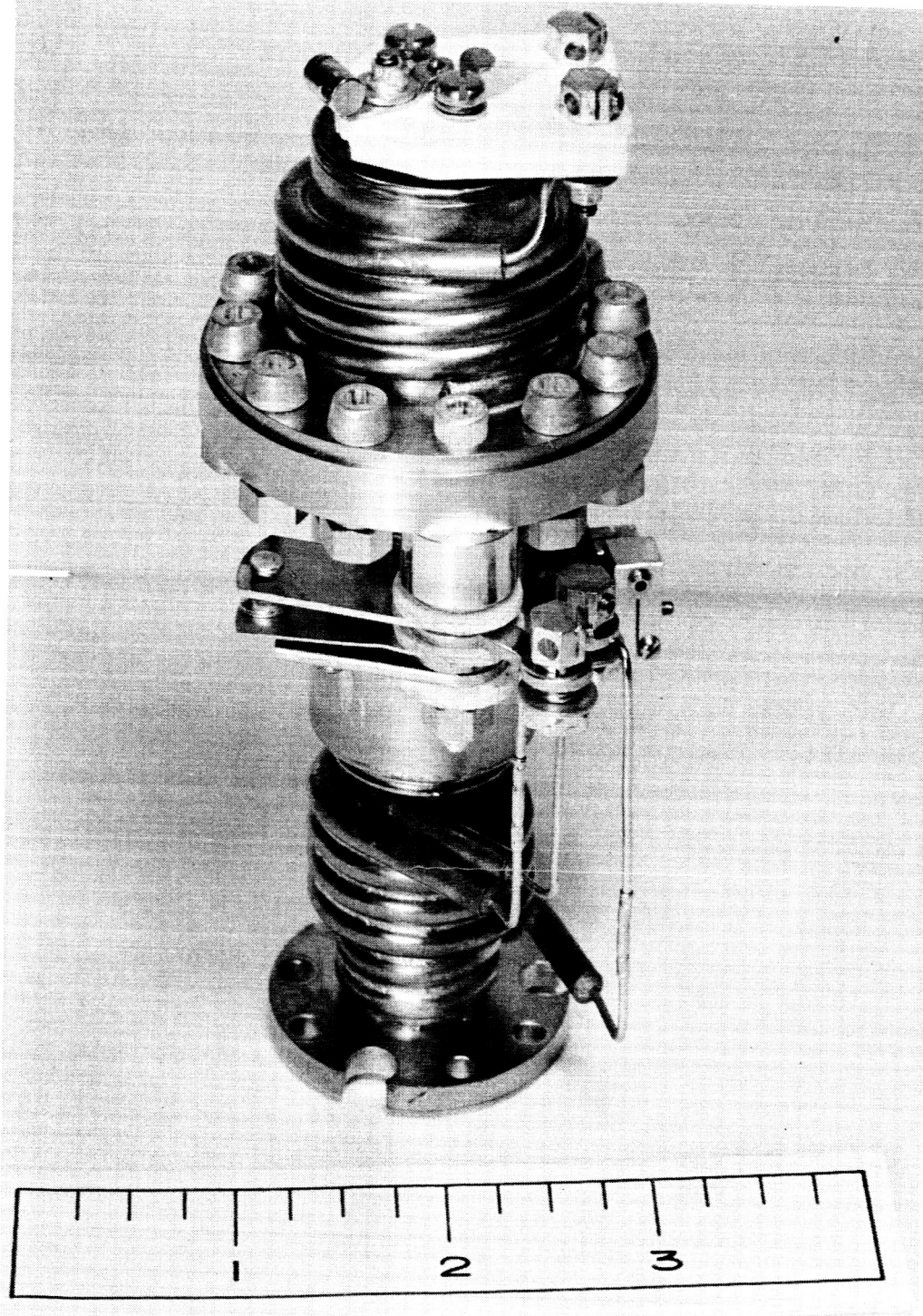


Fig. II-3. Three gram capacity flight-type cesium feed system originally developed for the SERT-I Program. (Scale in inches)

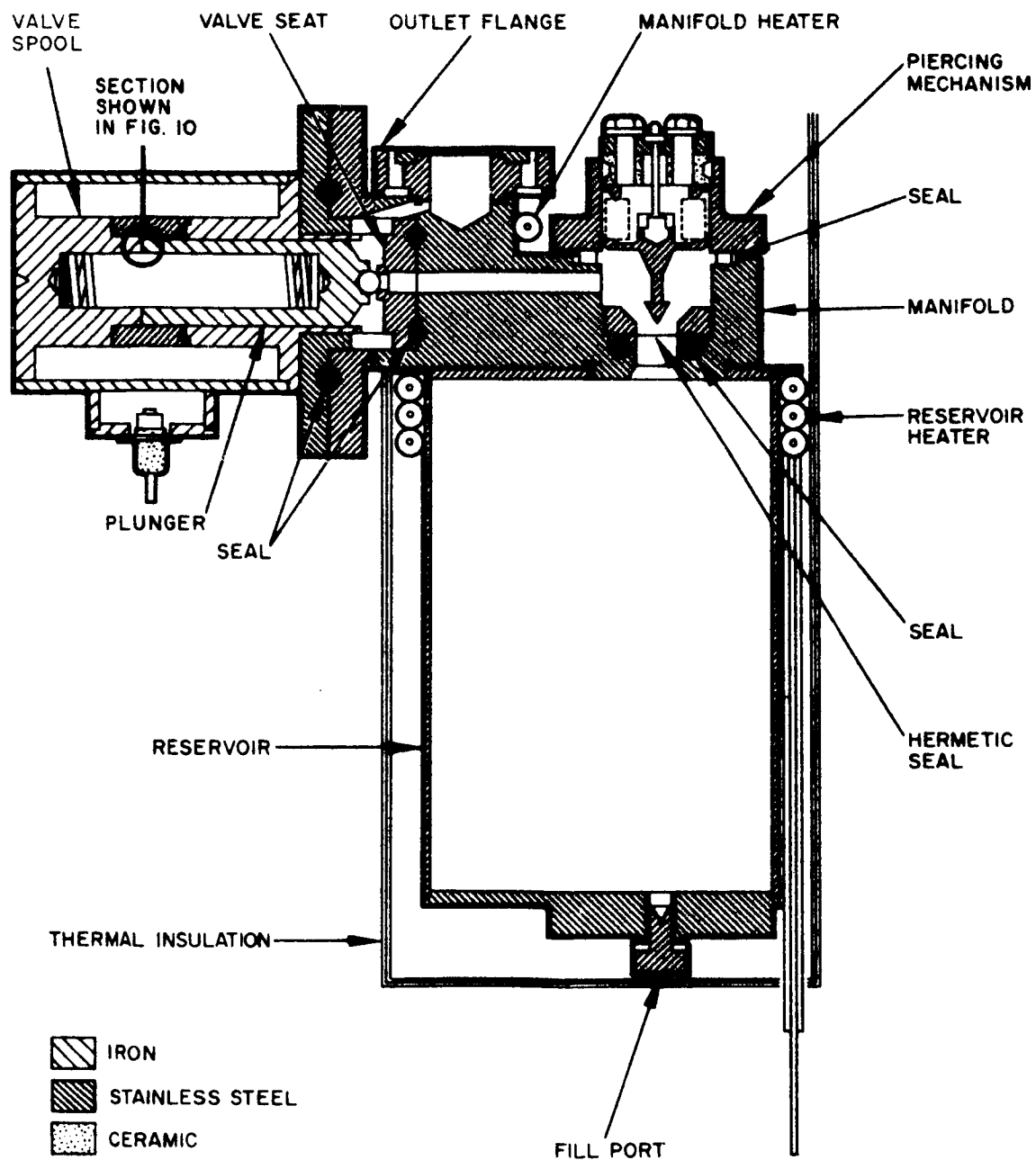


Fig. II-4. Cross section of 250 g laboratory feed system.

M 3927

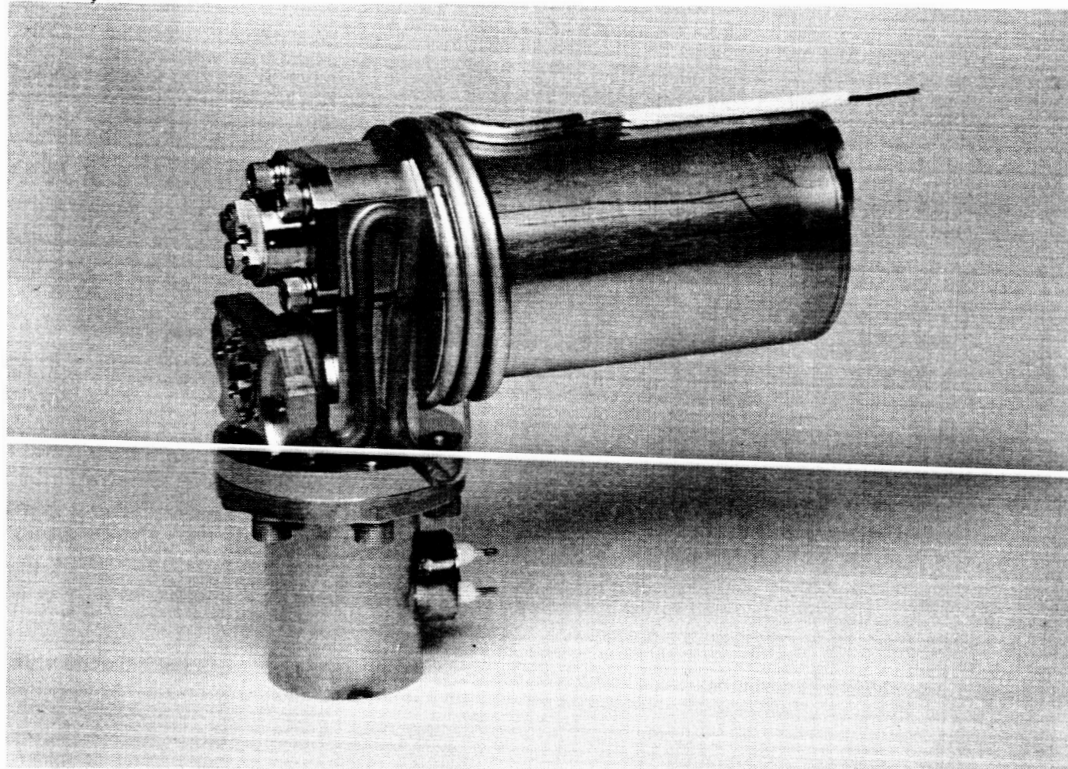


Fig. II-5. Photograph of 250 g laboratory feed system less heat shields.

with a special nut. The solenoid valve and a piercing mechanism were then added to complete the assembly. After the reservoir was filled with cesium, the fill port was sealed with a special screw and soft OFHC copper gasket.

To initiate feed system operation, the stainless steel diaphragm was ruptured by actuating the piercing mechanism, thus releasing cesium vapor to the control valve. The piercing mechanism was a welded metal bellows closed at one end by a plate and TIG welded at the other end to its housing. A pointed probe to rupture the diaphragm was machined integral with the bellows end plate. When the device was armed, the bellows was compressed and retained by a stainless steel wire tension link. To actuate the device an electric current was passed through this tension link which caused it to rupture like a fuse, thus releasing the bellows. Bellows spring force drove the probe through the diaphragm allowing cesium vapor to flow to the solenoid flow control valve. The piercing mechanism was flange mounted on the reservoir with a copper gasket used as a static seal.

The repackaged piercing mechanism was completely successful. It is compared to the old unit in Fig. II-6. The static seal design was verified by temperature cycling of the operating range while checking leakage on a helium mass spectrometer. No development work was done beyond the static seal design verification test on this piercing mechanism or on the hermetic seal used with it. Both elements were incorporated in the feed system design and used with no failures or other difficulties.

The only component in this feed system that required a significant amount of new engineering was the solenoid valve. Several changes were made in this component to improve system design for laboratory use. Referring to Fig. II-4, the cesium flow path goes from the reservoir, across the valve seat, and then directly to the outlet flange so that there is no flow through the valve spool. A poppet seating force of 7.0 lb was used (instead of 0.5 lb as on the SERT-I valve) to reduce leakage and permit deletion of the manual valve heretofore used in laboratory feed systems. All valve elements, including the valve seat, were removable for cleaning and/or repair. This last feature was

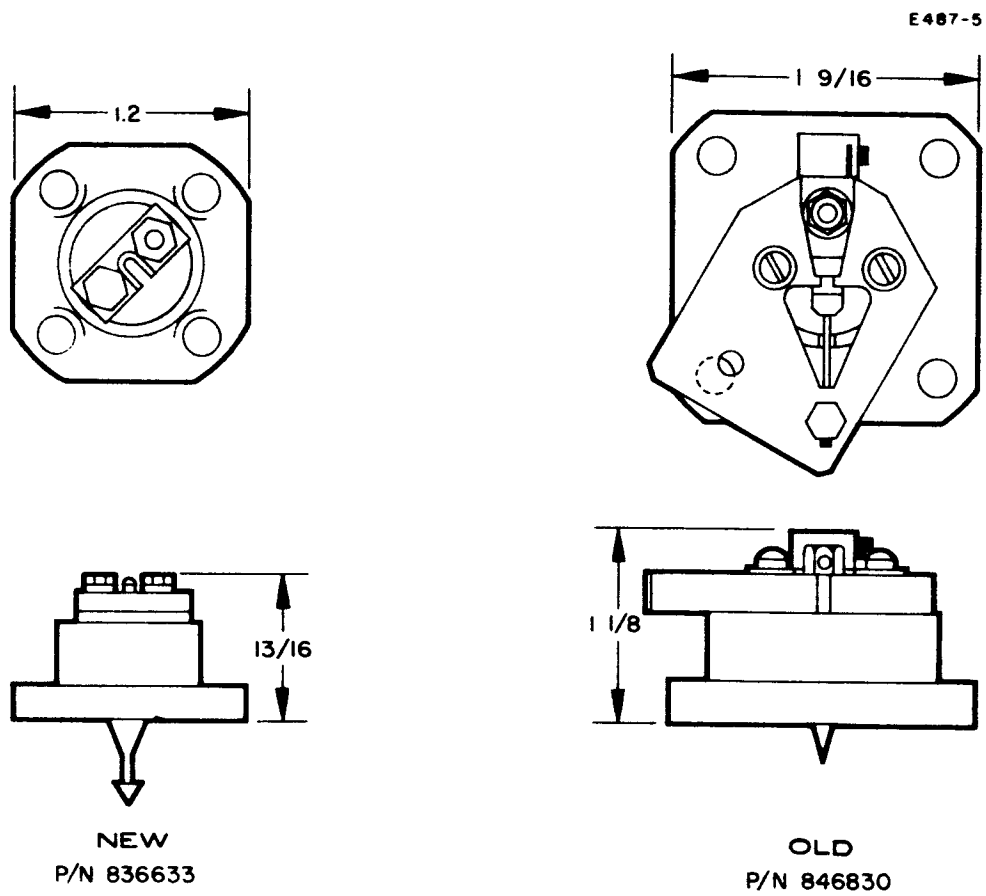


Fig. II-6. Piercing mechanisms for cesium feed systems.

practical because of successful application of a new type of static seal. One copper ring seals the valve seat to the reservoir outlet and a second ring seals the valve flange to the valve mounting block and feed system outlet flange. Both seals are retained, in series, by a single flange.

Increased poppet seating force required design of a new coil. In conjunction with the new coil, the valve spool was redesigned to reduce manufacturing costs by simplifying the machining operations and by replacing several welding operations with a single furnace brazing operation. A commercially available, high-temperature insulation system² was successfully applied to provide a rugged, fully potted solenoid coil capable of operation at temperatures up to 650°C.

The key element in the new valve design was the double static seal since the obvious alternates to the design used herein resulted in a considerable increase in valve mounting complexity. Therefore, a seal test fixture was built. Helium leakage through the seals was not detectable on a mass spectrometer (maximum sensitivity of 10^{-10} cc/sec) during five complete cycles from room temperature to 350°C and back to room temperature. Pressure differential across the seal during this test was one atmosphere, which was the maximum pressure the seal would experience in service.

Required valve performance was demonstrated, both during component performance testing and during engine tests. Feed systems and engines were removed from the vacuum chamber several times to have faulty feed valve coils replaced. No unacceptable contamination of the cesium in the reservoir occurred. In addition, system design was such that the feed system and engine assembly could be removed from the vacuum chamber to a controlled atmosphere dry box and the cesium in the reservoir replenished without extensive disassembly or overhaul.

The first feed system was assembled and tested to verify its performance. Solenoid valve leakage was zero bubbles of nitrogen in 0.5 hour with a differential pressure of one atmosphere across the valve. During temperature tests in vacuum, a suitable thermal balance was obtained by adjusting the boiler heater and manifold heater power. A boiler temperature of 296°C was maintained with the following heater power inputs:

Reservoir heater:	6.6 W
Manifold heater:	5.6 W
Ionizer heater:	58.0 W

The only feed system failures that occurred during this program were solenoid coil failures during thruster life tests. Two such failures occurred during the 226 hour test of thruster LB-4. Analysis showed that a major contributing factor to failure of the solenoid was manual operation with a Variac control which resulted in over-heating of the solenoid during those periods of high input power. Consequently, the feed valve power supply was modified so as to include a capacitive discharge circuit which would supply enough energy to open the valve within 50 msec. Once the valve opened, a small amount of dc power was maintained continuously to keep the valve in the open position. This mode of operation, coupled with a solenoid which met the required specifications, resulted in successful operation of the feed valve from $t = 122$ hr until the end of the LB-4 test. Total time at temperature for this last valve was 331 hours. In summary, it is believed that this failure mode was corrected.

During the 2000 hr life test of thruster LB-7, the solenoid coil failed at $t = 137$ hours. Analysis of this failure showed that the solenoid power supply generated 600 V of back emf whenever the power supply shut off. Repeated application of this back emf resulted in a local breakdown of wire insulation and potting compound at a point where the coil windings crossed. Eventually the wire burned

through, resulting in an open solenoid. To prevent this failure mode, the winding procedure was changed to provide more insulation and the valve control circuit in the console was modified to eliminate the back emf.

These valve failures, as well as a similar failure that terminated the life test of thruster LD-2, have resulted in several changes in coil potting techniques and have resulted in a general improvement in coil life. In addition, considerable effort was devoted to re-examination of the magnet wire and potting materials. This re-examination of coil materials showed that both magnet wire and potting compound composition had deteriorated in quality from the samples originally evaluated at HRL. Consultation with the vendor identified the problem as being in the vendor's manufacturing controls. We have been assured that this deterioration in quality will not be repeated.

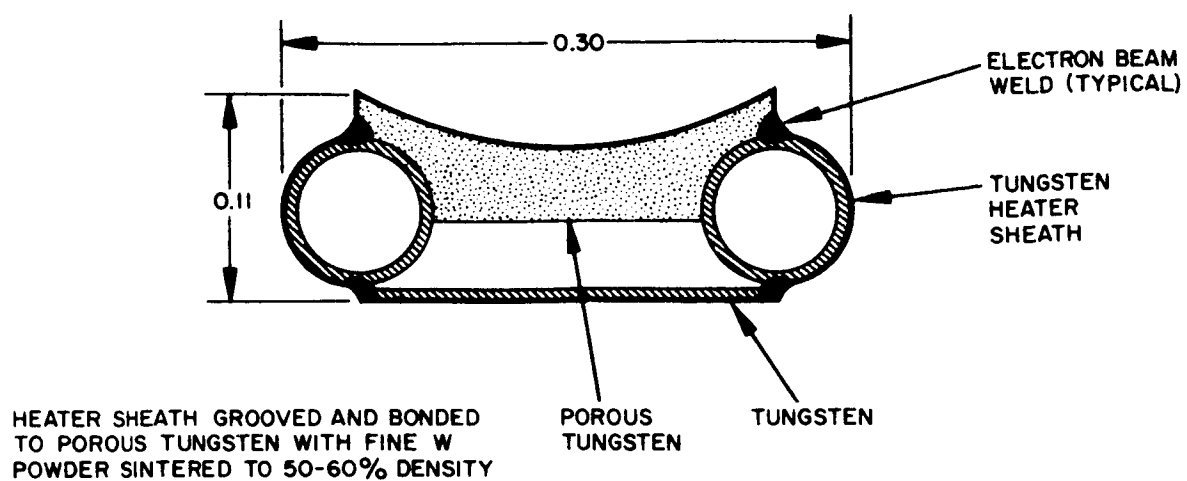
III. LOW-MASS IONIZER AND HEATER DEVELOPMENT

An early problem encountered in cyclic operation of ion thrusters was the design of an ionizer and ionizer heater which could be cycled from ambient to high temperatures ($\sim 1100^{\circ}\text{C}$) many tens of thousands of times but still be of sufficiently low mass so that the heat capacity of the assembly would permit rapid heatup with a relatively low energy requirement (0.75 W-hr or less). This required an approximately tenfold improvement over the then-existing state of the art in ionizer designs. To accomplish this task the problem was attacked from two points of view: (1) reduce the mass of the ionizer as much as possible consistent with thermomechanical integrity and distribution of cesium vapor to the emitting surface; (2) reduce the peak temperature of the ionizer heater by affecting the most efficient heat transfer consistent with electromechanical integrity.

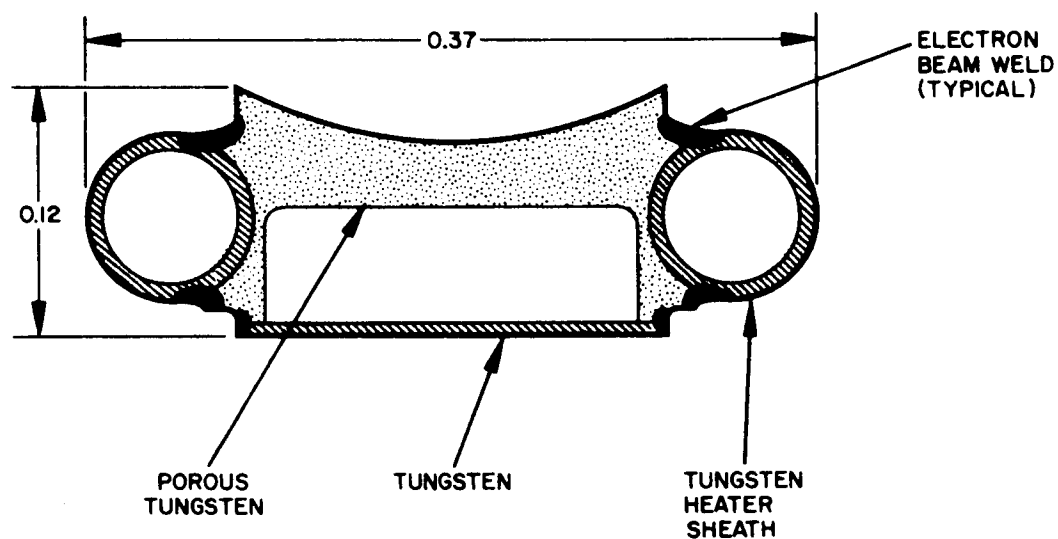
A. Low-Mass Ionizers

Two low-mass ionizers (LMI) were designed and evaluated for use in the Linear Ion Thruster. These ionizer designs, designated LMI-E and LMI-F, are shown in Fig. III-1. Mass of the LMI-E design is 1.5 g/cm of linear length including the accompanying support strips, feed tube and heaters. The LMI designs employed electron beam welding of the tungsten heater sheath to the porous emitter. The feasibility of electron beam welding a thin wall (0.005 in. to 0.010 in.) tungsten tube to a porous tungsten member is demonstrated in the photograph of Fig. III-2 which shows a cross-sectional region of an LMI-F.

A novel feature of the LMI-E design is the use of gravity sintered porous tungsten to provide a good thermal bond between the heater sheath and porous tungsten emitter without seriously impeding the cesium vapor flow. This sintered interface was not intended to provide the necessary mechanical support.



(a) DESIGN E



(b) DESIGN F

Fig. III-1. Cross-sectional drawings of two low-mass ionizer design.

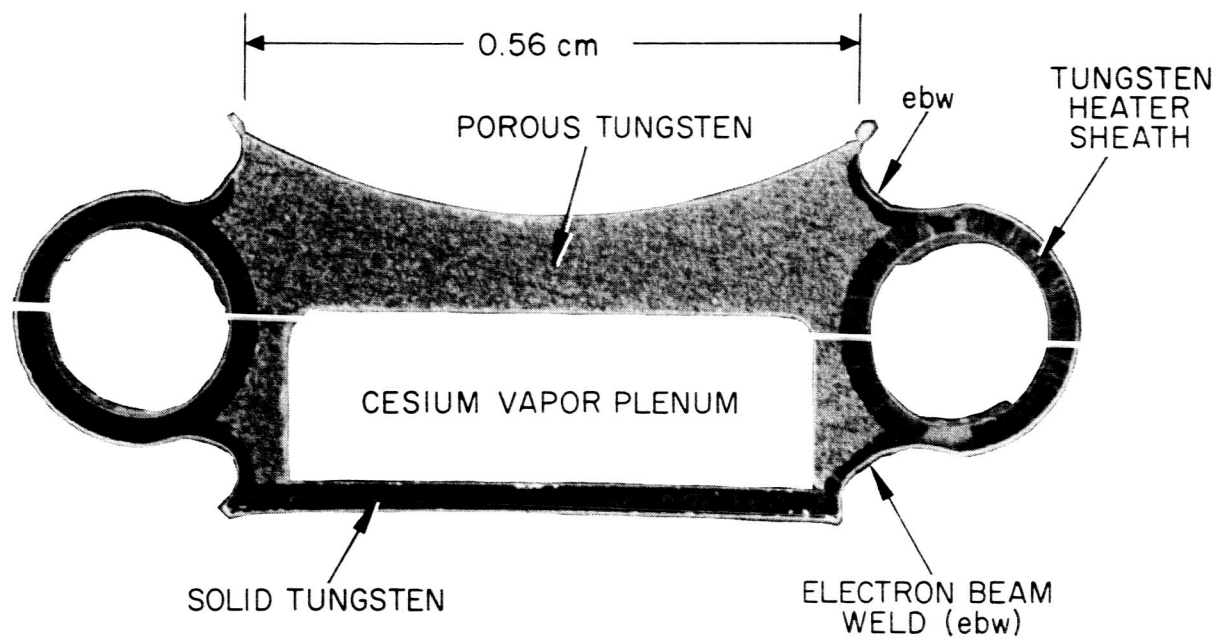


Fig. III-2. Photograph of low mass ionizer (LMI-F) cross section.

Gravity sintering experiments using three different fine tungsten powders, both cubic and spherical, were conducted to determine the density and degree of continuous bonding between solid tungsten and porous tungsten. The filler materials used were:

M-55

Supplied by Sylvania, coarse cubical, with size around 3 to 3.5 μ . Some fines from the particles fracturing. Two samples were sintered for 4 hours at 1800°C in vacuum.

U-4.0

Supplied by General Electric. Crystalline, needle structure with size range of 0.3 to 3.5 μ . Sintered at 1800°C for 4 hours in vacuum.

Linde No. 6

Supplied by Linde. Cut number 6. Spheroidized, small range of particle size centered at 4.8 μ . Sintered 20 hours at 1600°C in hydrogen.

The test conditions produced well-sintered joints. Figure III-3 in a cross section (50x magnification) of M-55 tungsten sintered in vacuum for 4 hours at 1800°C. The interface is very good where the radii match, with the interface being no thicker than the grain boundaries, but as the radii diverge, the joint becomes open with the filler material not adhering to the rod. In the gap between the rod and the porous tungsten, the filler material is present, sintered to the ionizer face only. There is some apparent "penetration" for a depth of 0.002 in. on the surface adjacent to the rod, but a close examination does not reveal any explanation as to the cause. The corrosion along the grain boundaries left no residue or trace compound. In one sample, at a single spot on the ionizer surface, a tungsten carbide structure was visible to a depth of 0.0005 in., but there was no connection to the "penetration" in other parts of the ionizer.

M3007

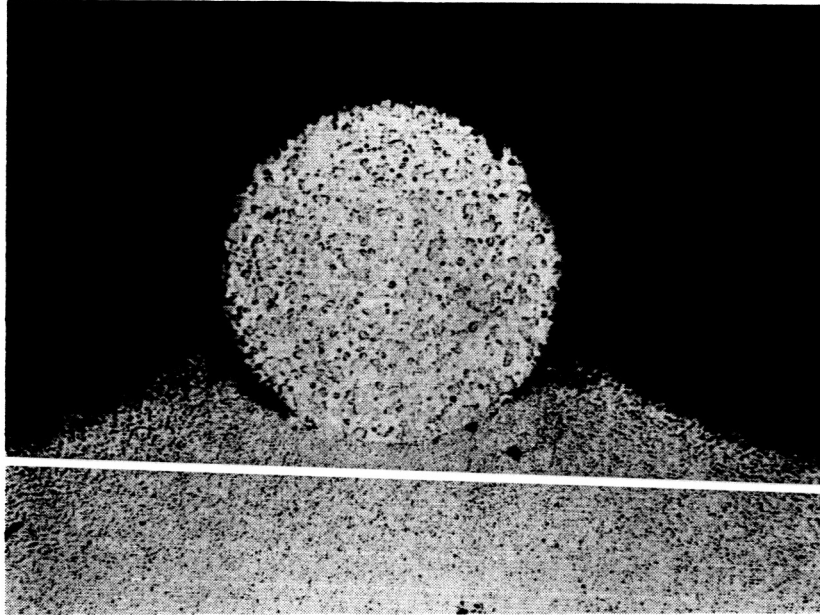


Fig. III-3. Cross section (50x) of tungsten rod sintered to porous tungsten with Sylvania M-55 tungsten powder.

The structure of the M-55 filler material is shown in Fig. III-4. The large voids are typical of the sintered filler material and would be quite porous to the flow of cesium vapor. In summary, good thermal and mechanical joints were made with all powders. A completed LMI-E made using the above technology is shown in the photograph of Fig. III-5.

As anticipated, the more rugged LMI-F design proved to be easier to fabricate and resulted in higher yields than the LMI-E. Although somewhat more massive than LMI-E, the LMI-F proved to be capable of meeting the warmup requirements. In addition, electrical performance tests indicated that the distribution of cesium vapor to the frontal ion emitting area was more favorable in the LMI-F design. Consequently, most of the later thrusters fabricated during this program utilized LMI-F ionizers.

Toward the latter part of the program, the electron beam welding of the 4.6 cm long low-mass ionizers was simplified by omitting end plates and having the cesium plenum milled into the back side of the porous tungsten. The elemental parts of such an ionizer are shown in the photograph of Fig. III-6. All metallic parts were tungsten except for the feed tube (75% W - 25% Re) and heater wire (97% W - 3% Re). A subsequent stage in the assembly is shown in Fig. III-7 prior to electron beam welding of the back plate. The ends of the ionizer were sealed by electron beam surface melting to 100% density to a depth of about 0.002 in. A similar treatment was applied to seal the ionizer sides to within 0.001 in. of the edge of the curved ion emitting surface.

B. Ionizer Heaters

Because of the requirement of cyclic operation of the linear strip thruster with warmup of the ionizer to operating temperature in 20 sec, the ionizer heater was one of the most critical components in this thruster. The severity of the operational mode for this heater is eased primarily by minimizing the peak temperature of the heater

M 3026

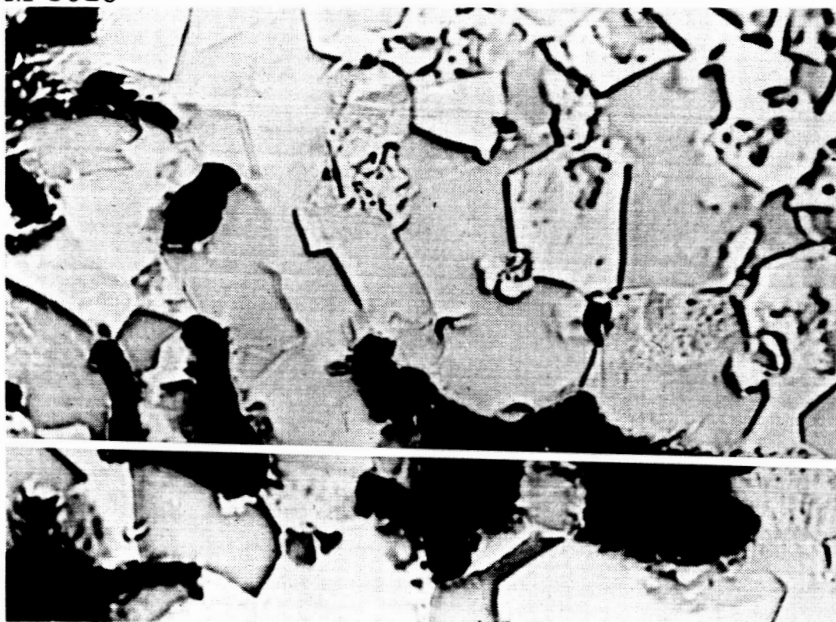


Fig. III-4. Photomicrograph (1600x) showing the structure of the porous ionizer and filler material.

M 3515

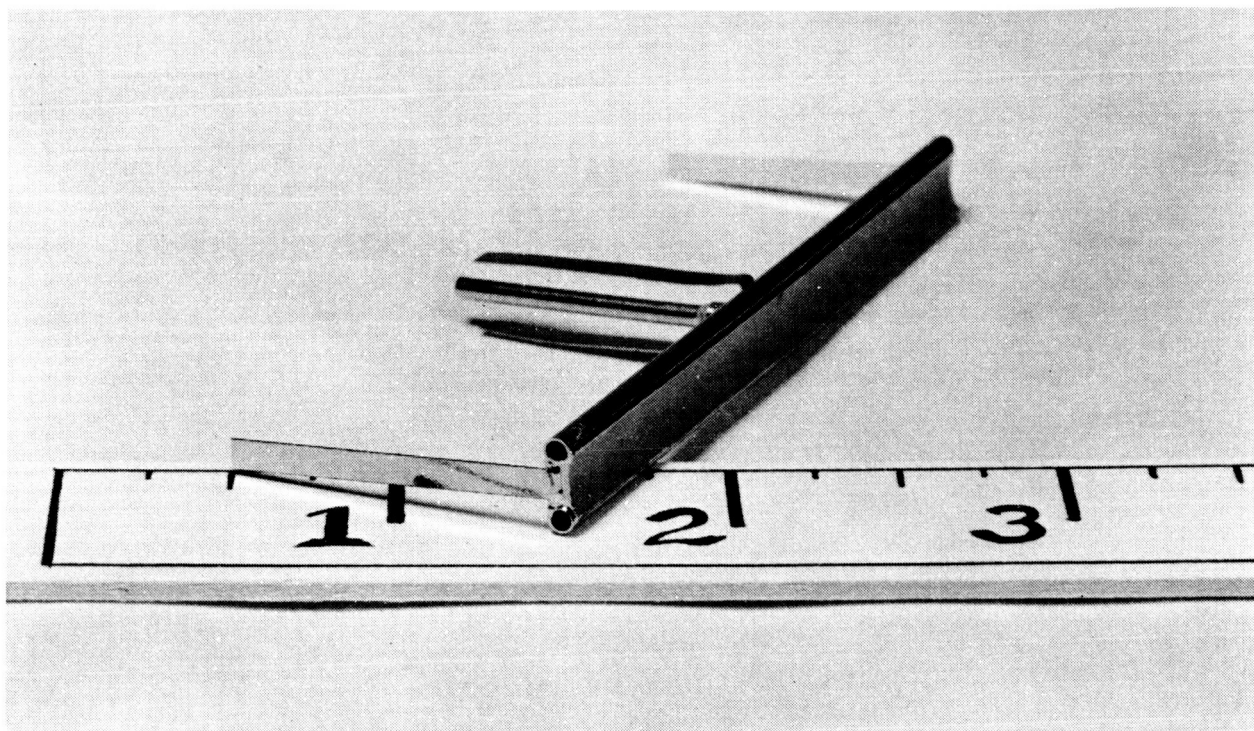


Fig. III-5. Low-mass ionizer (LMI-E), showing heater tubes, manifold plates, support straps and feed tube all electron beam welded to the porous emitter. (Scale in inches)

M4429

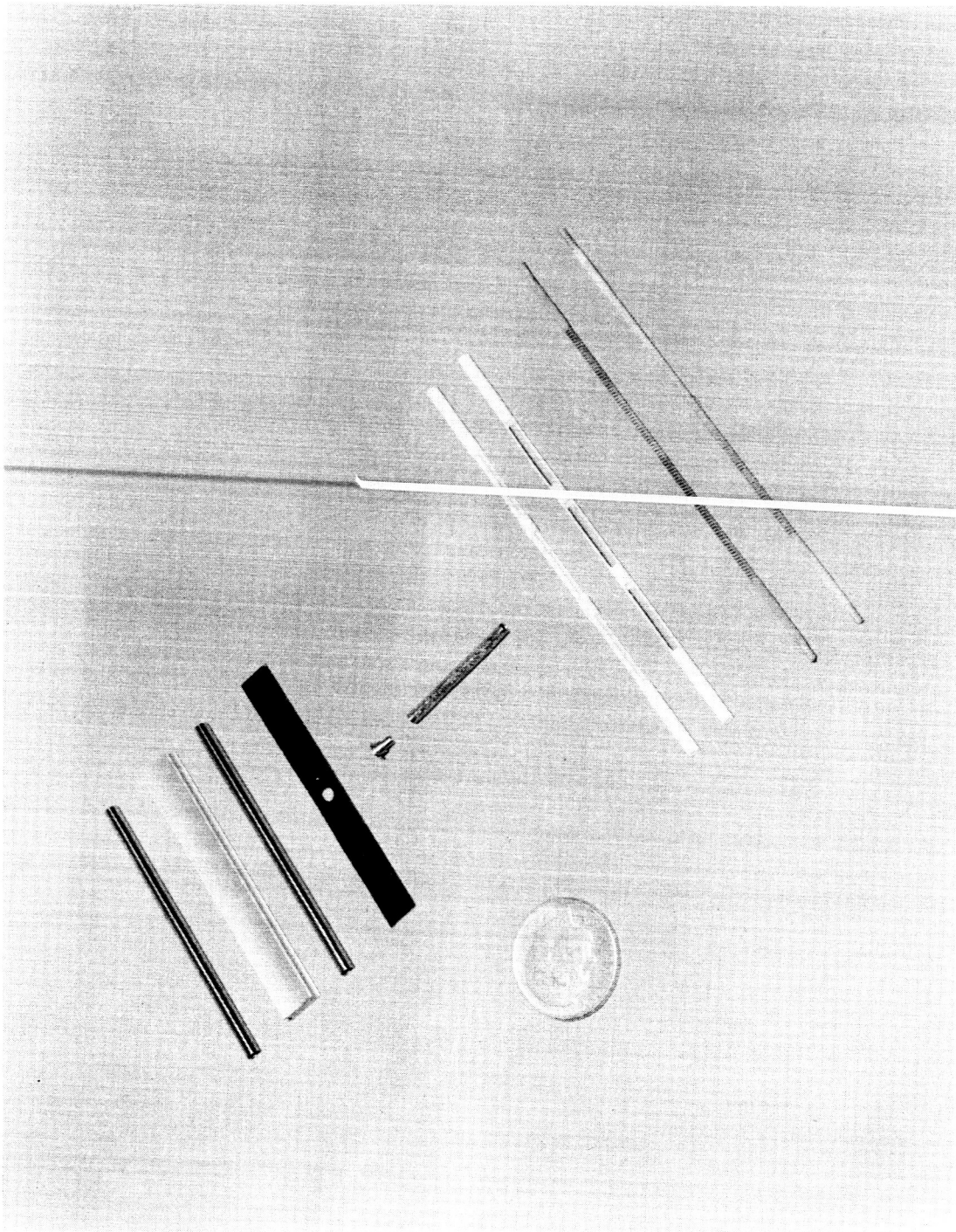


Fig. III-6. Parts comprising the basic elements of a low-mass ionizer.

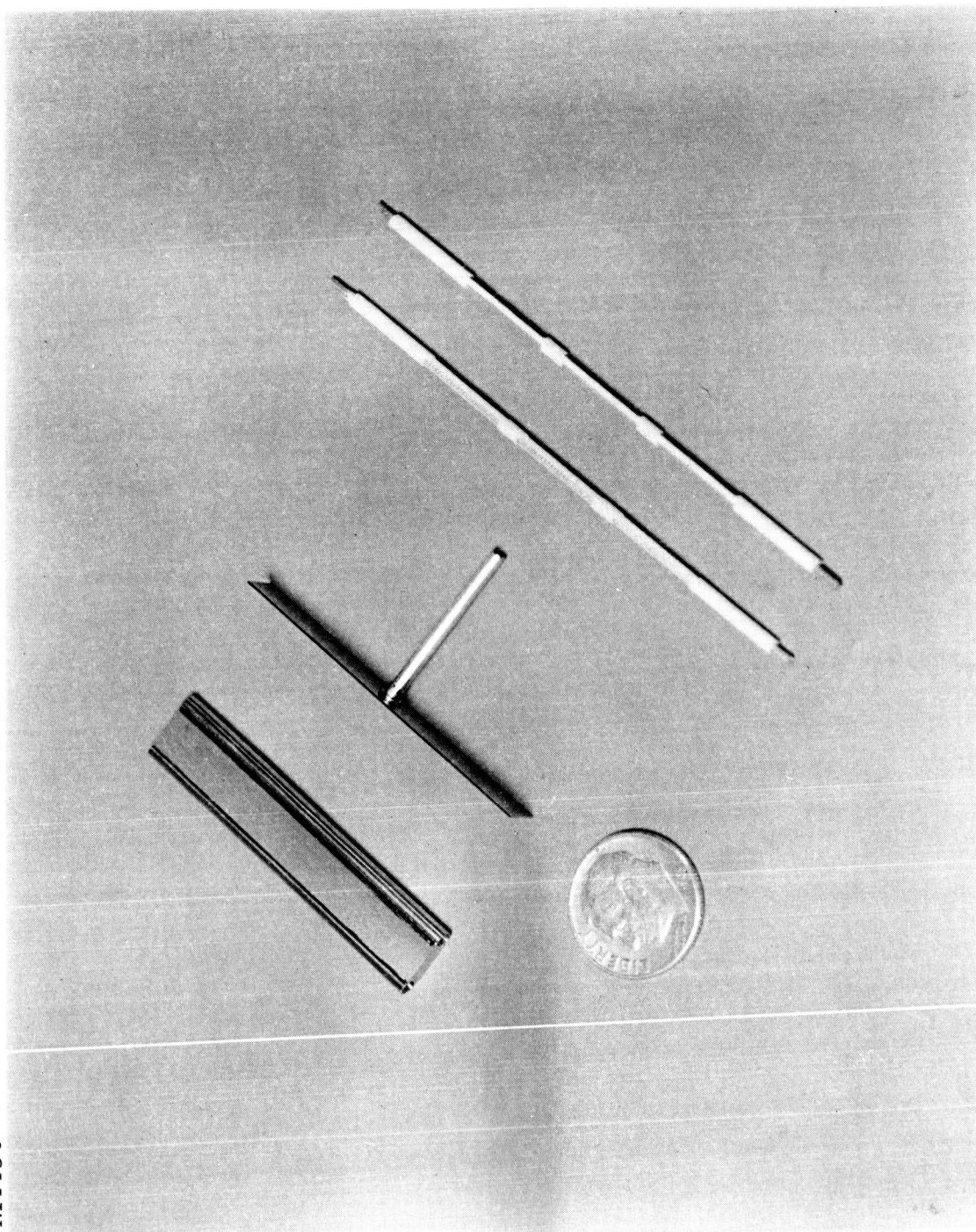


Fig. III-7. Low-mass ionizer parts in an intermediate stage of assembly.

assembly. This, in turn, implies relatively good heat transfer between the heater and porous tungsten ionizer body. The two most effective methods for realizing high heat transfer are: (1) maximum effective radiating area of the heater, and (2) high emittance of this radiating surface. Rapid warmup of the ionizer to operating temperature requires minimum mass not only in the ionizer body but in the heater also. Therefore, item (1) above is best affected by means of a coiled helix heater. It was decided to construct this heater coil from 97% W - 3% Re because of the advanced state of the art in manufacture of such small diameter wire and because this material has higher tensile strength than pure tungsten, particularly at elevated temperatures. A tightly wound helix approaches the radiating area of an equivalent cylinder by proper choice of the wire size, mandrel diameter, and pitch. The heater design used in the low mass ionizers has close to the maximum possible ratio of radiating area to coil diameter.

The emittance of the heater coil was increased over that of the bare wire by electrodeposition of a ceramic coating on the tungsten-rhenium wire. In particular, ceramic coatings such as thoria and magnesia have emittances approximately two times higher than that of bare tungsten at the typical operating temperatures in this heater. However, these materials have some properties less desirable than alumina. For example, in the case of magnesia the vapor pressure is relatively high so that the operating temperature in vacuum is limited to the neighborhood of 1600°C. Because of such considerations, the method devised was to electrodeposit alumina on the wire and then dope the alumina coating with chromium oxide so as to provide a surface having an emittance approaching twice that of the undoped alumina-coated heater coil. This is a relatively new technique for increasing the emittance of a surface.* Tests showed that this technique was effective in improving the heat transfer.

* In exploring the possibility of a patent disclosure covering this development, a literature search disclosed reports of work done by Mullard in England on similar coatings (British Patent 871, 375) covering the use of chromium doped heater coatings.

In addition to requiring a maximum heat transfer between the heater coil and ionizer body, cyclic operation demands high reliability of the heater subassembly. The prime failure mode exposed was parallel leakage resistance paths between the heater coil and the ionizer body. In this case a significant portion of the heater current was shunted through the parallel resistance so as to cause excess heating of the ceramic coating and consequent dielectric breakdown. To avoid this failure mode a leakage resistance of greater than $10^5 \Omega$ at operating temperature was required. This was achieved by placing a cylindrical ceramic spacer between the coated heater coil and the ionizer body. This ceramic spacer was high alumina. The mass of this ceramic cylinder had to be minimized because the specific heat of alumina is appreciably greater than that of tungsten and, therefore, would have been detrimental to the requirement of rapid warmup of the ionizer assembly. The simple means chosen for minimizing the mass of the ceramic insulator tube was to cut slots in the cylinder and thus decrease the volume of the ceramic by approximately 50%. Such heater assemblies were constructed and work quite effectively. A photograph of two such heaters is shown in Fig. III-8.

1. Heater Coating Tests

An attempt was made to determine the change in thermal emittance brought about by chromium oxide doping of alumina heater coatings. The coatings are easily prepared; the simplest method consisting of painting a water solution of the red chrome trioxide on to the previously sintered alumina heater coating. Firing in wet hydrogen at $1500-1600^\circ\text{C}$ will set the coating and produce a dark red color. Another method uses the green sesquioxide in the insulation solution. The doping agent is thus introduced during the cataphoretic application of the insulation coating. One firing is sufficient in this method but the firing is more critical since several competing processes are taking place.

M4530

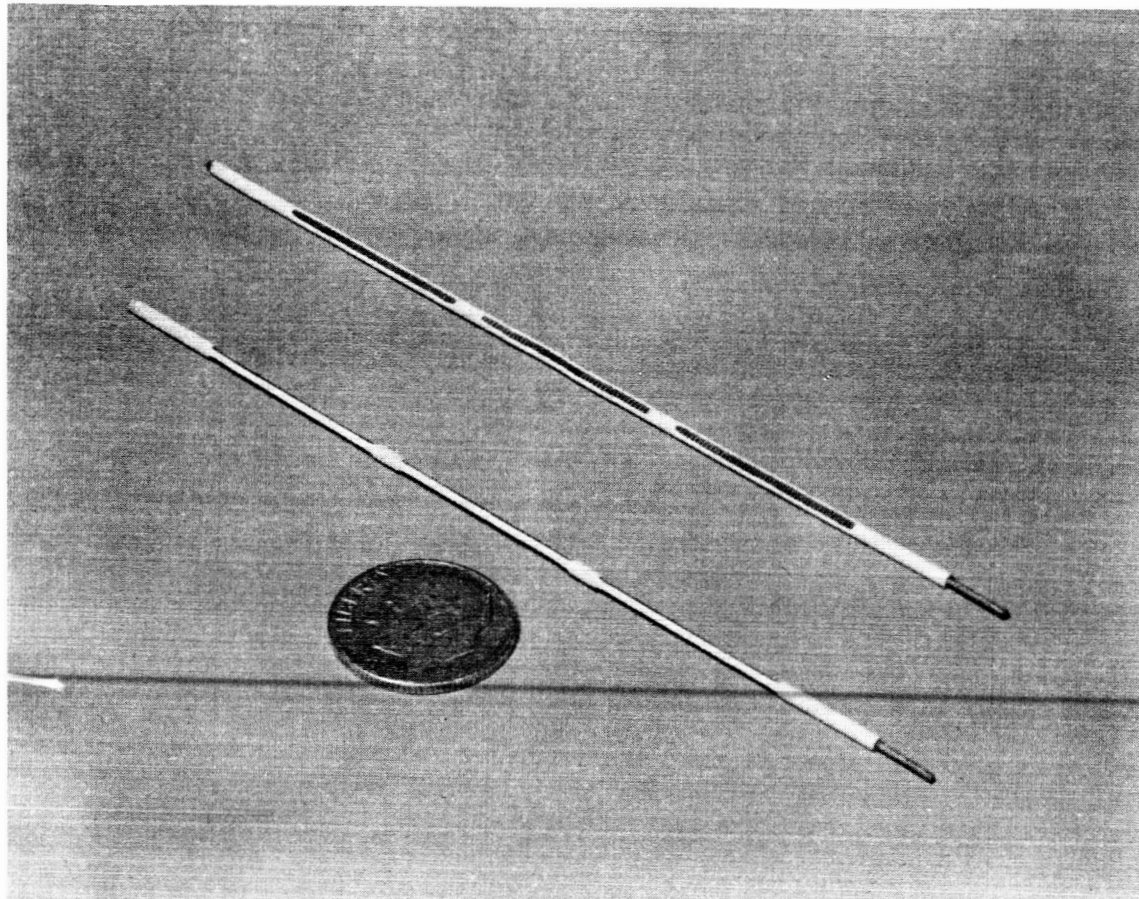


Fig. III-8. Photograph of two low-mass ionizer heaters.

Cataphoretic coating method:

Solution:

200 ml	commercial coating solution
50 g	Cr_2O_3
5 g	$\text{Al}(\text{NO}_3)_3 + 9 \text{H}_2\text{O}$
2 g	$\text{Mg}(\text{NO}_3)_2 + 6 \text{H}_2\text{O}$

Equal parts deionized water and alcohol to make
400 ml of solution.

Process:

Coat heater at 45 V dc for 5 to 6 sec to give about
0.003 in. thick coating. Fire in wet hydrogen at
1600-1700°C.

Filaments were prepared, consisting of six inches of 0.010 in. tungsten wire coated with a 0.005 in. thickness of fired-on alumina. Operating data were taken of voltage, current, and brightness temperature. The straight filament was then coated, while in place, with a water suspension of red CrO_3 . When heated in the vacuum, the chromium trioxide reduced to Cr_2O_3 , which is green. The green oxide gradually diffused into the alumina, producing a light pink. The temperature distribution along the wire was very nonuniform, due both to the uneven application of the oxide and to the amount of diffusion into the alumina. The green oxide was very effective in increasing the thermal emittance, the power radiated being twice the power radiated by the white coating before treating. The reduced wire temperature is evidenced by the resistance versus power characteristics as shown in Fig. III-9. Pyrometer readings of the green coating were approximately 50°C higher in brightness value than for the white coating. The difference would be 70°C for a change of thermal emittance from 0.15 to 0.3 at 1400°C true temperature. The experiment was not refined any further due to the difficulty in producing a uniform coating. From the results, it was concluded that the highest emittance was obtained with the partially reacted green chromium oxide, with lower values ranging on down from dark red through the pinks to pure white.

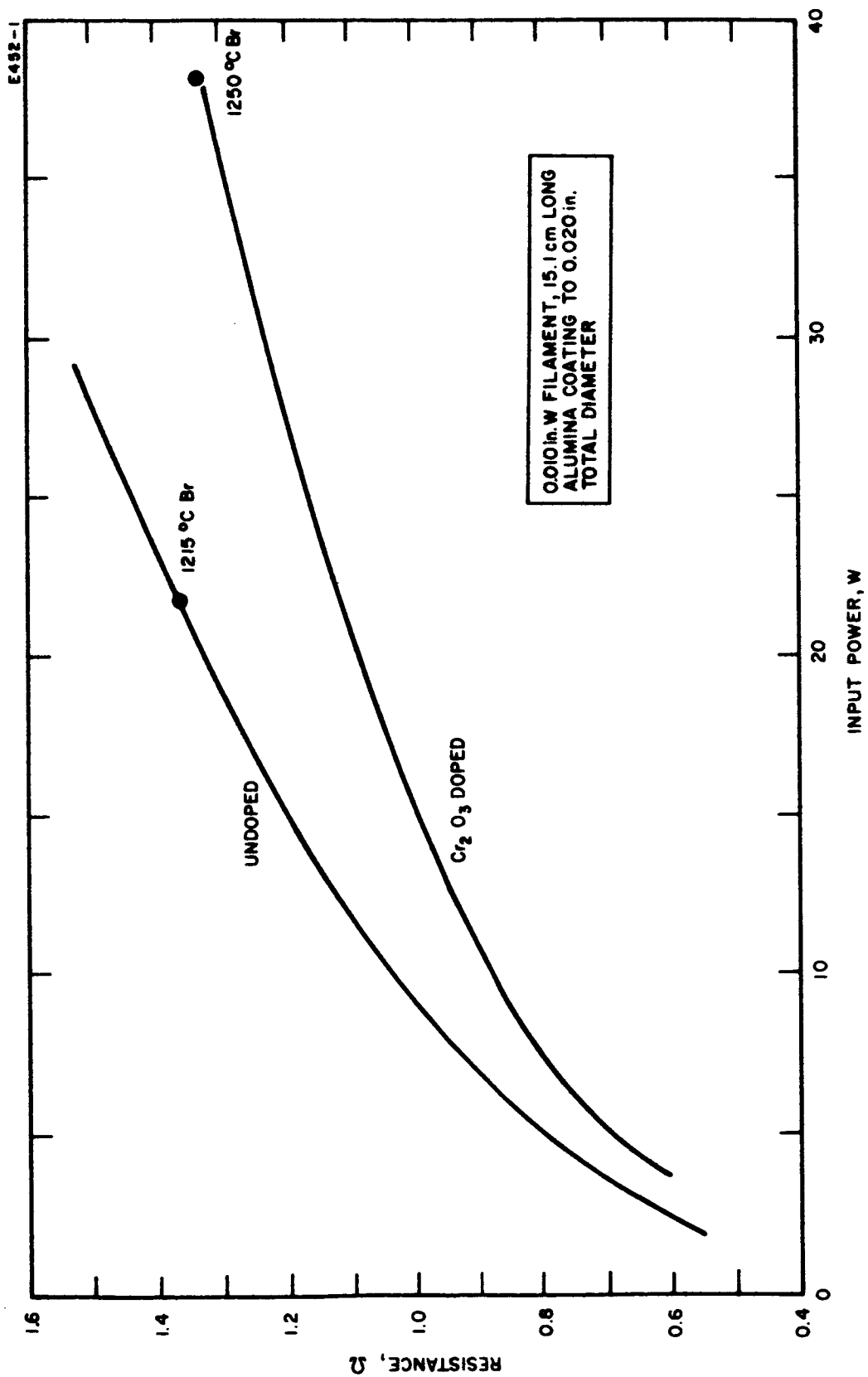


Fig. III-9. Heater resistance versus input power for doped and undoped alumina-coated tungsten filament.

2. Heater Lead Connections

A very useful method of joining tungsten parts was developed which has the advantage of extreme stability at high operating temperatures. The method was developed to make connections to high temperature heaters of tungsten wire and for joining tungsten parts.

The solution to the problem of connecting leads to coiled tungsten heaters was to insert a tightly fitting tungsten wire inside the heater coil. Fine tungsten powder was applied as a filler material between the heater coil turns and connecting lead. Sintering the filler material produced a stable joint with excellent electrical conductivity. Various braze materials had been used previously to improve the electrical conductivity between the coil and connection wire, but the joints were unsatisfactory due to the problems brought on by the high operating temperature. Evaporation and migration of the braze material were the major undesirable effects.

Metallographic studies were made to determine the quality of the sintered bond. Figure III-10 is a section (100x) through the axis of a connection wire showing the filler between the turns of a helix. The sample used M-55 tungsten powder as the filler material, applied with amyl acetate as the vehicle. M-55 is a pure tungsten powder supplied by Sylvania Electric Co., Towanda, Penna. It is coarse, cubical in structure, with particle size around 3 to 3.5 μ . Sintering was accomplished by heating to approximately 2000°C in a vacuum ($<10^{-4}$ Torr) for 10 sec. An analysis of the joint showed the following features:

Coil to connection wire bond:

When viewed under high magnification, approximately 20% of the turns had a good bond to the lead. The cross sectional area of a good joint on a turn was approximately 0.003 in. wide times the circumference, requiring one good turn to provide a cross sectional joint area equal to the cross sectional area of the heater wire. Thus, two or three turns with good joints were sufficient to provide a good current path.

M4554

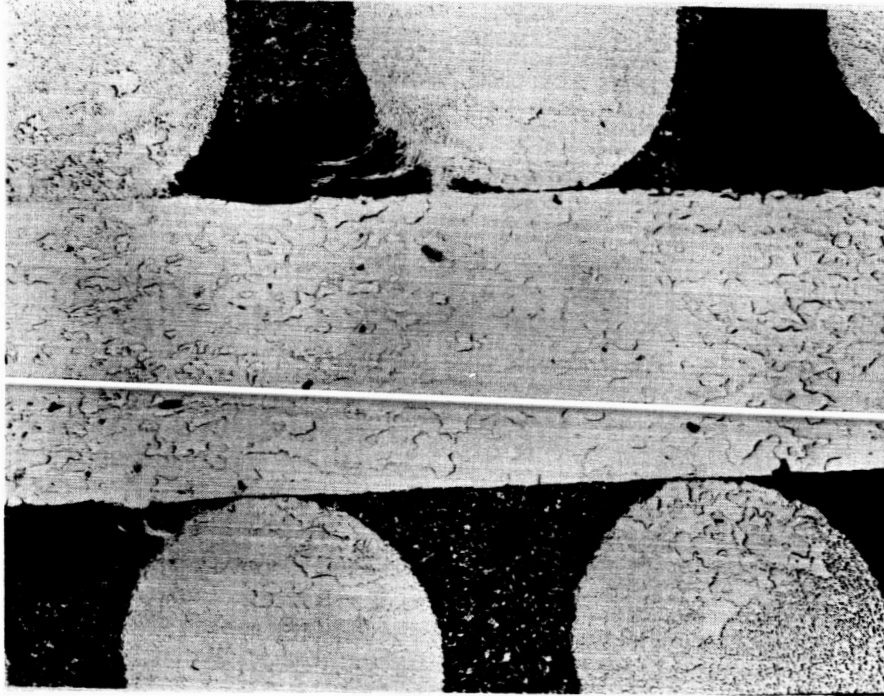


Fig. III-10. Photomicrograph (100x) showing the structure of the filler material in a sintered heater lead connection.

Heater lead to filler bond and coil to filler bond:

In both cases, the bond was very good with no evidence of separation or non-adherence. The polished detail was good and an estimation was made of the density by means of reflectometer readings on the filler material and on the solid tungsten. The ratio of the reading from the filler material to the reading from the solid tungsten was consistently 44 %.

In general, the joint was very good mechanically, in both appearance and performance. This type of joint was used on all heaters after the second month of the program, with no evidence of any deterioration of the joint during operation. Electrically, the resistance of the joint was much lower than the resistance of the coil because of the shunting effect of the center lead and the filler material. An analysis was made using 44% of the conductivity of tungsten for the filler material and assuming the filling to be complete to the outer diameter of the coil. The cross-sectional resistance of the joint was calculated to be 11% of the resistance of the heater wire. Good joints were made also with both porous and solid machined tungsten parts using several different grades and types of fine tungsten powder. By observing good practices in clearances and the application of pressure during sintering, very good mechanical and thermal joints were made in the 1500-2000°C sintering range.

3. Heater Summary

During the various thruster tests three different heater designs were employed. Their characteristic features are tabulated in Table III-1.

Based on test results obtained during this program, all three designs were satisfactory for their intended purpose. The Model F-2 was judged the most desirable for operation where excessive temperatures are expected since it has the largest safety factor in its design.

TABLE III-1

LINEAR-STRIP IONIZER HEATERS

Heater Model	Wire		Coil		Coating	Ceramic Tubing
	Material	Diam.	Diam.	tpi		
D-8	W	0.018 in.	0.055 in.	44	0.003 in. Al_2O_3 , Cr_2O_3 doped	None
F-1	97W-3Re	0.010 in.	0.033 in.	55	0.002 in. Al_2O_3 , Cr_2O_3 doped	0.036 I.D. x 0.060 O.D. alumina-slotted
F-2	97W-3Re	0.012 in.	0.043 in.	50	0.003 in. Al_2O_3 , Cr_2O_3 doped	0.050 I.D. x 0.073 O.D. alumina-slotted

IV. THRUSTOR DESIGN VERIFICATION

Prior to commencement of any steady-state life tests or long-duration thermal cyclic tests, three model LB thrusters (8 cm long ionizer) were fabricated and subjected to both thermal and electrical tests to verify the over-all thruster design. All three thrusters were subjected to a series of thermal tests to determine steady-state, transient, and cyclic characteristics. Because of excellent electrical performance, meeting all objectives during a 16 hour test, only thruster LB-1 was performance tested with cesium.

At about the midpoint in the program, a contract amendment re-directed some effort to investigate a thruster scaled down to an ionizer length of 5 cm. This thruster design, designated Model LC was initiated because of potential requirements of a 0.3 mlbf thrust device for control of a synchronous satellite. Three such LC thrusters were evaluated both thermally and electrically. An additional contract amendment near the end of the contract period, called for an improved 0.3 mlbf thruster which was designed and fabricated in order to decrease the thruster power requirements. This thruster was designated Model LD and used an ionizer 4.6 cm long.

A. Thermal Tests

Low-mass ionizer designs E and F were compared in their thermal characteristics during tests of the first three LB thrusters. Both LB-1 and LB-2 utilized LMI-F ionizers whereas thruster LB-3 utilized an LMI-E. All ionizers were manufactured from Philips Metalonics, Mod-E porous tungsten, 75% density. Heater design D-8 was used in thrusters LB-1 and LB-3 while the F-1 heater was utilized in the thermal tests of LB-2.

For steady-state thermal performance the principal objective was to maintain an accel electrode temperature less than 300°C for an ionizer temperature of 1200°C and also have the focus electrode temperature be 500°C or less. The reason for these requirements was to minimize any thermionic electron emission from the accel electrode to the positive high voltage electrode and also to reduce surface ionization of stray neutral cesium on the focus electrode to a negligible level. These steady-state thermal objectives were attained as is shown by the data presented in Fig. IV-1 for thruster LB-2. Notice that a steady state accel temperature of 212°C was measured with the ionizer operating at 1160°C . This low accel temperature is highly favorable for long-term stable operation of a cesium-contact ion thruster. Focus electrode ionization was no problem in any cesium tests because the electrode temperature was so low (400°C) that the ratio of ions originating at the focus electrode to charge exchange ions was on the order of 10^{-6} .

Equilibrium temperatures during thermal cycling of the ionizer were determined on thruster LB-3. The temperature-time profiles are shown in Fig. IV-2 for the ionizer when heated to 1130°C in 20 sec and held at temperature for 5 to 10 sec followed by a 3 min cool period. Of course, variations about these equilibrium temperatures for the accel and focus electrodes result from changes in the ionizer operating temperature or variations in its duty cycle.

Warmup characteristics were measured on all three thrusters for the case of constant input power. The family of characteristic curves for the LMI-F ionizers is presented in Fig. IV-3. These data show that the LMI-F (8 cm version) was heated to 1100°C with a warmup energy of 0.75 W-hr in a time of about 17 sec. However, this required a fairly high input power of 160 W to the ionizer heater to achieve this result.

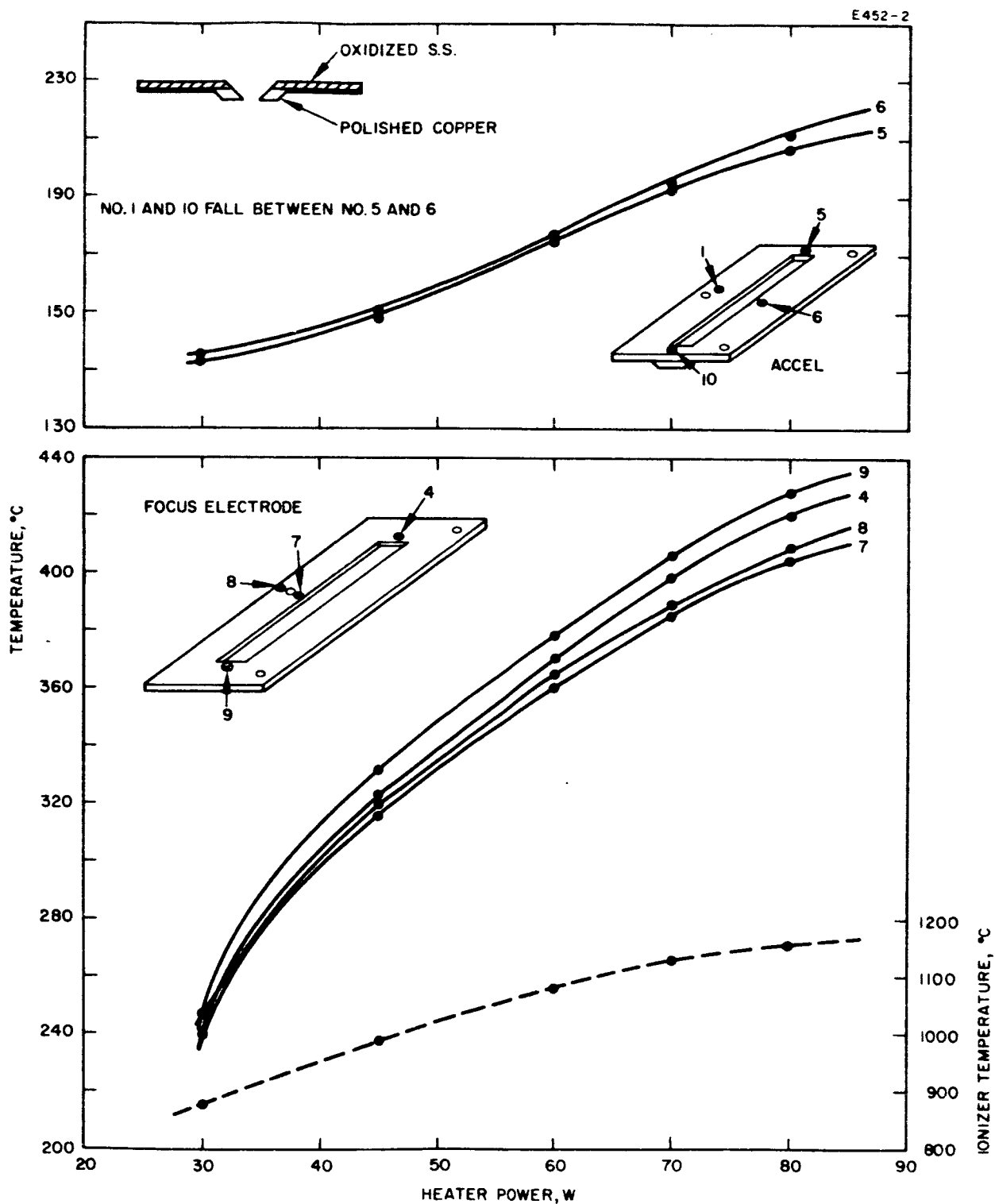


Fig. IV-1. Steady-state thermal characteristics of the LB thrutor.

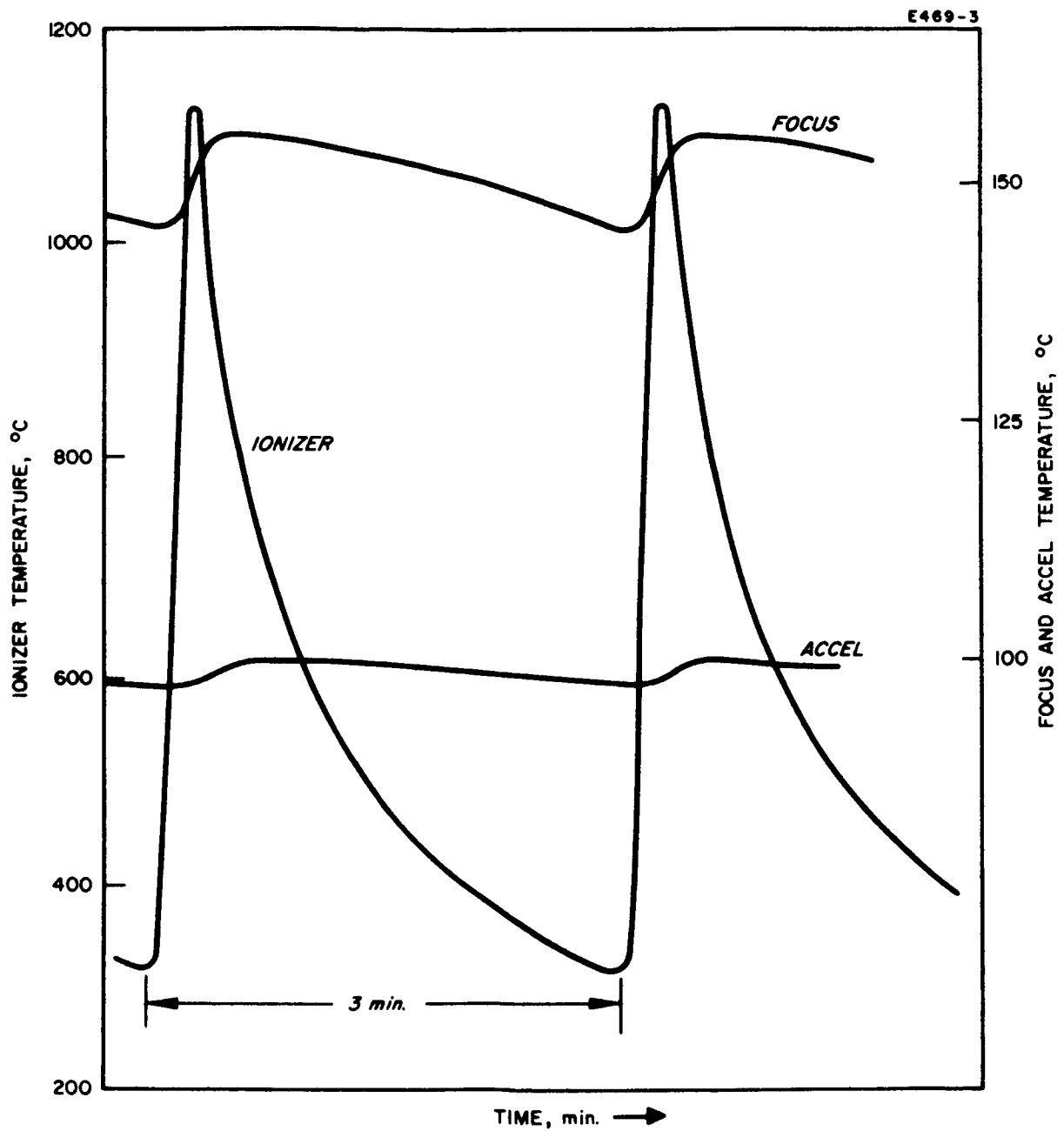


Fig. IV-2. Equilibrium temperatures measured during repeated thermal cycling of the LB thruster.

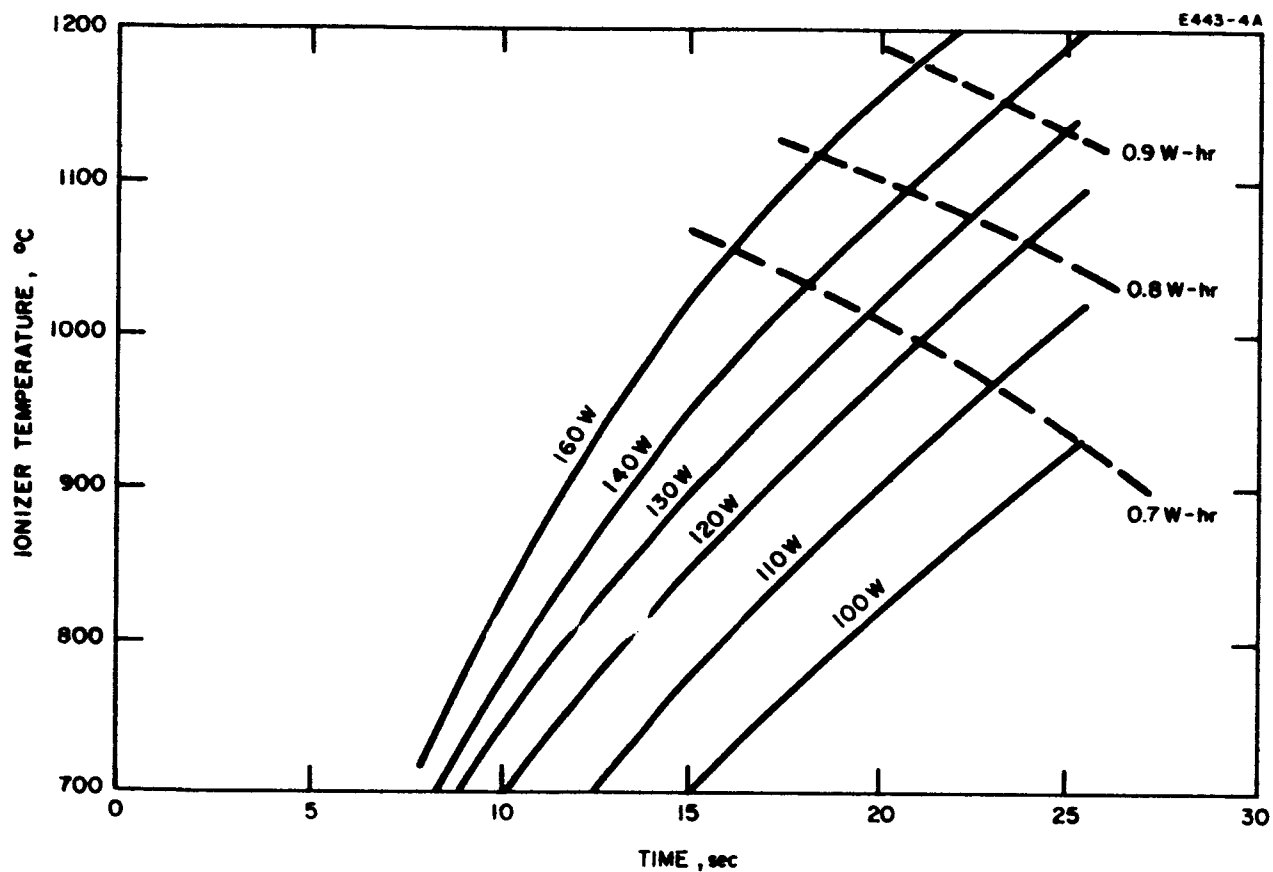


Fig. IV-3. Heatup characteristics for the LB thruster with an 8 cm long Model F low-mass ionizer.

Since the LMI-E is a lower mass ionizer than the LMI-F, it is of interest to compare the results obtained with thruster LB-3. The ionizer warmup characteristics for this thruster, using an LMI-E are presented in Fig. IV-4. Notice that the LMI-E ionizer was heated to 1100°C in a time of 14 sec with a warmup energy of only 0.63 W-hr for the same power level of 160 W as shown in Fig. IV-3 for the LMI-F. Now, however, it is feasible to consider lower input powers to the LMI-E ionizer and still attain the 1100°C operating temperature within a time of 20 sec. Figure IV-4 shows that this was achieved at an input power of about 120 W with little increase in the warmup energy.

Carrying this line of experimentation further to the 5 cm long ionizer, the results obtained are shown in Fig. IV-5. Notice that an energy requirement of only 0.44 W-hr was required to heat this ionizer to 1100°C in a time of approximately 11 sec for a constant input power of 140 W. Conversely, for a 20 sec warmup time, the ionizer was heated to its operating temperature with an input power of only 80 W and the warmup energy increased only slightly to about 0.47 W-hr. The data presented in Figs, IV-3, IV-4, and IV-5 demonstrate a significant advance in the state of the art with regard to heating ion thrusters from ambient to temperatures on the order of 1100°C .

B. Electrical Tests

The first electrical test during the Contract was completed successfully on thruster LB-1. As mentioned previously, the ionizer was fabricated from Philips Mod E, 75% dense porous tungsten. The thruster was subjected to 33 hours of total test time with a cesium beam. Of this test period 20 hours was logged at an ionizer current density of 7 mA/cm^2 , including a 16 hour continuous run to determine the short-term stability of the thruster design. During this 16 hour period, the electronic accel drain current, due to the presence of cesium, averaged 0.7%. Drain currents were stable during this time.

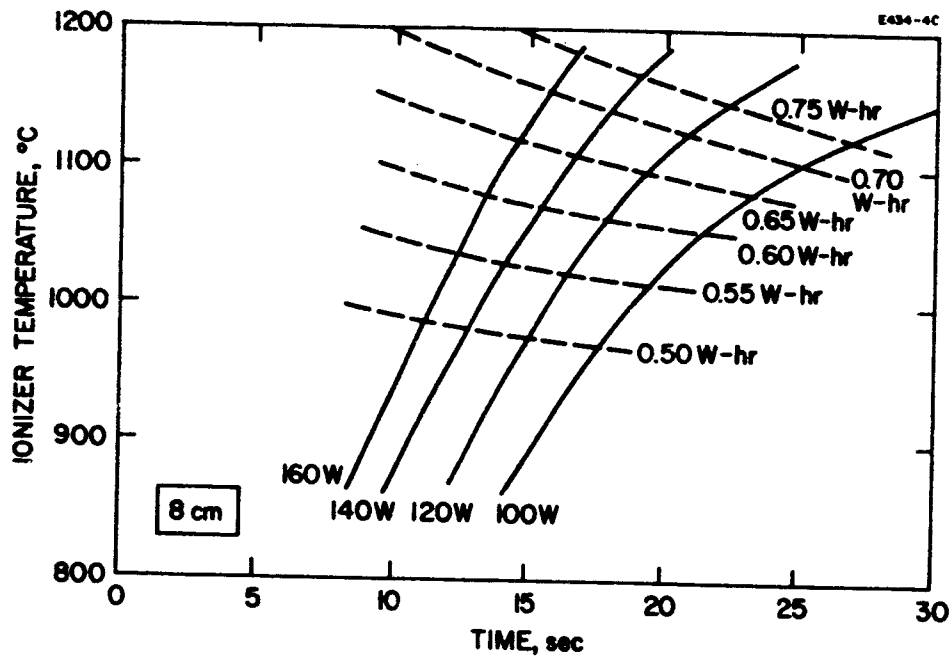


Fig. IV-4. Heatup characteristics for the LB thruster with an 8 cm long Model E low-mass ionizer.

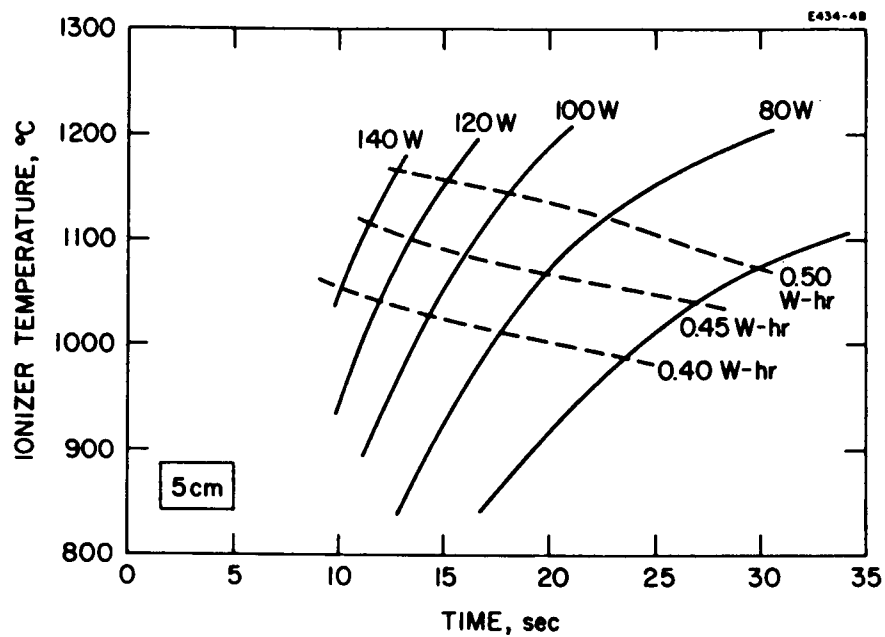


Fig. IV-5. Heatup characteristics for the LC thruster with an 5 cm long Model E low-mass ionizer.

The time history of several thruster parameters during the continuous test period is presented in Fig. IV-6. Because of a decrease in emittance, due to deposition of sputtered copper from the collector, the accel electrode temperature increased from 287°C to 357°C at the end of the 16 hour period. (The ionizer was operated 150°C hotter than clean tungsten because of oxygen on the surface.) The somewhat higher accel currents during the latter portion of this test may have been due to increasing thermionic electron emission as the accel temperature rose.

Maximum accel to ionizer voltage that could be sustained in the presence of cesium was 8.4 kV. The arc frequency reduced to one every 6 hours in the last 14 hours of the 16 hour continuous test. Specific impulse was varied between 4500 and 9000 sec.

The nominal design perveance of the accelerator structure was $70 \times 10^{-9} \text{ A/V}^{3/2}$. The current-voltage characteristics as shown in Fig. IV-7 demonstrate that this design perveance was verified experimentally.

Prior to electrical tests the ionizer was subjected to an oxygen treatment in the hope of removing any carbon contaminants. As a result of this prolonged treatment at 1600°C in vacuum with a partial pressure of oxygen, the ionizer was oxidized. This was evidenced by an electron function of 5.3 eV, which is considerably above the value for clean tungsten (4.54 eV). Attempts to remove this oxygen layer by operation of the ionizer above 1300°C and with a small flow rate of cesium proved to be rather unfruitful; consequently, the electrical tests of the thruster required a higher than normal ionizer temperature. In this sense the design verification tests on this thruster were more severe than expected to be encountered. Subsequent experience showed that wet hydrogen firing was the most effective method of minimizing carbon impurities.

Typical critical temperature data observed during the testing are presented in Fig. IV-8. The sequence of order of data measured is indicated by the circled numbers. Notice that in the case of the first two critical temperature measurements, curves 1 and 2, the J_i versus

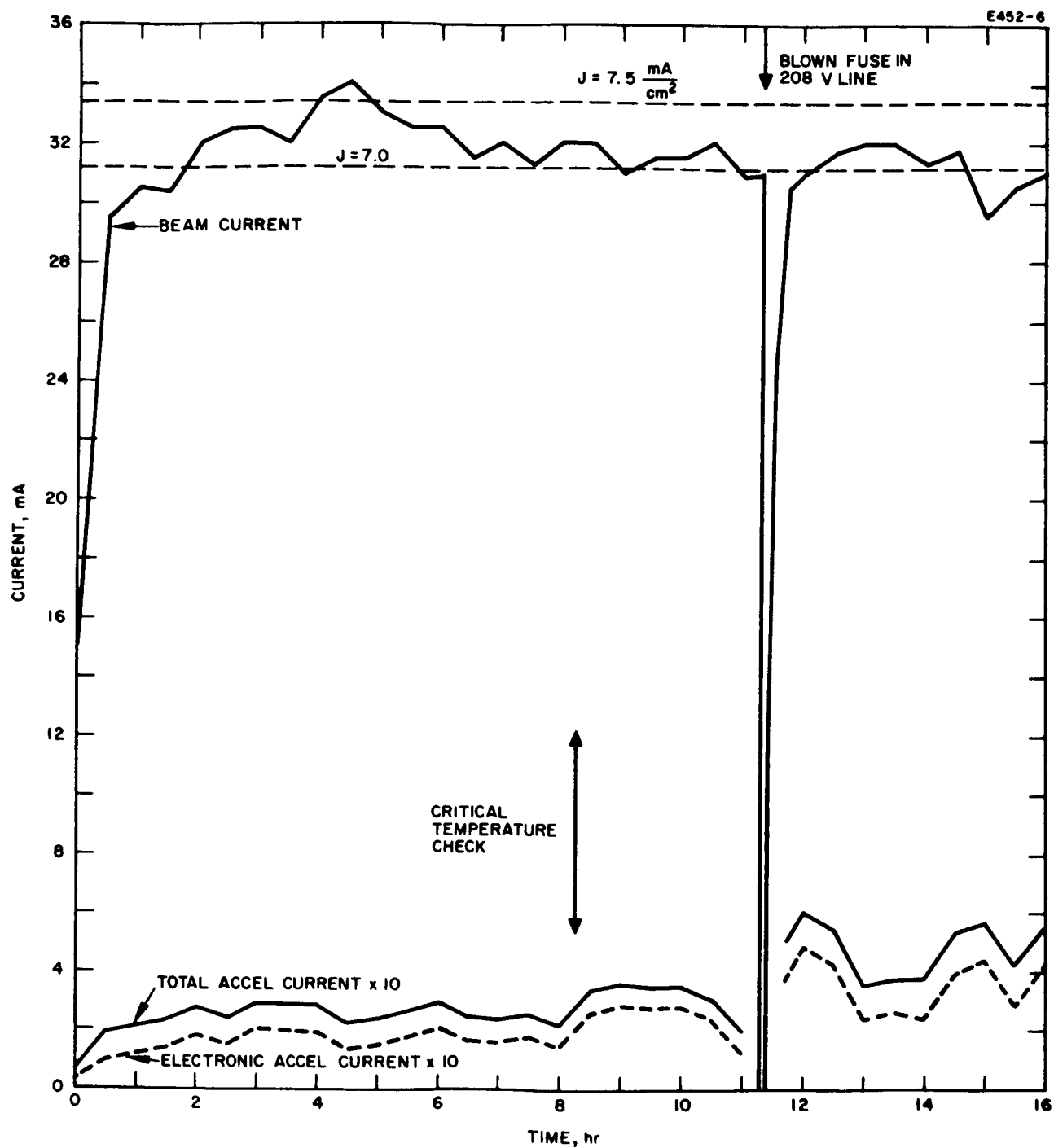


Fig. IV-6. Time profile of beam and accel currents during 16 hour period of design verification.

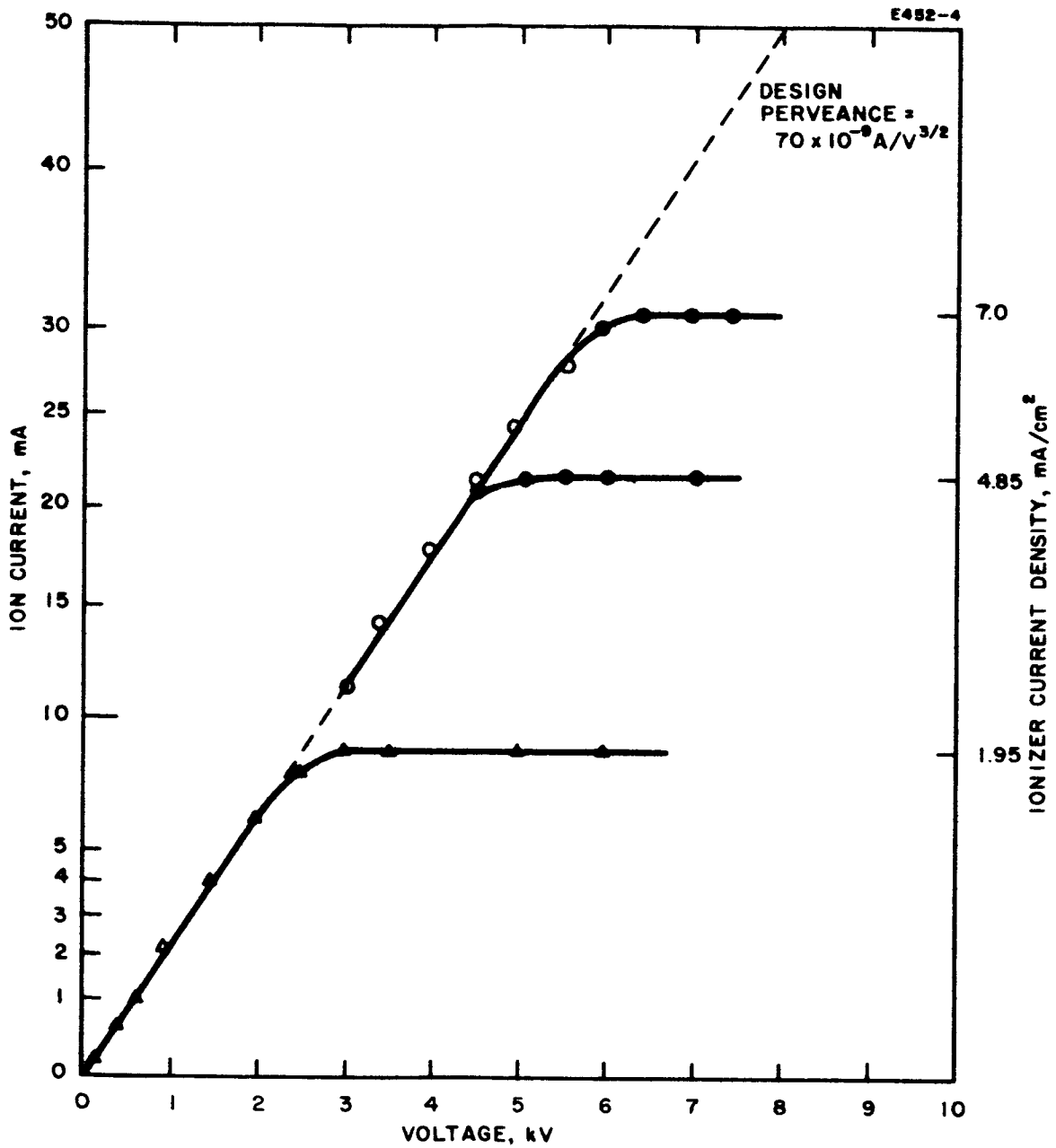


Fig. IV-7. Current-voltage characteristics measured on thruster LB-1.

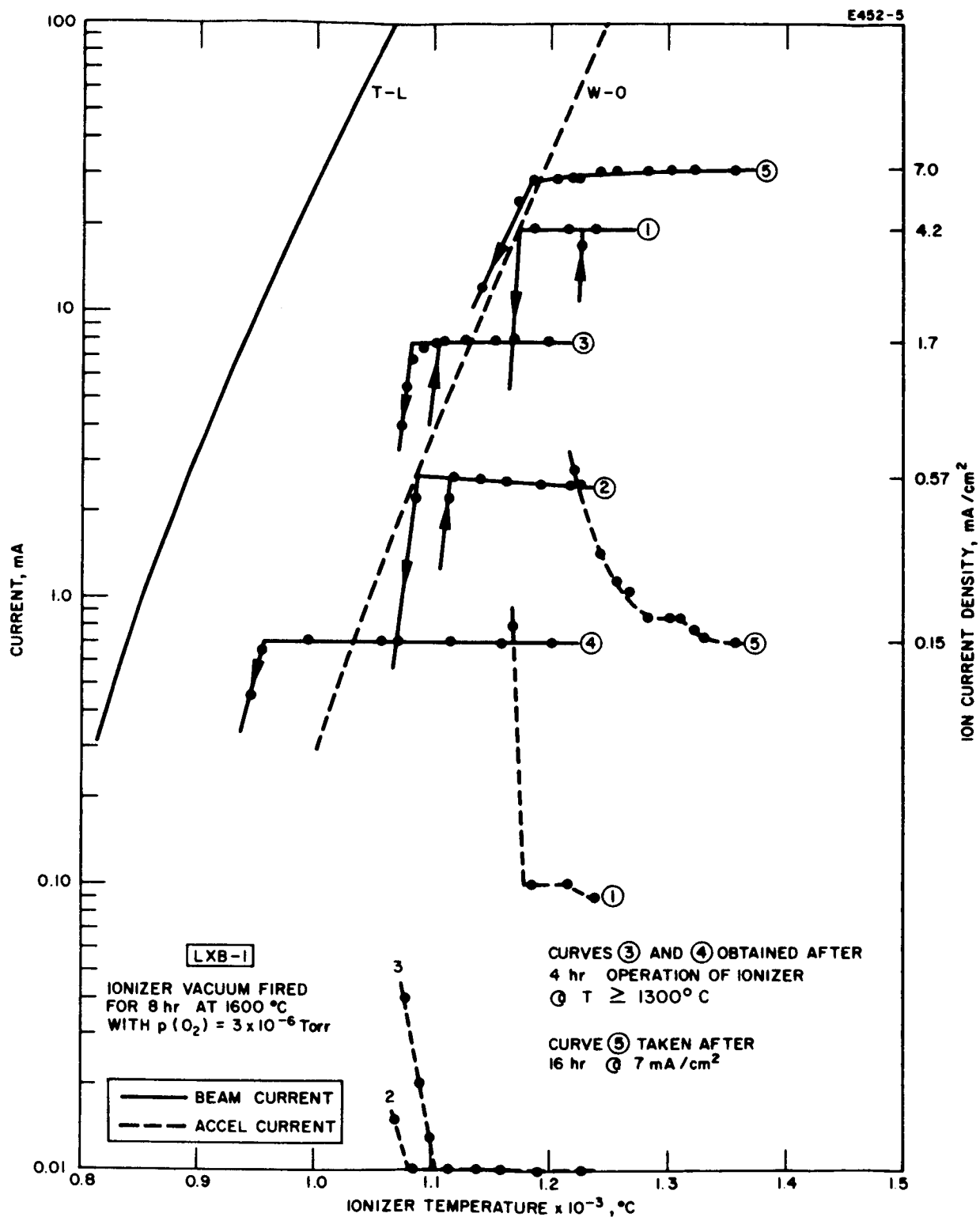


Fig. IV-8. Ion emission and accel current characteristics as a function of ionizer temperature for thruster LB-1.

T_i characteristic is quite sharp and a hysteresis is observed which is definite evidence of the presence of oxygen on the emitting surface. Curves 3 and 4 obtained after 4 hours of operation at temperatures above 1300°C show some indication of a clean-up in the sense that the critical temperature has now moved to the left of the oxygenated tungsten curve. However, hysteresis is still present, although to a lesser degree, and hence the oxygen has not been removed completely. The corresponding accel electrode currents are plotted for curves 1, 2, and 3. Since in this operating condition the accel current is a very sensitive indicator of neutral flux, these curves would correspond closely to the variation of neutral efflux with ionizer temperature. Notice that in all three cases, the accel current remains constant until the critical temperature for ionization is reached and then the accel current together with the ion current exhibit sharp discontinuities. This behavior is clear evidence of the absence of any significant effect due to carburization. Curve 5 of this figure represents a critical temperature curve measured at the end of the 16-hour continuous test.

As a result of a Contract amendment effective at approximately the midpoint of the original contract period, several of the scheduled 8 cm thrusters were replaced with scaled down units having ionizers 5 cm long. This thruster design, designated the LC series, had as its primary objective general performance mapping including 1000 thermal cycles and a 24 hour continuous test with cesium.

Following the thermal evaluation, which included 1636 temperature cycles, thruster LC-1 was tested with cesium for a period of 36 hours at an average ionizer current density of 7 mA/cm^2 . The thruster used on LMI-E ionizer manufactured from Philips, Mod E porous tungsten. During this period the ionizer cleaned up so that a low critical temperature of approximately 1020°C was observed at the above current density. This is shown in the curves of Fig. IV-9. Also presented in this graph is the critical temperature obtained during an earlier test on

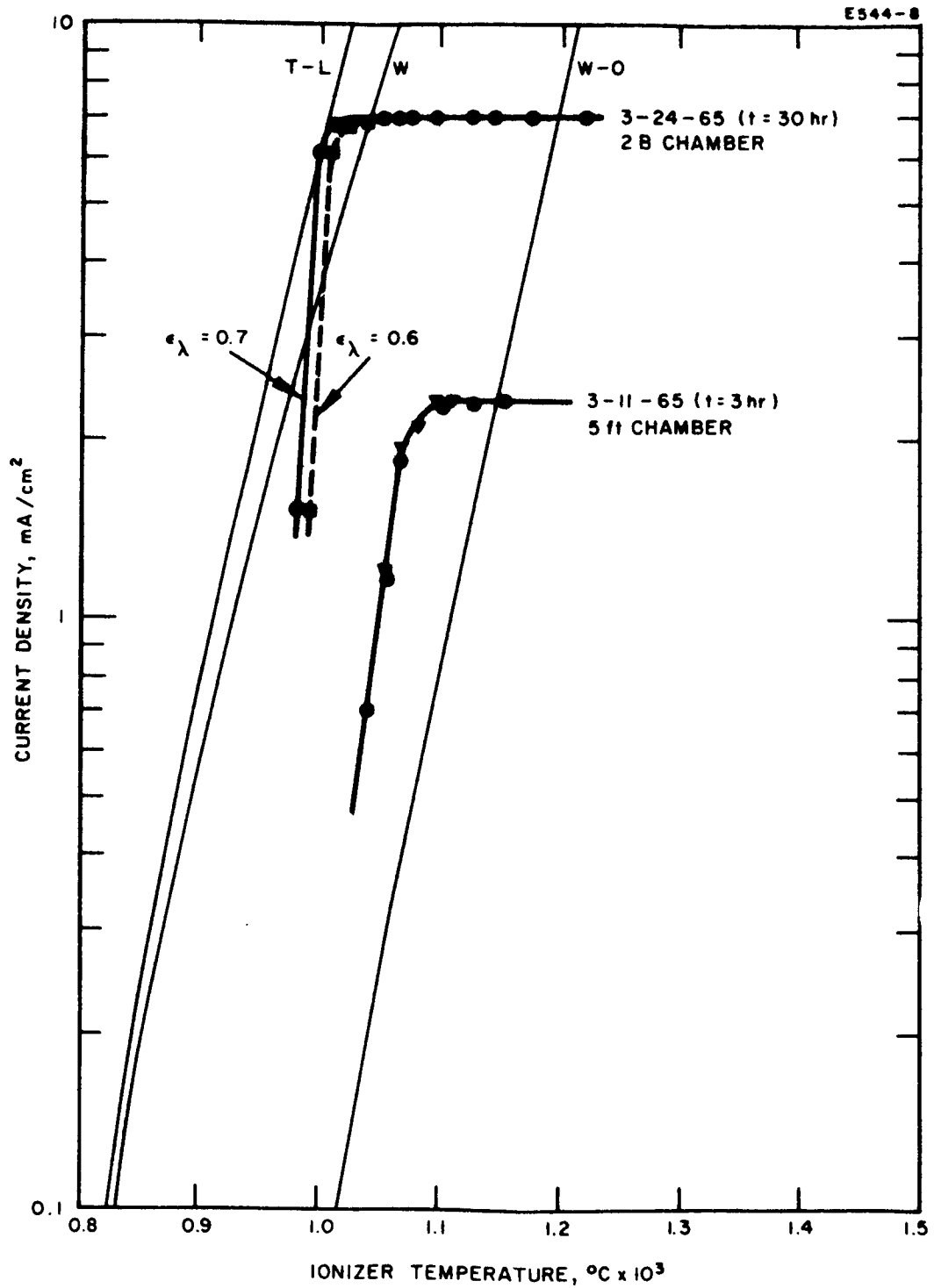


Fig. IV-9. Ionizer current density versus temperature for thruster LC-1.

the same thruster when it was mounted in the 5 ft by 15 ft vacuum chamber. Evidence of partial cleanup was present, even during the early testing of this thruster. During assembly the ionizer was fired in wet hydrogen for two hours at 1150°C followed by a one hour dry hydrogen firing at the same temperature.

Perveance characteristics as measured on this thruster are presented in Fig. IV-10. Notice that there is a very gradual roll-over from flow-limited to space-charge limited operation with the transition region covering a 2.5 kV span. Similar perveance characteristics for thrusters using LMI-F ionizers exhibited a sharper transition ($\Delta V = 0.5$ to 1.0 kV) from flow-limited to space-charge-limited operation. Consequently, the larger transition region of the LMI-E perveance characteristic was taken to be evidence of less effective distribution of cesium vapor to the front ion emitting surface of the ionizer. Since such an effect requires higher operating voltage to produce an ion current equivalent to that obtained from LMI-F, all subsequent thrusters that were subjected to electrical performance or life tests utilized the LMI-F ionizer design.

The power-to-thrust characteristic, as measured on thruster LC-1, is presented in Fig. IV-11. Even with the low critical temperature of the ionizer it was not possible to reduce the power-to-thrust ratio to below 247 W/mlbf at the indicated current density. Primarily, this was because conduction losses from the ionizer did not scale linearly with ionizer length and thus contributed more to the ionizer power requirement in the shorter LC series thrusters.

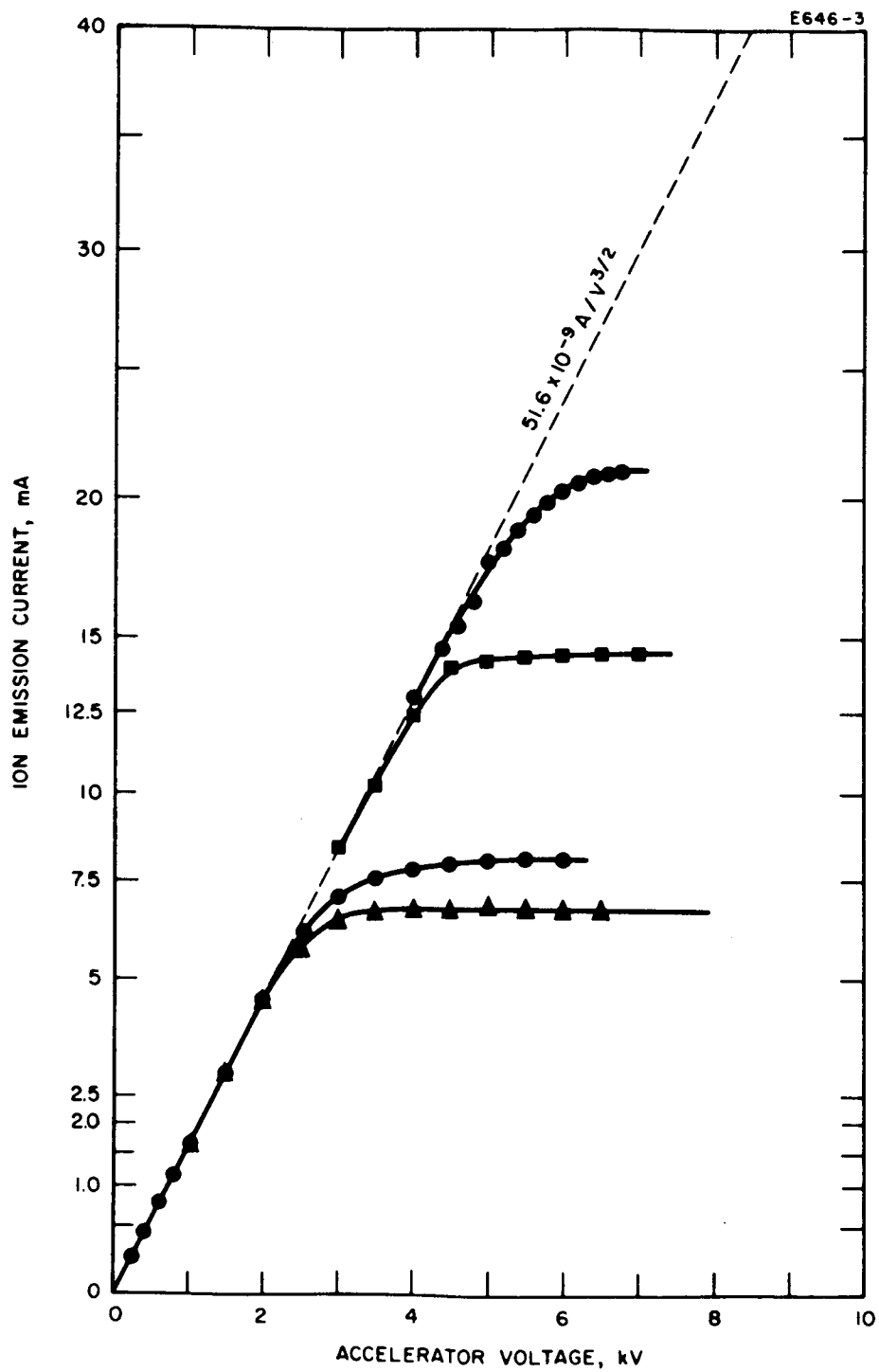


Fig. IV-10. Current-voltage characteristics for thruster LC-1.

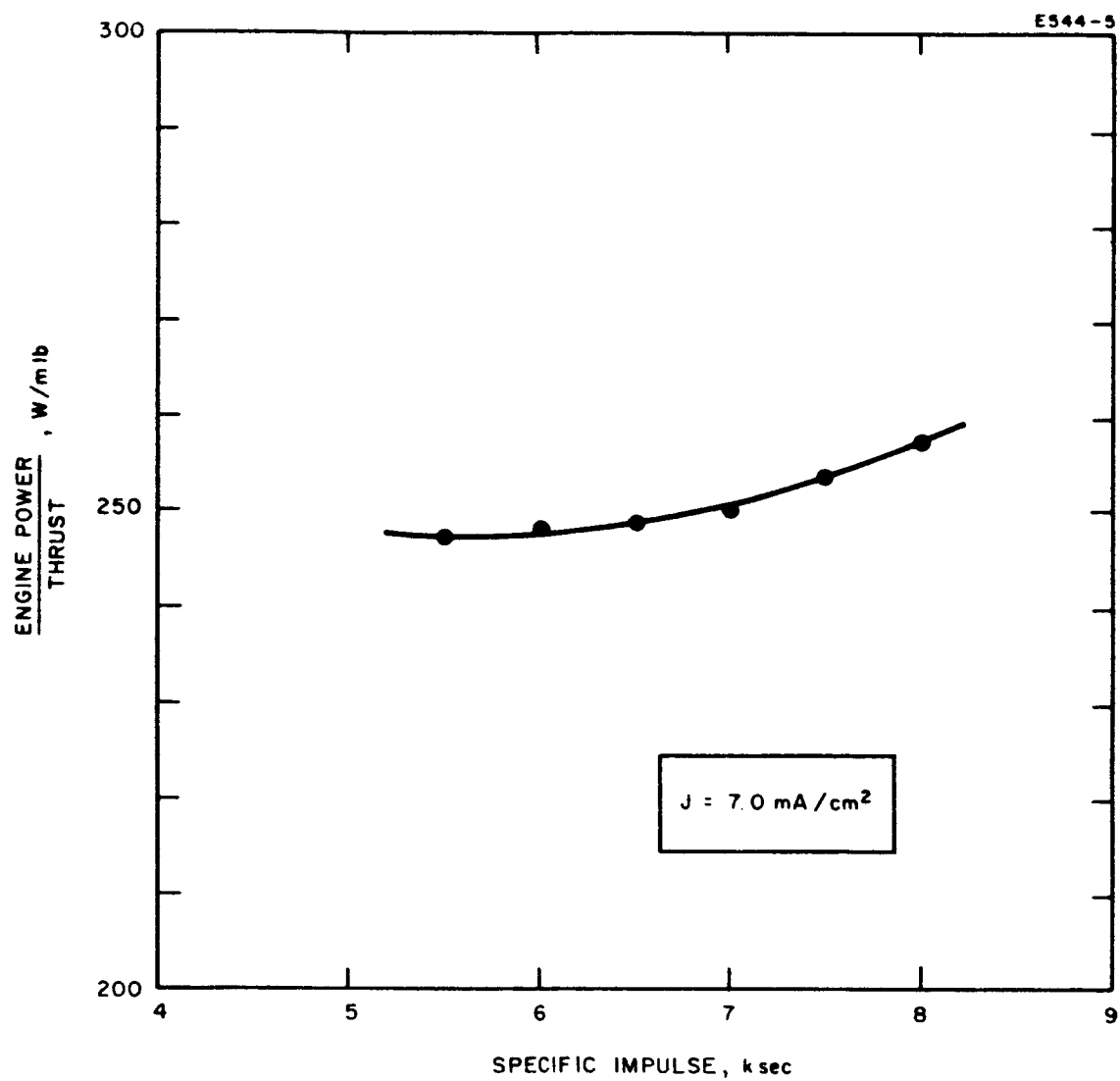


Fig. IV-11. Power-to-thrust characteristics of thruster LC-1.

V. LONG-DURATION CYCLIC THERMAL TESTS

To demonstrate that ion rockets can be cycled many tens of thousands of times without deterioration in their thermal or mechanical characteristics, four linear-strip LB thrusters were subjected to long-duration cyclic tests. A fifth thruster was fabricated and assembled but never tested because all test objectives had been met and exceeded. Test objectives were two thrusters to 10,000 cycles and three thrusters to 50,000 thermal cycles. Warmup time was required to be 20 sec with a warmup energy of 0.75 W-hr or less.

For convenience, the thrusters were mounted into stems and sealed into evacuated glass bottles (see Fig. V-1). Vacuum was maintained by means of attached ion pumps. The bulk of the gas was removed prior to the life test by baking and degassing while attached to an exhaust system. Cyclic operation was checked at this time and the tubes then sealed off as shown in Fig. V-1.

The tests were run using power supplies from the SERT-I program with additional timing and counting circuits provided to operate two engines alternately. The cyclic mode for all tests consisted of a warmup phase for 20 sec, a 5 sec simulated thrust period during which the ionizer temperature was regulated to a preset value between 1100 and 1200°C, followed by a 3 min cool period after which the cycle was repeated.

A schematic diagram of the cyclic life test circuit is shown in Fig. V-2. The power supply was a solid state inverter circuit operating on 34 V dc supplied by storage batteries. The batteries were maintained by a battery charger supplying 2.6 A continuously. The output of the power supply was a 42 V peak-to-peak square wave with a frequency of 2 kc (see Fig. V-3a). Control was by means of pulse width modulation so that when the heater reached the desired resistance as it warmed up the pulse width was reduced to maintain heater resistance (see Fig. V-3b). If the load resistance remained within the proper

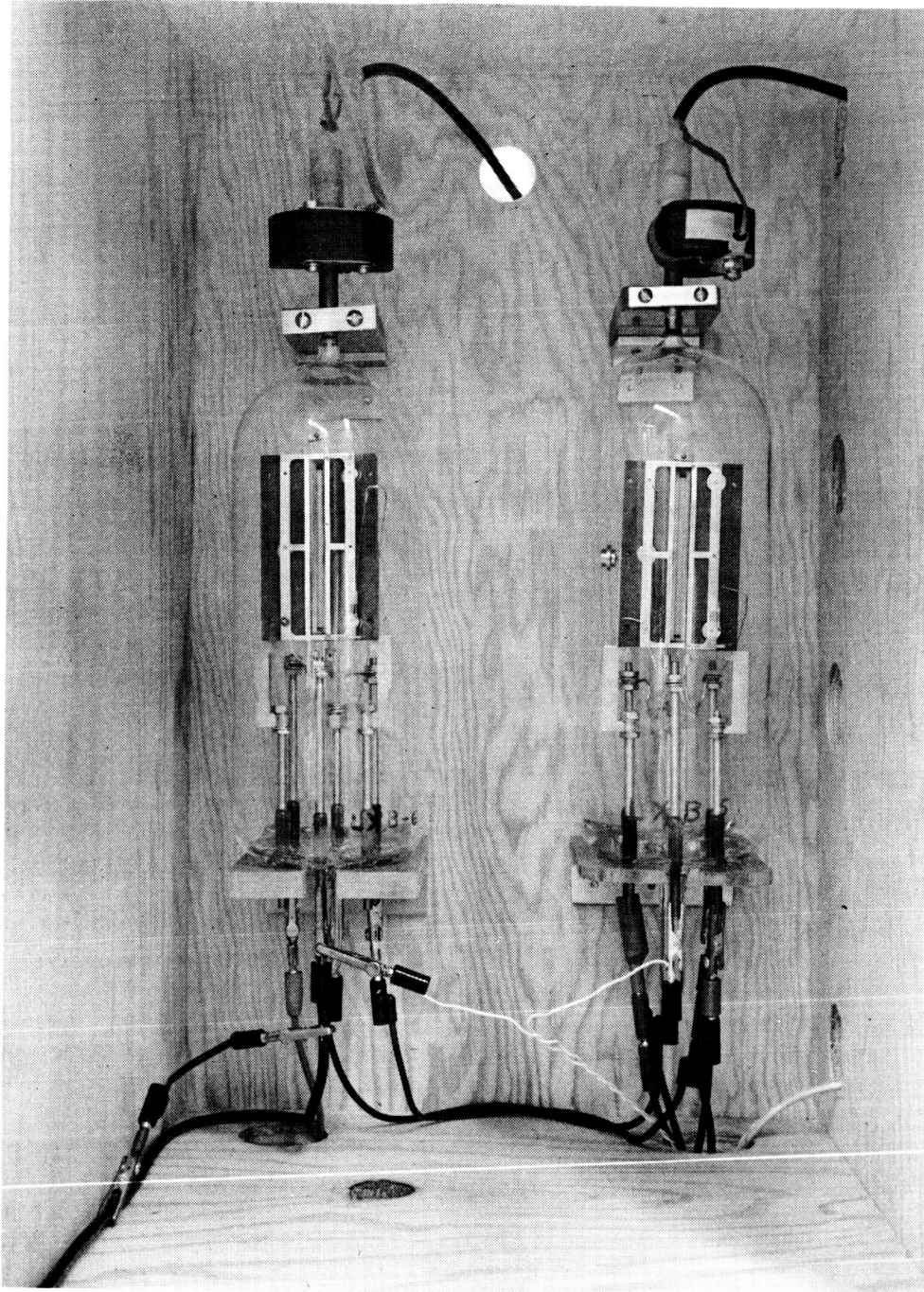


Fig. V-1. Model LB thrusters mounted in evacuated sealed bottles for long-duration cyclic thermal life tests.

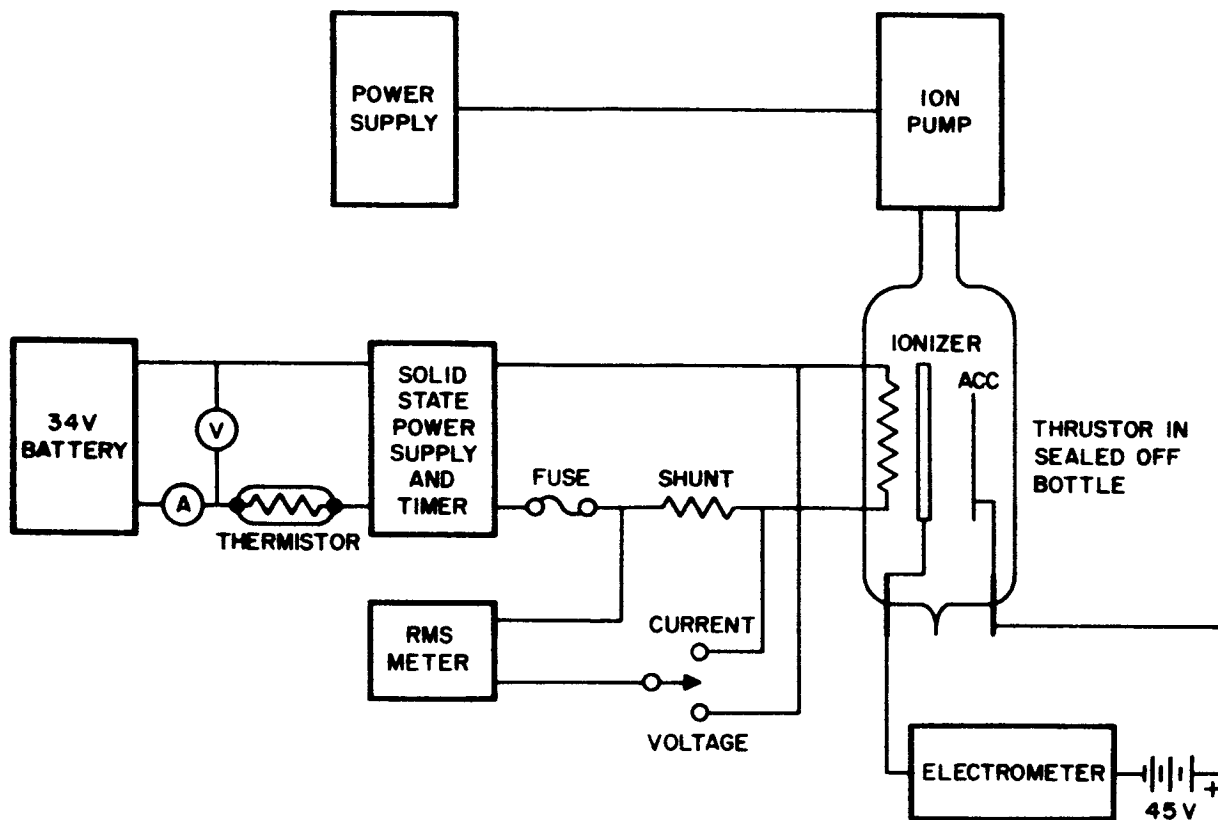


Fig. V-2. Block diagram of cycling test circuit.

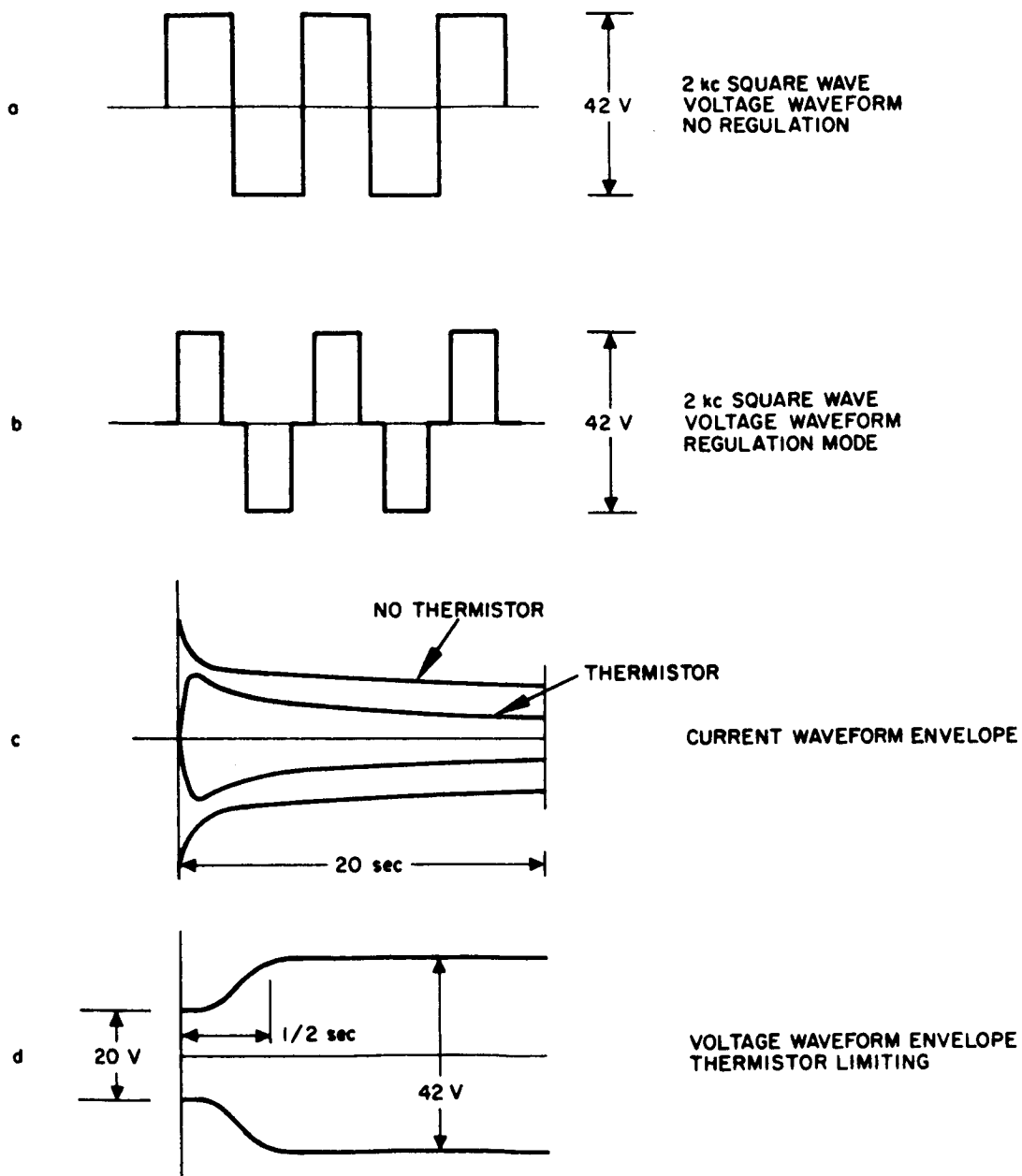


Fig. V-3. Voltage and current waveforms for cyclic tests.

range, peak-to-peak voltage and current readings remained constant, but in our test operation, two additional factors influenced the shape of the voltage and current envelope. During the initial inrush of current to the ionizer heater, due to application of full voltage to the cold heater, the value of current was too high for the regulator to function properly. As the heater warmed up and the resistance increased, the current reduced to a value permitting the regulator to function. In Fig. V-3c the curve marked "no thermistor" is a typical trace of the current waveform envelope for this type of operation. Because of the 3 min cool portion of the cycle, the heater resistance drops to a value of approximately 20-25% of the maximum resistance. This combined with the higher currents required for rapid warmup operation resulted in an initial current which was 500% of the steady state value. Thermal stresses and abnormal local heating of parts with low thermal mass frequently resulted in premature failure of a heater. Control of initial current was achieved by use of a thermistor in the 34 V line supplying power to the inverter. The preferred current waveform envelope can be seen in the curve marked "thermistor" in Fig. V-3c while the voltage waveform envelope is shown in Fig. V-3d.

The thermal cyclic tests were quite successful. The thrusters were cycled up to 85,035 cycles each. No mechanical failures occurred and no deterioration in any characteristics of the ionizer heaters was observed, although one heater did develop an intermittent open circuit at 40,493 cycles. However, in this case the ionizer was purposely heated to 1200°C for the last 27,000 cycles. A summary of the thruster characteristics and thermal cyclic performance is presented in Table V-1.

TABLE V-1
THERMAL CYCLIC THRUSTORS

Serial	Ionizer	Heaters	Cycles	Heatup Energy	Reason for Termination
LB-5	LMI-F Philips, Mod E, 75%	D-8	33, 000 to 1100°C 17, 000 to 1200°C	0.75 W-hr	Test objective achieved.
LB-6	LMI-F Philips, Mod E, 75%	F-1	13, 425 to 1100°C 27, 068 to 1200°C	0.77 W-hr	Intermittent open in one heater.
LB-8	LMI-F Philips, Mod E, 73.8%	F-1	85, 035 to 1100°C	0.76 W-hr	Power supplies required elsewhere.
LB-9	LMI-E Philips, Mod E, 73.5%	F-2	64, 119 to 1100°C	0.65 W-hr	Power supplies required elsewhere.
LB-11	LMI-E Philips, Mod E, 73.5%	F-2	Backup unit; Not tested		

VI. STEADY-STATE LIFE TEST

A. Introduction

To gain insight into the lifetime capability of the single-strip ion thruster, a limited, but flexible, steady-state life test plan was the major part of the program described in this Summary Report. Initial objectives were operational tests of 200 hours and 1000 hours each on two different thrusters with 8 cm long ionizers. Ionizer current density was required to be 7 mA/cm^2 . Based on the good performance observed during the second life test, the above plan was augmented by extending the second test to 2000 hours and adding another test of a thruster scaled to an ionizer length of 4.6 cm. Objectives of the third life test were: 700 hour operation, thrust level of $0.3 \pm 0.06 \text{ mlbf}$, power-to-thrust ratio less than 200 W/mlbf in the 4000 to 5000 sec specific impulse range. In general, these long-duration tests were highly successful in attaining the original objectives. It is believed that the test results and analyses presented in the following sections represent a contribution to the state of knowledge of cesium-contact ion thrusters which raises significantly the confidence level in long-life capability of this class of thruster.

B. Test Results

1. Thruster LB-4 (226 hour Test)

The first life test under this Contract was scheduled for 200 hour duration. This was accomplished with thruster LB-4 which completed 226 hours of operation at an average current density of 7 mA/cm^2 .

The thruster employed a low mass ionizer, Design F, with a D-8 heater. The porous tungsten emitter was manufactured from Philips, Mod E 74% dense material. The test was conducted with a laboratory type feed system and was terminated arbitrarily at 226 hours

of cesium beam-on time because of commitments of the limited project manpower to other aspects of the program, and because of the lack of an automated test console.

A time history chart of the major performance parameters on thruster LXB-4 is presented in Fig. VI-1. The average ionizer current density during the test was 7 mA/cm^2 . Accel drains averaged 1.08% through 200 hours and increased to 1.27% if averaged through the total of 226 hours. The drain current increase during the latter portion of the test resulted from operating the thruster about 8 hours per day during the normal working period instead of continuously. This type of operation required about 4 hours after each turn-on to stabilize the accel current at a minimum value.

Experimental evidence indicates that the major portion of the accel electrode current drain was electrons field emitted from the accel to the focus electrode. This is supported by visual observation of numerous protrusions on the accel surface after disassembly of the engine. The surface of the accel electrode in the vicinity of the end of the accel slot is shown in the photograph of Fig. VI-2. In addition to the presence of surface protrusions which enhance the local electric field and increase the field emission current, the other feature to be noted in Fig. VI-2 is the absence of any clean portion of the surface, particularly around the end of the accel slot. This lack of a clean surface region indicates that ion bombardment was not significant during this test. Metallographic analysis of the accel electrode after the test showed that any erosion due to sputtering was less than 10 microns. A photomicrograph of a cross section of the beam forming part of the accel is presented in Fig. VI-3.

A total of 540 trips were logged during the test which averages to an arc frequency of 2.4/hr. However, as indicated in Fig. VI-1, periods of up to 28 hours were recorded during which no arcs occurred.

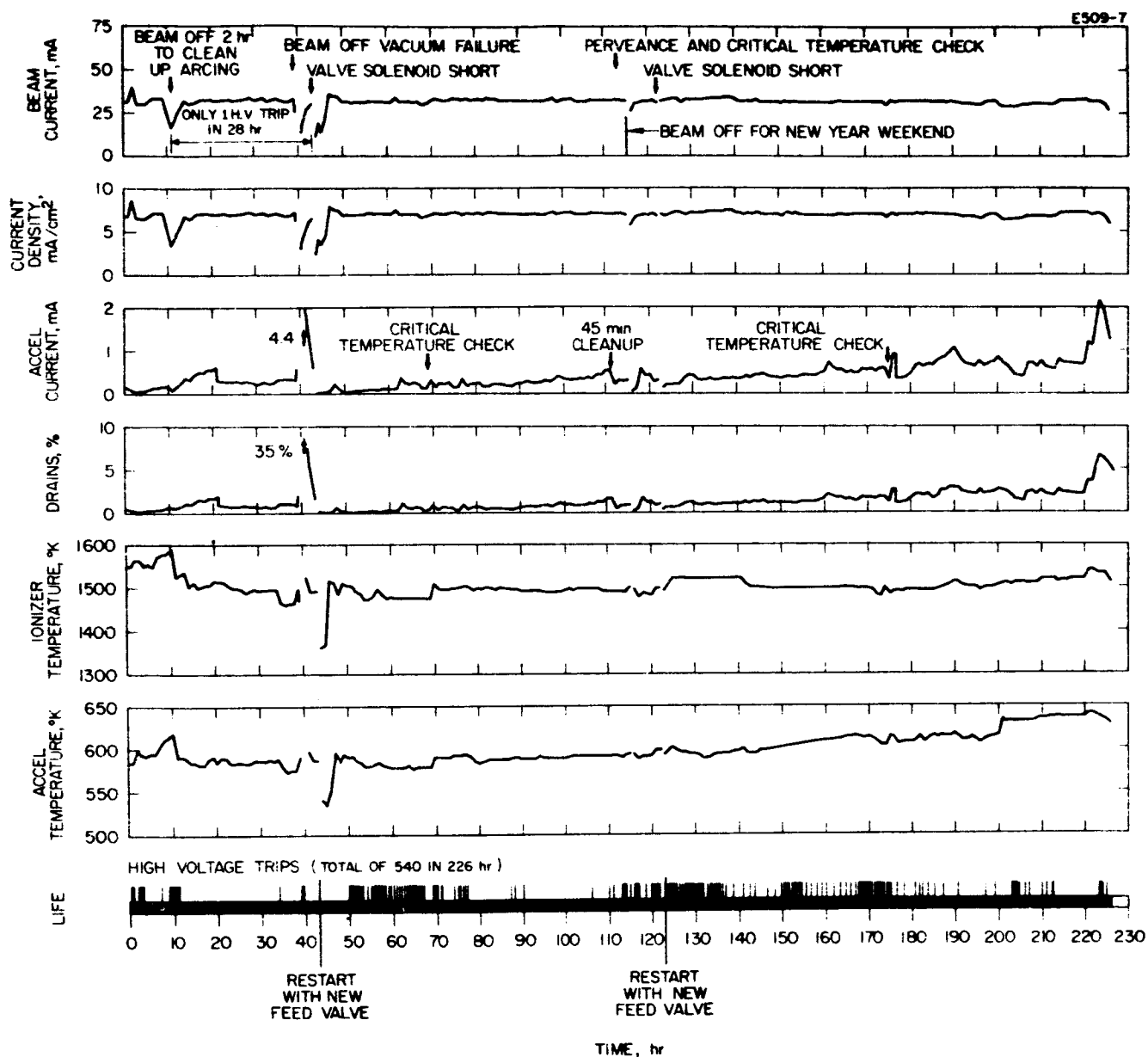


Fig. VI-1. Performance history chart for steady-state life test of thruster LB-4.

1497



Fig. VI-2. 15x photograph of surface of accel electrode after 226 hour life test in LB-4. Note the "globules" which are really surface protrusions. The absence of any clean areas indicates negligible sputtering.

M3937

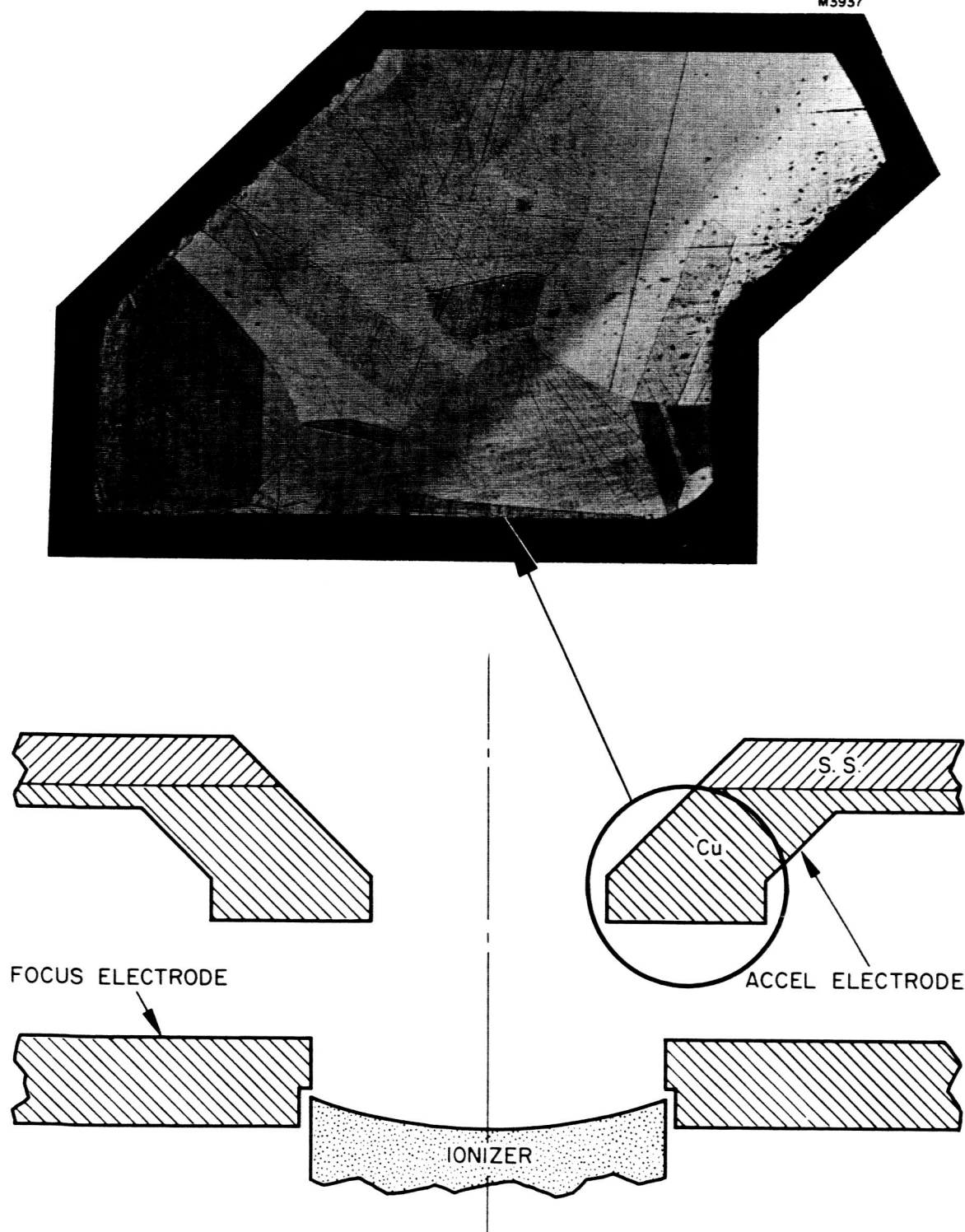


Fig. VI-3. 50x photograph of copper section of accel electrode after 226 hour life test at 7 mA/cm^2 in thruster LB-4.

Referring again to the chart of Fig. VI-1, notice that at no time during this life test was it possible to operate the ionizer at temperatures approaching the critical temperature for clean tungsten. Evidence indicates that oxygen on the porous tungsten ionizer was regenerated during operation with the cesium beam. Possible explanations are that:

(1) some ions escaping from the thruster struck the liquid nitrogen cryogenic surfaces, releasing oxygen-bearing adsorbed molecules or atomic or molecular oxygen; (2) a small air leak was present which resulted in an oxygen partial pressure of about 10^{-7} Torr.

Installation of a conical optical baffle to intercept ions before they struck the cryowall was partially successful in reducing the critical temperature of the tungsten emitter. However, it was observed in later tests that as long as 200 hours of continuous operation was required before clean porous tungsten performance was attained.

2. Thruster LB-7 (2000 hour Test)

The most significant accomplishment under this Contract, and a major milestone in the development of cesium-contact ion thrusters, was a 2000 hour endurance test of single-strip thruster LB-7 which was completed successfully on 30 July 1965. The test was conducted in two 1000 hour segments because of the necessity of reloading the cesium feed system. The low mass ionizer in this thruster was 8 cm long and was manufactured from Philips, Mod E, 74% dense porous tungsten. The major design parameters are listed in Table VI-I.

TABLE VI-1

8 cm THRUSTOR ELECTRICAL PARAMETERS
(Nominal Design Values)

Thrust	0.5 mlbf
Specific Impulse	5000 sec
Beam Current	32 mA
Beam Voltage	1.7 kV
Ionizer Current Density	7.0 mA/cm ²
Power-Thrust Ratio	225 W/mlbf
Weight	0.5 lb

The thruster was powered and controlled by an Automatic Life Test Console which used SERT-I power conditioning equipment mounted on a water-cooled heat sink to permit steady-state operation. A control loop could be closed between the beam current and boiler temperature to maintain a constant output current from the thruster. Also included in the console logic was a control loop which could minimize accel current by adjusting the ionizer temperature. Details of the console design and operation are presented in Section VII.

Life test of the ion thruster was conducted in a vacuum chamber 2 ft in diameter by 6 ft long. Liquid nitrogen cryowalls lined most of the interior surface area of the vacuum facility. Approximately 950 hours of the life test were accomplished with the chamber being pumped by a getter ion pump while the remaining portion of the test was conducted using an oil diffusion pump. Total pressure in the chamber with the beam on varied from 1.5×10^{-7} Torr with the ion pump system to 4×10^{-8} Torr when using the oil diffusion pump which had a higher pumping speed than the ion pump. Mass spectrometer analysis of the residual gas environment is discussed in Section VI-C.

In general, the performance of the thruster was stable, with little high voltage arcing. High voltage trips averaged one per hour. A time history of the key parameters during this 2000 hour life test is presented in the chart of Fig. VI-4. Average current density throughout this test was approximately 6.5 mA/cm^2 . Accel drain varied from a low of less than 1% up to 15%, depending upon the temperature of the accel electrode. Most, if not all, of these drain currents were electrons from the negative accel electrode to the positive high voltage electrodes. This type of drain current is nondestructive with regard to any limitations on thruster life.

The only performance figure that changed significantly was the ionizer critical temperature. Notice in Fig. VI-4 that the critical temperature (solid black dots) decreased during the first 200 hours of operation and maintained a value corresponding to clean tungsten throughout the remainder of the test except for a short interval following cesium reload at the 1000 hour mark. The critical temperature, as measured at the 2000 hour point, was 1020°C at an ionizer current density of 7 mA/cm^2 . This value is only about 20°C higher than the Taylor-Langmuir value for solid tungsten (see Fig. VI-5). However, the ionizer temperature generally was not maintained close to this critical value because the accel temperature increased abnormally due to a decrease in emittance of the radiating surface. In fact, thermionic electron emission was a maximum at the point of minimum ionizer temperature.

A check of the perveance characteristics of this thruster prior to the life test and at intervals during the life test showed no detectable change of the perveance. The data are presented in Fig. VI-6. The implication that erosion of the accel electrode surfaces which are critical to the ion optical structure was negligible was confirmed upon visual examination of the exposed accel electrode edges after removal from the vacuum chamber.

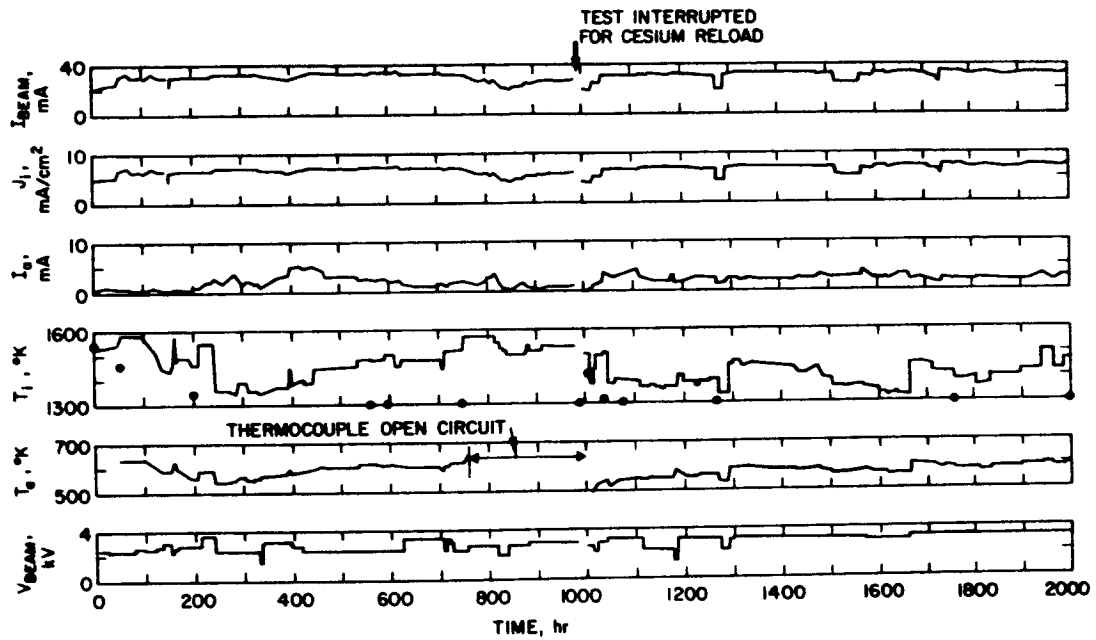


Fig. VI-4. Performance history chart for 2000 hour life test of thruster LB-7.

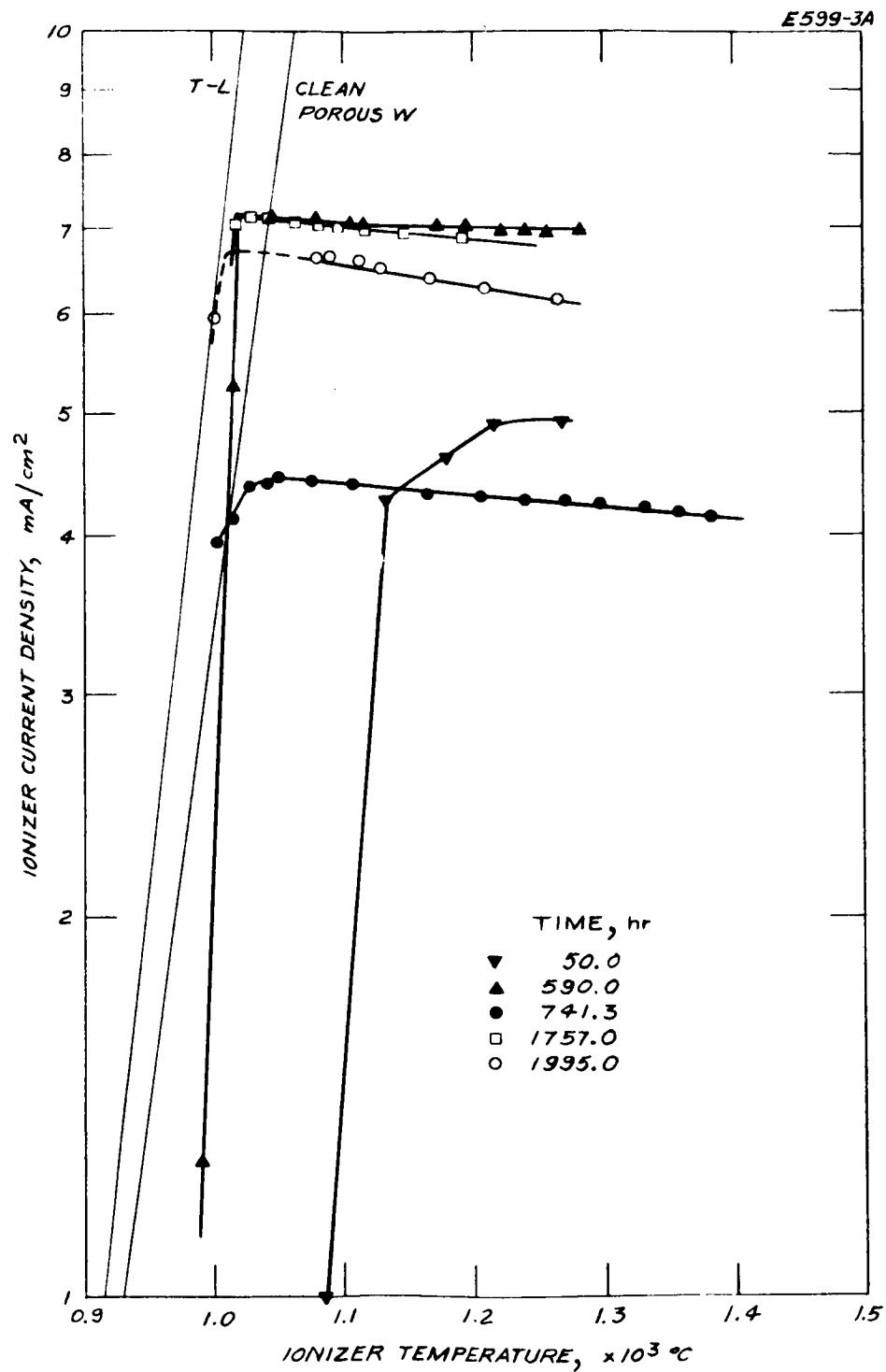


Fig. VI-5. Ionizer current density versus temperature during 2000 hour test of thruster LB-7.

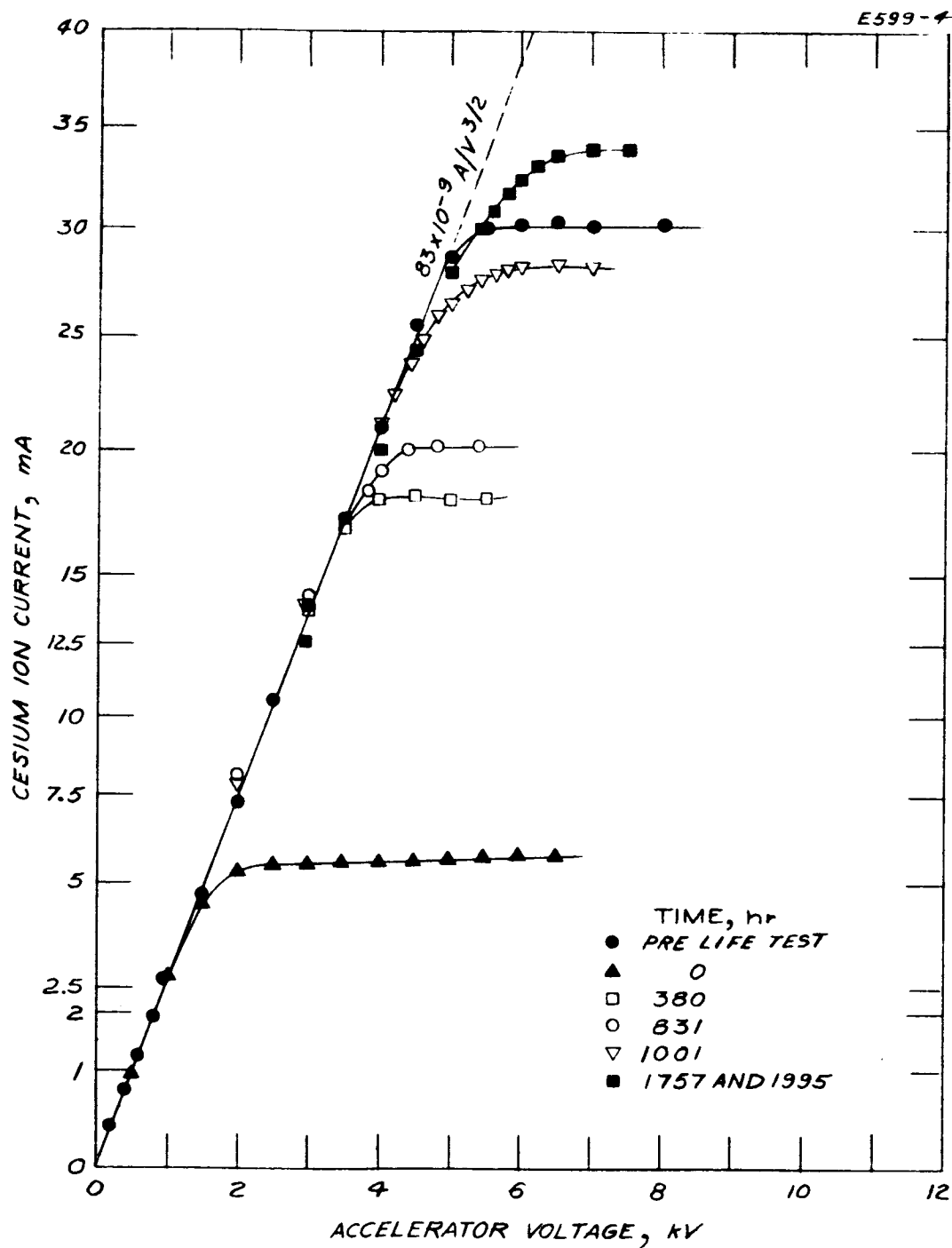


Fig. VI-6. Perveance characteristics of thruster LB-7.

The transition region from space-charge-limited operation to flow-limited operation became less well defined toward the end of the life test. Since critical accel surfaces remained undamaged, it is believed that this change in the behavior of the transition region of the I-V characteristics is related to ionizer permeability. Available qualitative macroscopic information shows that the ends of the porous tungsten ionizer were less permeable than the central region after the 2000 hour test. This could result in a broader transition region from space-charge to flow-limited operation. The effect in the transition region of the perveance curve did not cause any deterioration of thruster performance because the thruster was normally operated well into the flow-limited region.

A graph of total thruster power-to-thrust ratio versus specific impulse is shown in Fig. VI-7. A minimum power-to-thrust ratio of 220 W/mlb was measured at a beam-on time of 1177 hours. This compares favorably with the predicted minimum of 225 W/mlb and is a significant improvement over the power-to-thrust ratio minimum measured prior to start of the 2000 hour life test. Included in these power calculations, in addition to ionizer and beam power, are the accel drain power and the neutralizer power. Feed system power is not included. Maximum power efficiency measured on this thruster during the life test was 72 percent at a specific impulse of 7500 sec.

A number of partial S-curves of the electron emission from the accel electrode were obtained during the life test and a typical group is shown in Fig. VI-8. The peak in the thermionic electron emission from the accel occurs predominantly at a temperature of about 550°K. Because of back sputtering from the collector the accel electrode in LB-7 became coated with copper. The resultant reduction in emittance of the radiating surface caused this electrode to operate very near the peak in thermionic electron emission when the ionizer was maintained close to the low critical temperature. Even so, no detrimental effects were observed in thruster performance and no run-away conditions were observed during the 2000 hour life test. Operation even at high drain current (up to 15%) was stable.

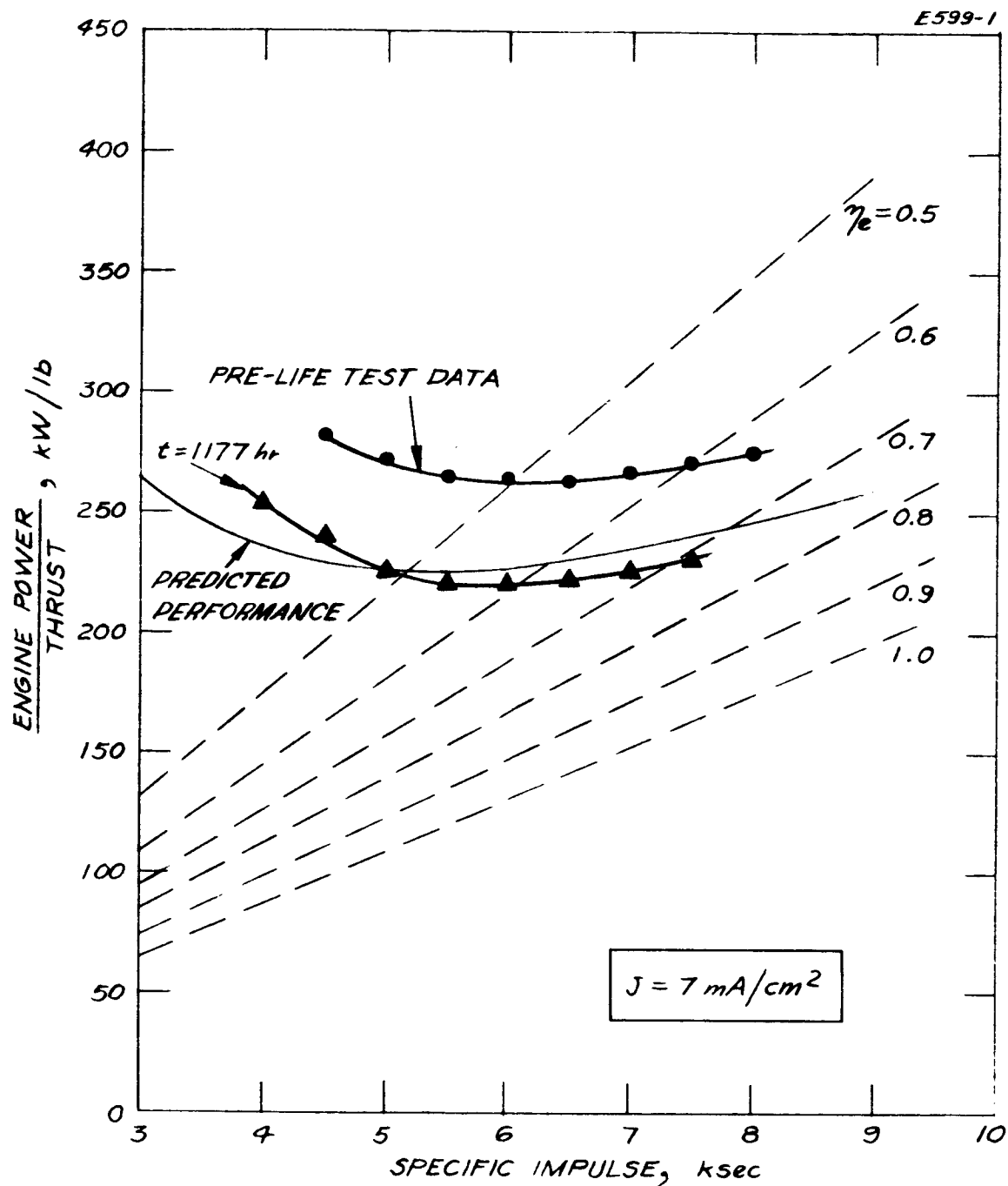


Fig. VI-7. Power-to-thrust ratio versus specific impulse for thruster LB-7 as compared to empirical calculation. Feed system power is not included.

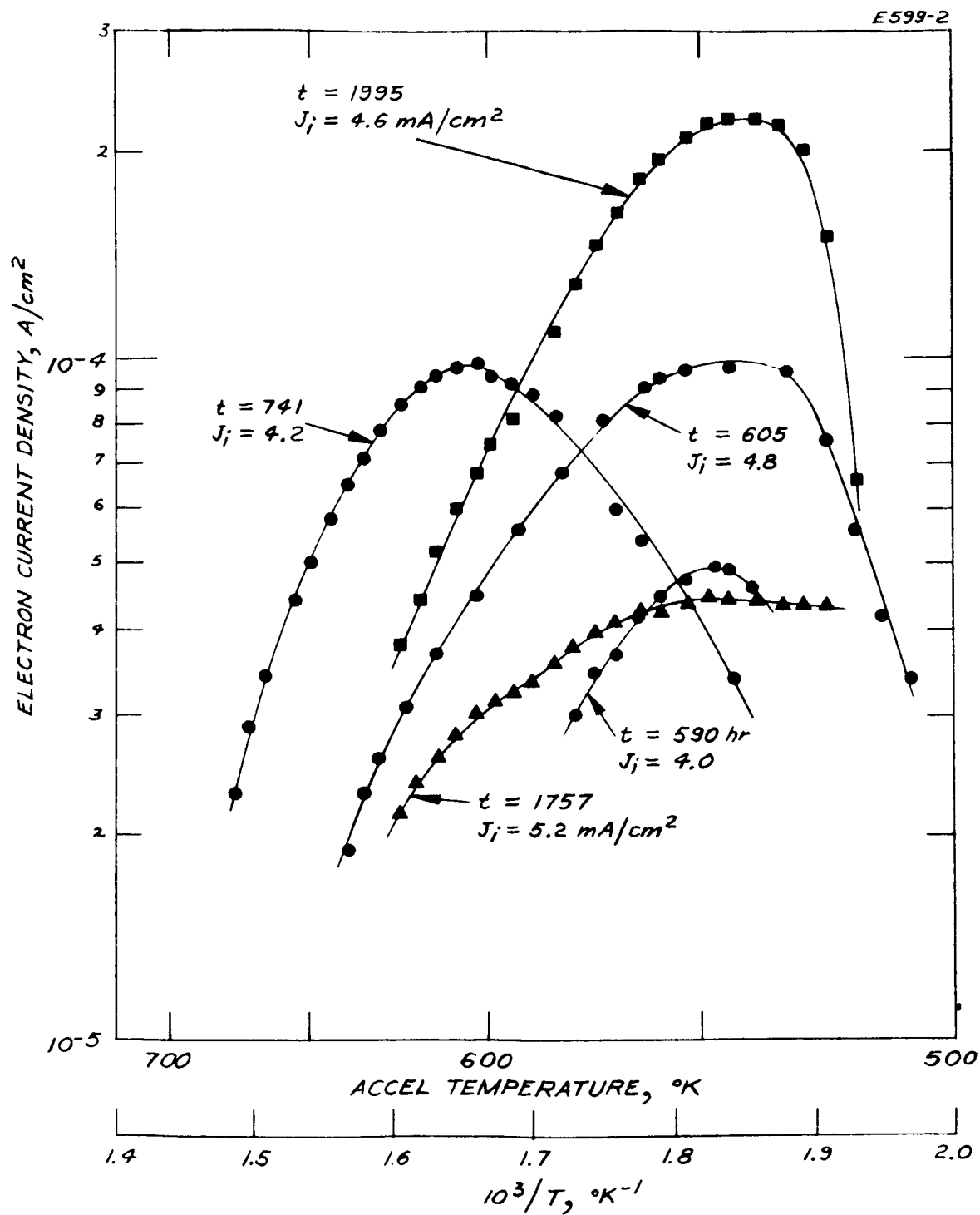


Fig. VI-8. Electron back emission from accel electrode to the positive electrodes during test of LB-7.

In a free space environment, where there would be no back sputtering of copper to change the emittance, the accel electrode equilibrium temperature would be about 470°K with the ionizer operating at 1350°K .^{*} In this true operating situation Fig. VI-8 shows that the accel electron drain should be reduced by a factor of ten or more from the peak value.

A most encouraging aspect of the life test was the fact that the neutralizer which is a simple carburized, thoriated-tungsten filament, remained intact and suffered almost no erosion throughout the 2000 hour period. Furthermore, the specific electron emission as measured after completion of 2000 hours of beam-on time, was 50 mA/W at 1900°K . This is an excellent value for this type of electron emitter. Filament lifetimes of over 10,000 hours are predicted at a temperature of 1950°K and a specific electron emission of 35 mA/W. Hence, we have considerable confidence in the applicability of this neutralizer design to ion thrusters of this type.

3. Thruster LD-2 (610 hour Test)

A single-strip thruster scaled from an ionizer length of 8 cm to 4.6 cm was tested for 610 hours. The principal objective was a power-to-thrust ratio of 200 W/mlbf at a thrust level of about 0.3 mlbf in the specific impulse range of 4000 to 5000 sec. The ionizer was manufactured at the Hughes Research Laboratories from classified spherical tungsten powder, 3.92 μ mean particle size, 78.2% dense. Figure VI-9 shows the time profile of the major thruster parameters. The test falls into two time periods separated at hour 332, when a neutralizer to accel short occurred and an ionizer heater transformer failed. The accel high

^{*}For a discussion of other factors affecting ion engine life test data see J. R. Anderson, S. A. Thompson, and H. J. King, "Factors in Life Testing Ion Engines," J. Spacecraft and Rockets, 3, (March 1966).

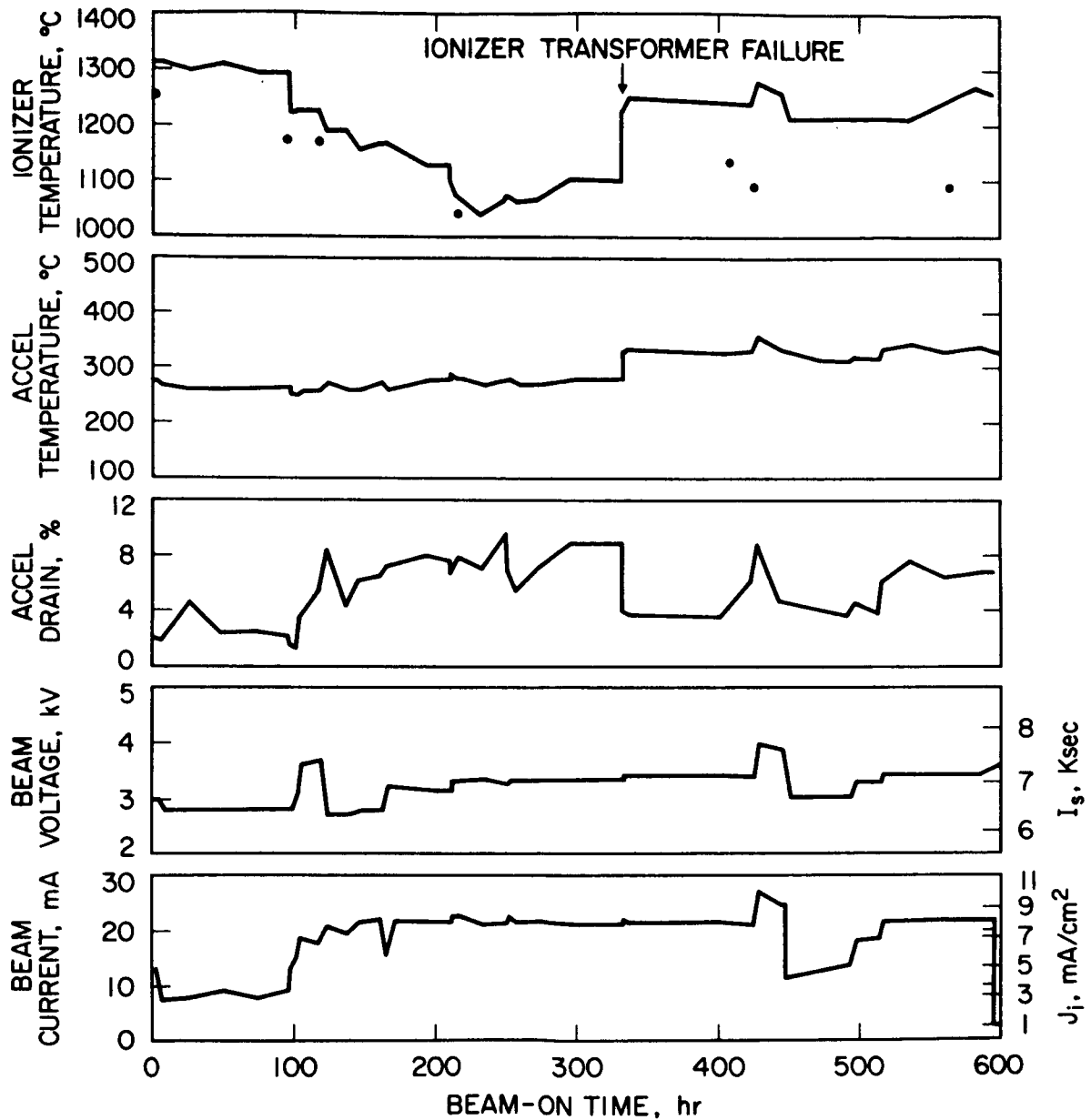


Fig. VI-9. Time profile of major thruster parameters during 610 hour life test of thruster LD-2.

voltage supply output level and ripple control failed. The resultant time varying electrostatic field between the neutralizer and accel electrode caused the neutralizer filament to vibrate in a resonant mode. The amplitude of this resonance was sufficient for the filament to touch the accel electrode and become welded to the latter, thus causing the short circuit. The console was repaired and the neutralizer replaced prior to continuing the test. An ionizer current density of 8 mA/cm^2 was recorded during 435 hours and averaged 7 mA/cm^2 over-all. Thrustor perveance data are presented in Fig. VI-10. Since the LD thrustor is merely a shorter LB design, perveance/ cm^2 is identical to that of the LB class of thrustor.

As expected the critical temperature was high initially, but decreased during the early phase of testing until clean porous tungsten performance was measured at hour 215. This can be seen in Fig. VI-11. The dots on the ionizer temperature profile in Fig. VI-9 also show the critical temperature decrease with time. After the neutralizer had been repaired, the ionizer again went through a short clean-up process.

Accel drain current averaged 6% but was strongly dependent on accel temperature. The accel temperature-accel current relationship is depicted in Fig. VI-12. Accel current reached its maximum at an accel temperature of 280°C . Very early in the test this was of little concern because accel temperature was less than this value. As the test progressed, the accel temperature versus ionizer temperature characteristic underwent a translation that resulted in a higher accel temperature for a given ionizer temperature. The difference was about 90°C . Figure VI-13 shows this characteristic during early operation, during translation, and during the final portion of the test. The cause of this temperature change was the same as experienced during the LB-7 life test, viz., sputtered copper from the collector coated the accel surface of oxidized stainless steel and lowered the emittance. This required the accel to assume a higher temperature in order to continue rejecting power radiated to it from the ionizer and focus electrodes. A factor of two reduction in emittance is adequate to explain the observed shift in accel temperature.

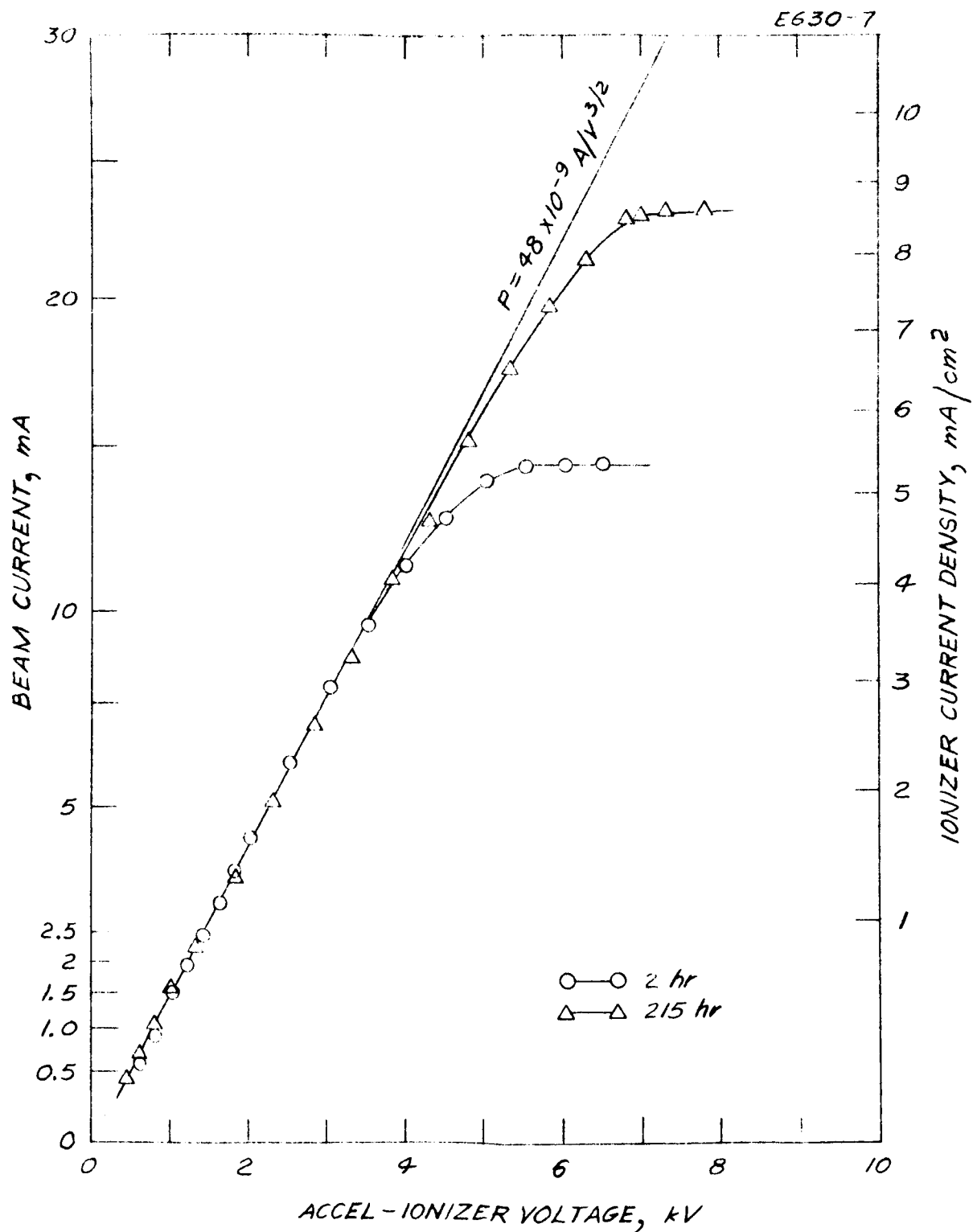


Fig. VI-10. Perveance data measured on thruster LD-2 during 610 hour life test.

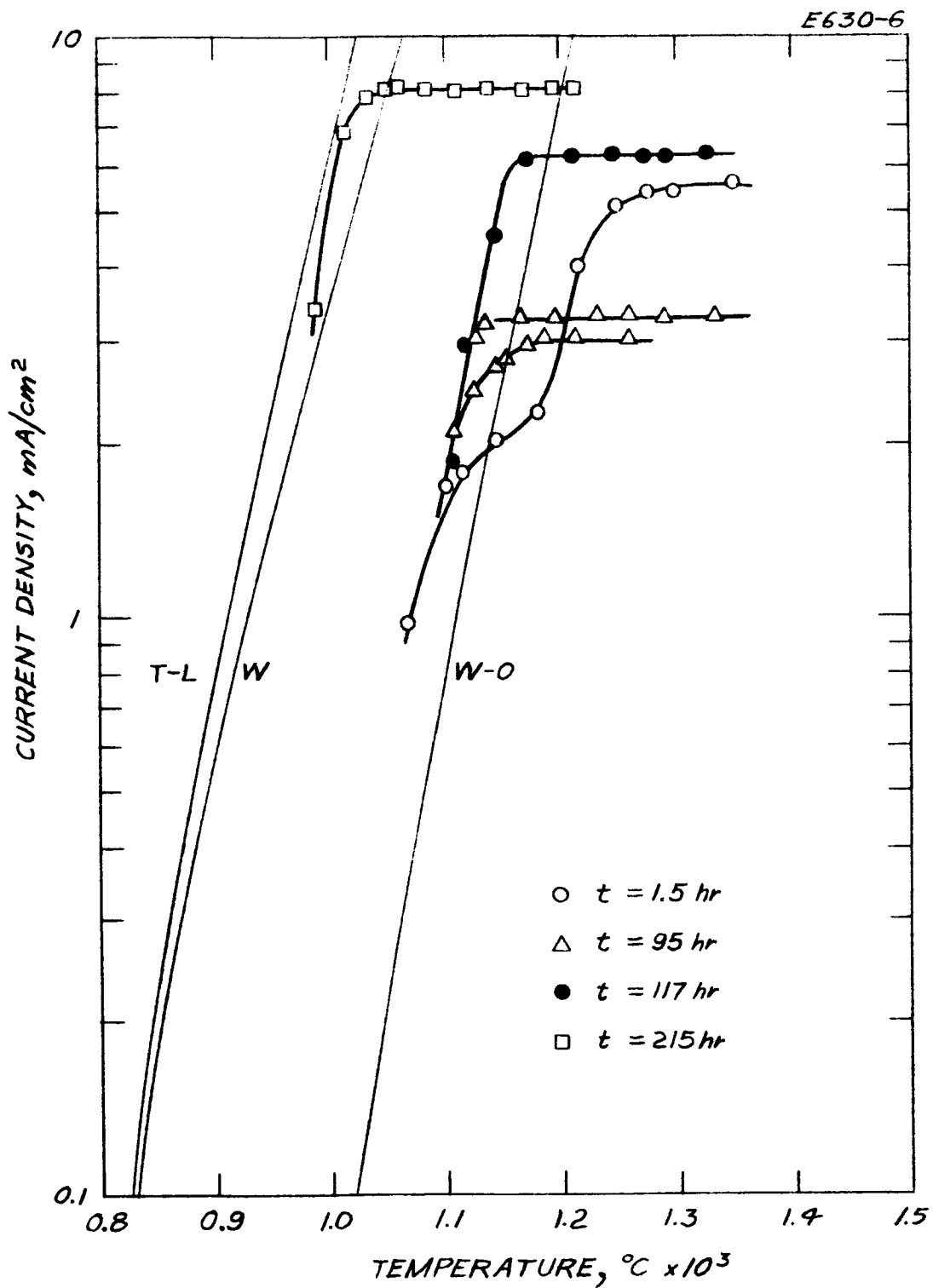


Fig. VI-11. Ionizer current density versus temperature characteristics measured on ion thruster LD-2 during 610 hour life test.

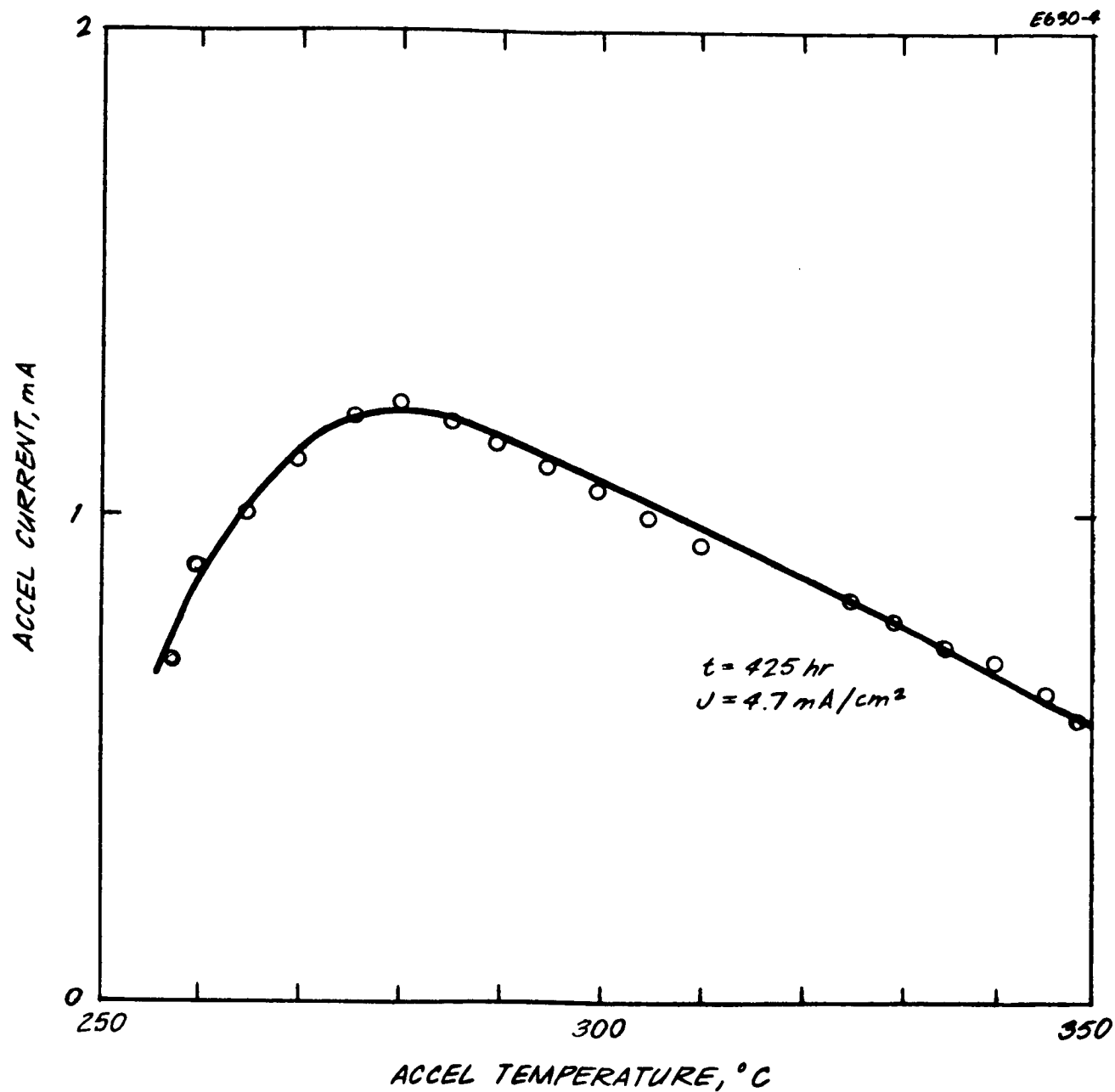


Fig. VI-12. Dependence of accel current on accel temperature in thruster LD-2.

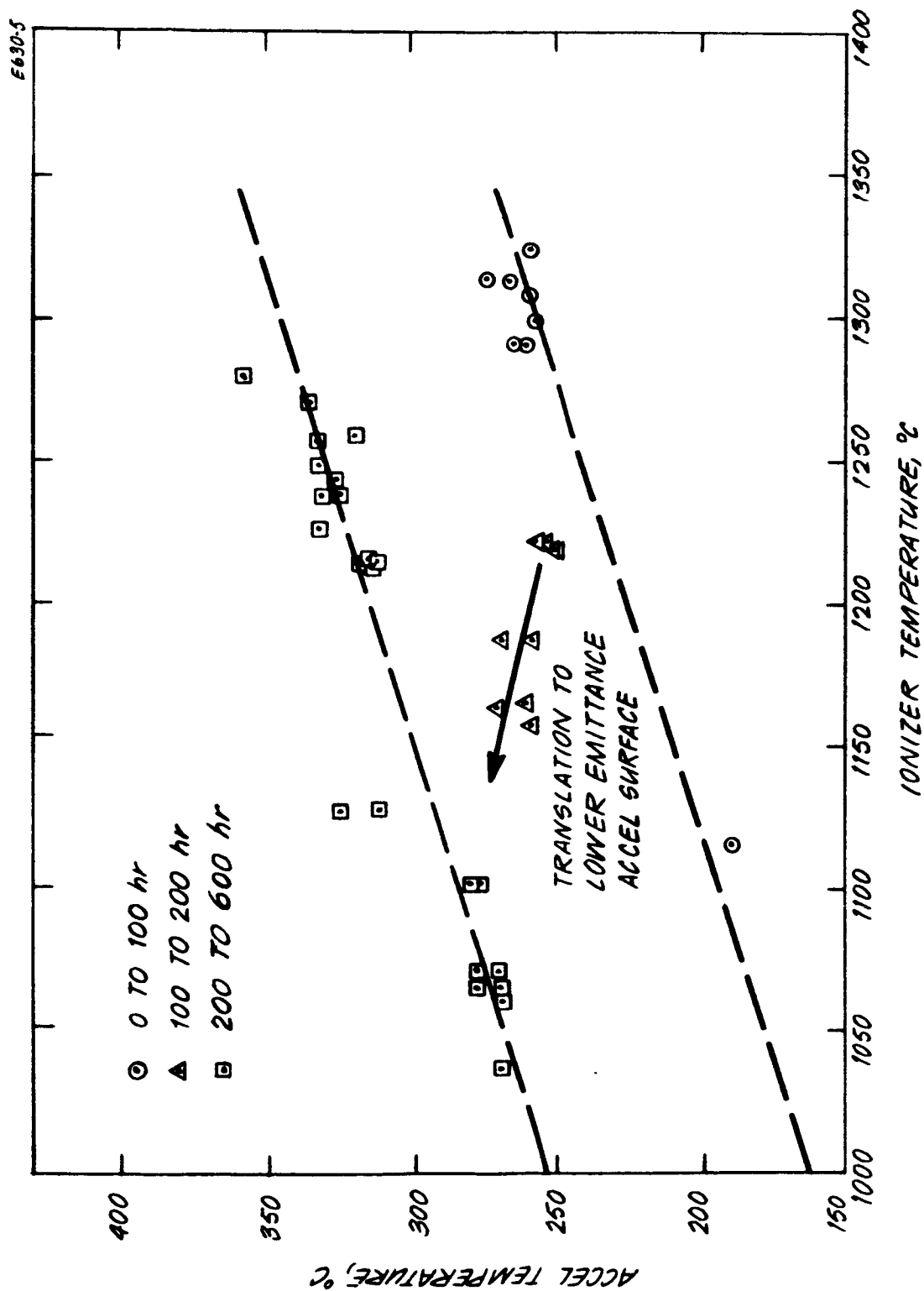


Fig. VI-13. Accel temperature as a function of ionizer temperature during life test of thruster LD-2.

Once the ionizer surface was in the clean tungsten state, the ionizer temperature could be lowered to between 1040 and 1100°C with no degradation in ion beam current. However, because of the accel temperature shift, the accel then operated in the worst possible temperature range for electron emission. Consequently, ionizer temperature was usually kept higher than required in order to reduce accel drain currents.

The phenomenon of altered accel emittance is not representative of thruster performance in free space. Several corrections are incorporated in power-thrust data in Fig. VI-14 to reflect the fact that accel drain power should be greatly decreased from that encountered in ground test facilities.

Curve (1) is a plot of the power to thrust computed directly from the raw data. The current density was 9.16 mA/cm² during this test at hour 448. Curve (2) shows the data if accel drain power is ignored. This curve is not corrected for the fact that some of the back electron emission from the accel helps to heat the ionizer. Curve (3) represents the data totally corrected for free space performance, including the normal accel drain expectation and corrected ionizer heater power. The minimum P/T value of 196 W/mlbf should occur between 4500 sec and 5000 sec.

Electron emission characteristics of the neutralizer filament are presented in Fig. VI-15. These data were obtained by biasing the accel positive with respect to the neutralizer. No more than 2 W would be required for the neutralizer electron emission to accommodate the beam current in free space. Since the collector was grounded during the life test, electrons from the neutralizer were not needed.

C. Residual Gas Environment

Adverse effects on ionizer performance, arising from contamination by the residual gases in a vacuum test chamber, have been conjectured from time to time. The merits of an oil diffusion pumped system versus systems evacuated by other methods have also been debated. The 2 ft diameter by 6 ft long vacuum chamber used for the steady-state life tests was instrumented with a C.E.C. 21-612 Residual Gas Analyzer.

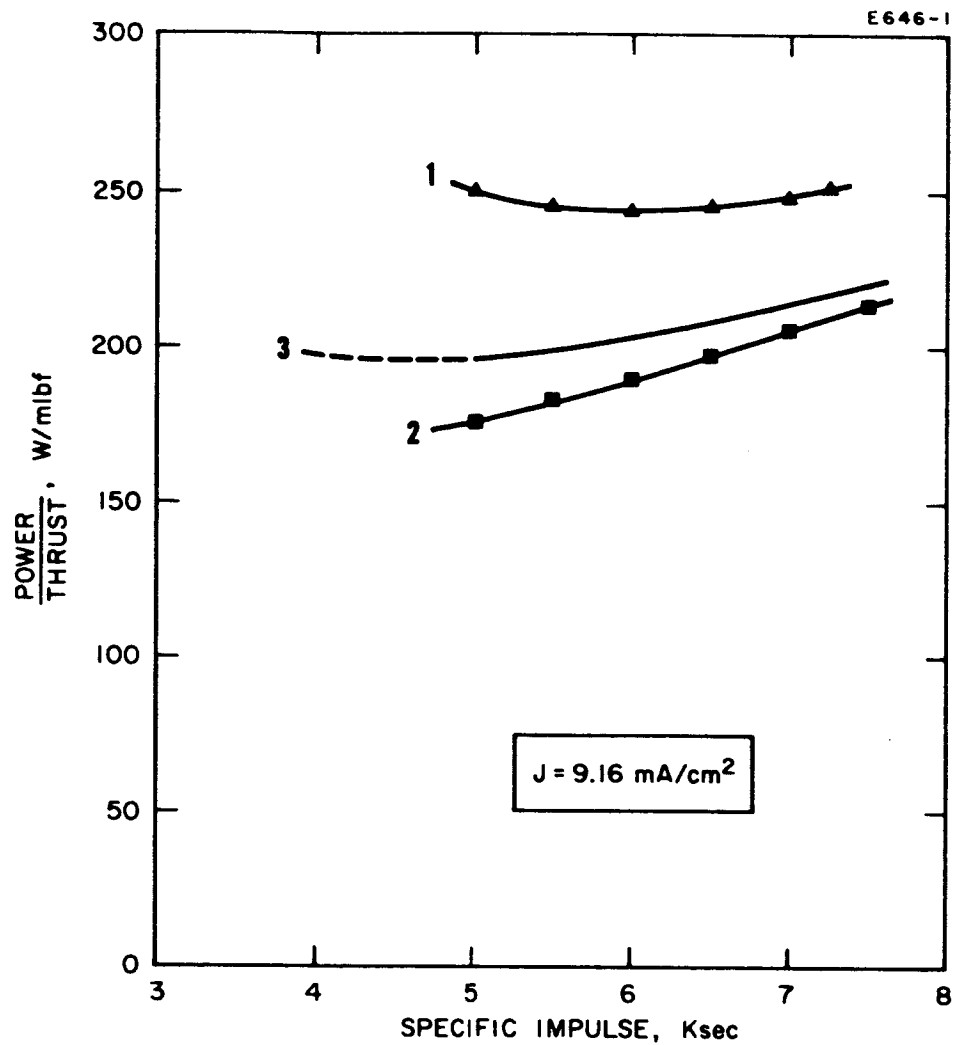


Fig. VI-14. Power-thrust characteristics of thruster LD-2. Curve (1) is based on the raw data. Curve (2) was calculated assuming zero accel drain power. Curve (3) was calculated by extrapolation of the thruster data to free-space operation.

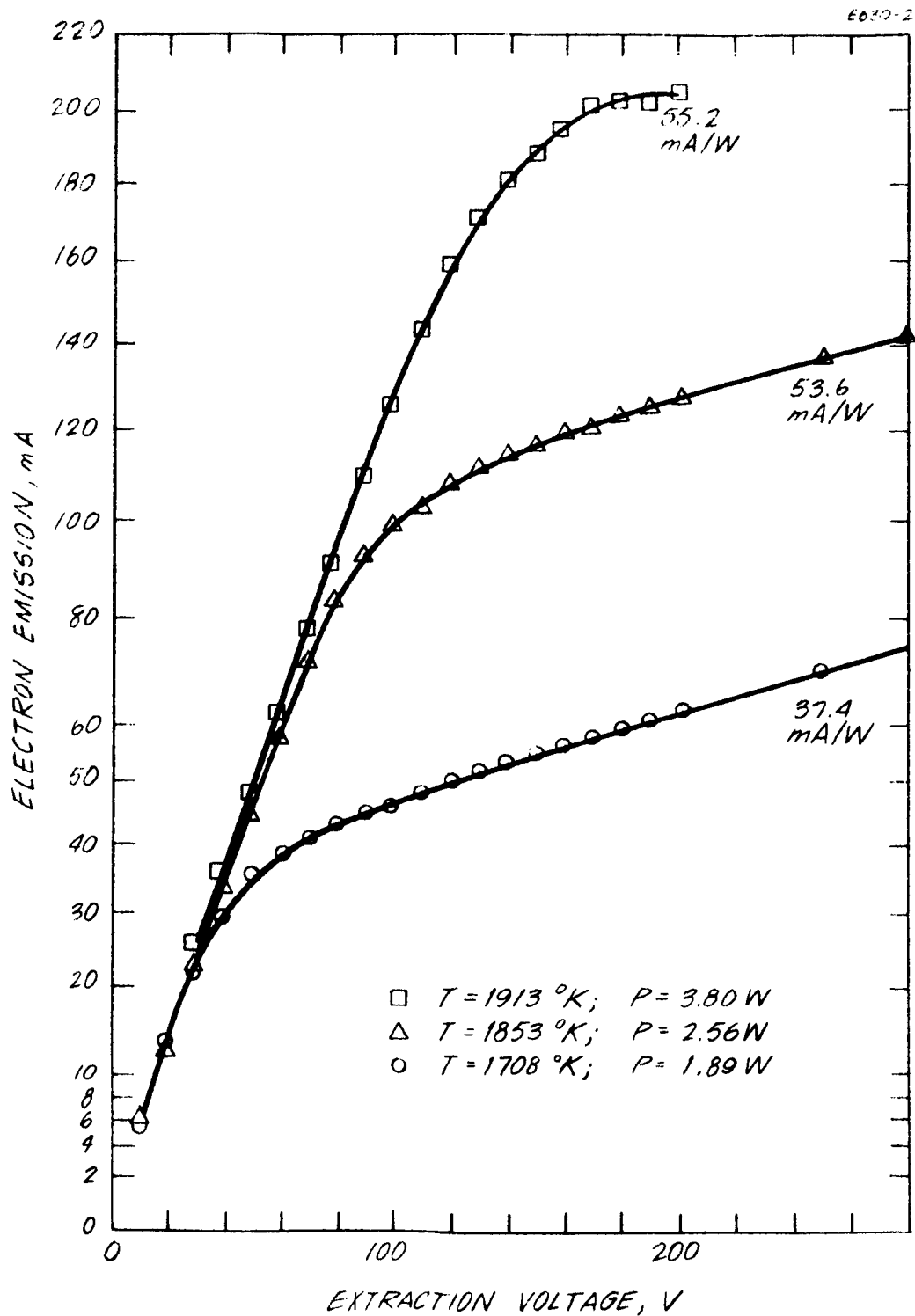


Fig. VI-15. Neutralizer current-voltage characteristics for thruster LD-2.

In addition, the chamber was pumped by either a 10 inch oil diffusion pump (DC 705 oil) with an effective pumping speed of 1800 liters/sec or a 300 liters/sec ion pump, or both simultaneously. A tray containing Linde 16X zeolite pellets. 1/16 in. in diameter, was placed on the bottom of the vacuum chamber between the cryowall and the chamber outer wall. The zeolite was dehydrated by outgassing at 350°C for 2 hours. The purpose of the zeolite was to increase the pumping and trapping of water vapor and hydrocarbon gases.

Results of analysis of the residual gas in the chamber during the 2000 hour life test are presented in Table VI-2.* During 950 hours of the first 1000 hour segment of the test only the ion pump was used. In this configuration over 80% of the residual gas was hydrogen. With both pumps operating, the total pressure dropped significantly. However, a large portion of the pressure reduction was achieved by pumping of hydrogen. The highest carbonaceous gas component with the ion pump only was that of CH₄ which had a partial pressure of 2.93×10^{-9} Torr. Other carbon-bearing gases such as CO₂, CO, and C₂H₆ were all in the 10^{-10} Torr range or lower.

The ion pump was turned off during most of the second 1000 hour period. Because the diffusion pump had a higher pumping speed, all partial pressures except those of N₂ and O₂ were reduced and CO and C₂H₆ were not detected. A minute air leak was probably responsible for the rise in partial pressure of N₂ and O₂ since they were present in approximately the same proportion as found in air. There is no evidence that the ionizer became contaminated when using either the oil diffusion pump or the ion pump.

The influence of adsorbed carbon on ionizer work function and critical temperature is a function of the carbonaceous gas species, its partial pressure, the ionizer temperature and time.³ Because critical temperature remained low after an initial ionizer cleanup, it can be concluded that the temperature-pressure relationship for carburization was such as not to be detectable during the 2000 hour life test.

*Very close agreement with these data was recorded during the 610 hour test of thruster LD-2.

A factor that clouded earlier observations about ionizer performance was that tests simply were not long enough. It has been observed several times that a stabilization period of up to 200 hours was required before ionizers exhibited clean tungsten performance. Operating times of this order of magnitude were achieved consistently only in the past year or so. It now appears that ionizer surfaces start with adsorption impurities that are gradually reduced until a clean surface results. From the 200 hour point until the conclusion of the 2000 hour test, no deterioration attributable to the residual gases was observed.

D. Post-Test Analysis

1. Thruster LB-7

This section deals with post-test examination of thruster LB-7 which accumulated 2000 hours of beam-on time. The distinguishing feature of all post-test examinations was the integrity of thruster components. No area could be pinpointed where failure was imminent.

a. Accel Electrodes

Upon successful completion of the first 1000 hour test interval, thruster LB-7 was removed from the vacuum chamber for visual inspection and cesium reload. Macroscopic examination of the accel electrode by HRL personnel and a representative of the NASA Project Manager showed no detectable erosion of the accel electrode at a magnification of 50X. The lack of any significant sputtering of this electrode was also indicated by the absence of any clean surfaces. Instead, the electrode was coated with copper sputtered from the collector

TABLE VI-2
AVERAGE PARTIAL PRESSURES (TORR)

GAS	ION PUMP ONLY	DIFFUSION PUMP ONLY
H ₂	1.29 x 10 ⁻⁷	8.61 x 10 ⁻¹⁰
H ₂ O	1.75 x 10 ⁻⁸	7.99 x 10 ⁻⁹
N ₂	5.9 x 10 ⁻⁹	3.99 x 10 ⁻⁸
CH ₄	2.93 x 10 ⁻⁹	6.43 x 10 ⁻¹⁰
Ar	9.5 x 10 ⁻¹⁰	4.02 x 10 ⁻¹⁰
C ₂ H ₆	6.61 x 10 ⁻¹⁰	—
CO	4.71 x 10 ⁻¹⁰	—
CO ₂	4.26 x 10 ⁻¹⁰	4.01 x 10 ⁻¹⁰
O ₂	—	8.77 x 10 ⁻¹⁰
Total	1.57 x 10 ⁻⁷	5.59 x 10 ⁻⁸

and copper re-evaporated from the hot ionizer. A photograph of a portion of the critical slit region of the accel electrode is shown in Fig. VI-16. Notice the good definition of the ion optical edges and surfaces in this slit region.

A photograph of the thruster immediately after removal from the vacuum chamber following completion of 2000 hours of beam-on time is shown in Fig. VI-17. A photograph of the thruster in the disassembled state is shown in Fig. VI-18. Of immediate interest is the presence of four pit-type erosion regions located at the ends of the accel electrode on the downstream side. Figure VI-19 is a closeup photograph of two of these pitted areas.

Photomicrographs of the accel electrode at the central slit area and a pitted area are presented in Fig. VI-17. In the central slit area charge exchange erosion was so little that deposition of copper from the collector completely masked it. Even in the pitted area, no erosion was observed on the upstream side (facing the ionizer) or in the slit region of the accel electrode. Since material sputtered from the downstream side of the accel has a very low probability of returning to the ionizer, a simple solution to reducing the erosion in this region is available; namely, fabricate all downstream surfaces of the accel electrode from a low sputter yield material rather than copper.

For the optical design used in this thruster, an end effect correction was included at the end regions of the optical structure to prevent impingement of primary ions on the accel electrode. The Model 70 optical design with end effect correction was successful in achieving this goal. However, measurements made on the ion beam from this ion optical design show that the current density near the ends of the strip beam is higher than in the central portions of the beam. Quantitative measurements indicate that the peak value of the current density near the ends of the strip is approximately four times that in the central regions of the beam. Since the charge exchange collision probability varies approximately as the ion current density times the

M 4001

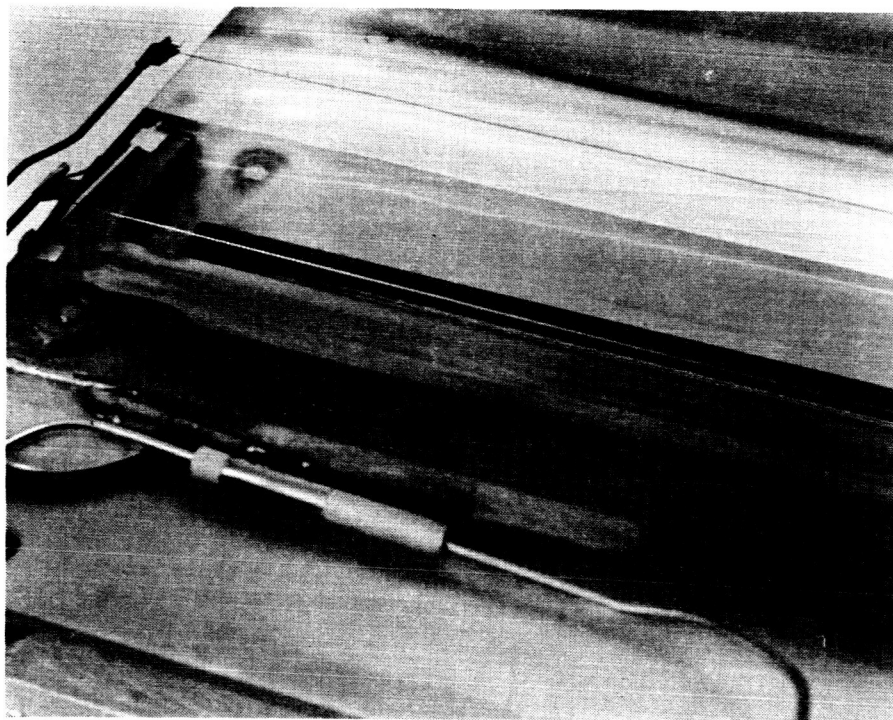


Fig. VI-16. Closeup photograph of portion of accel electrode aperture after 1000 hours of cesium life test. Note the absence of any macroscopic erosion of the critical ion-optical edges and surfaces.

M4138

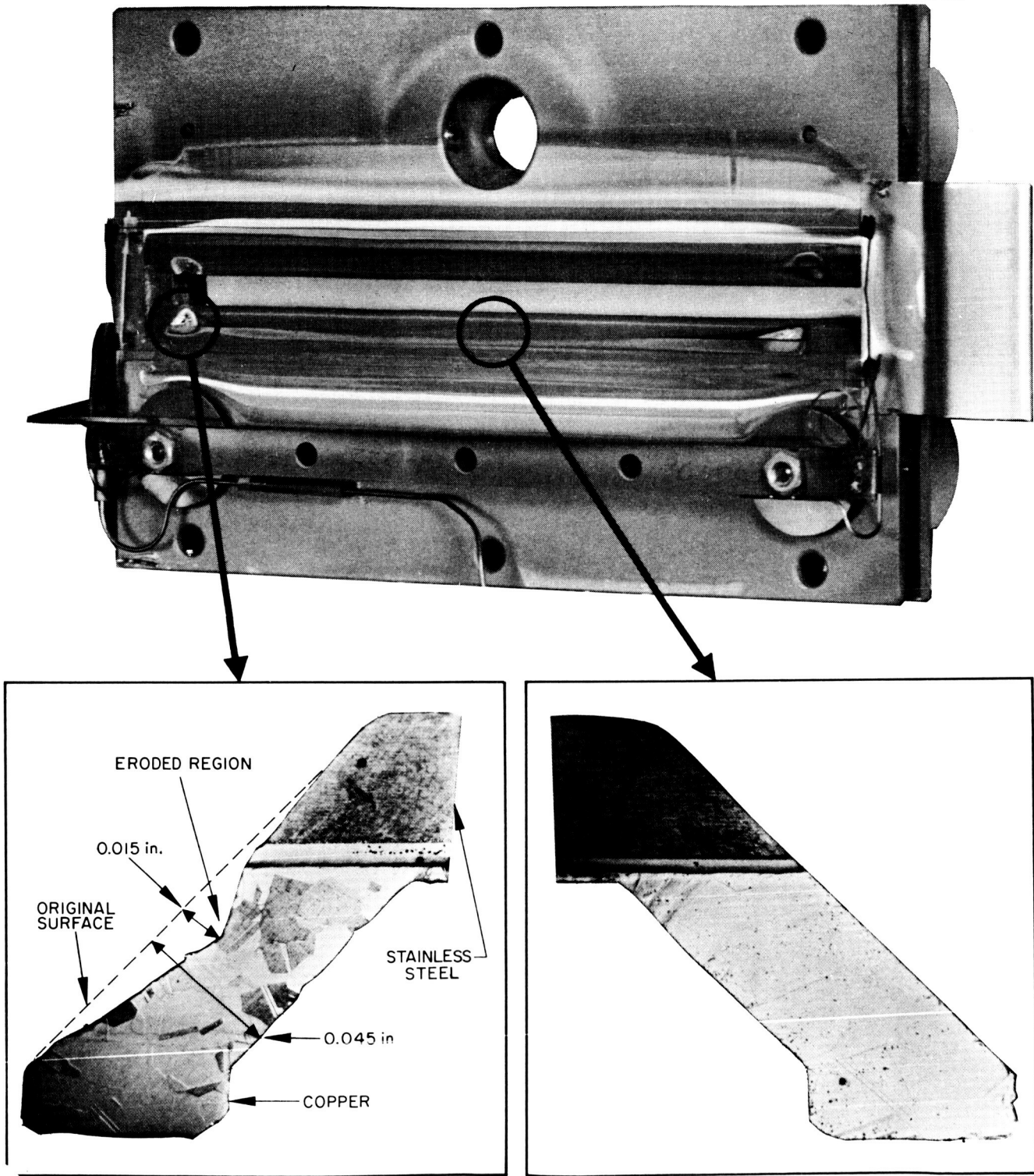


Fig. VI-17. Ion thruster LB-7 upon removal from vacuum chamber following successful completion of 2000 hour steady-state life test.

M 4159

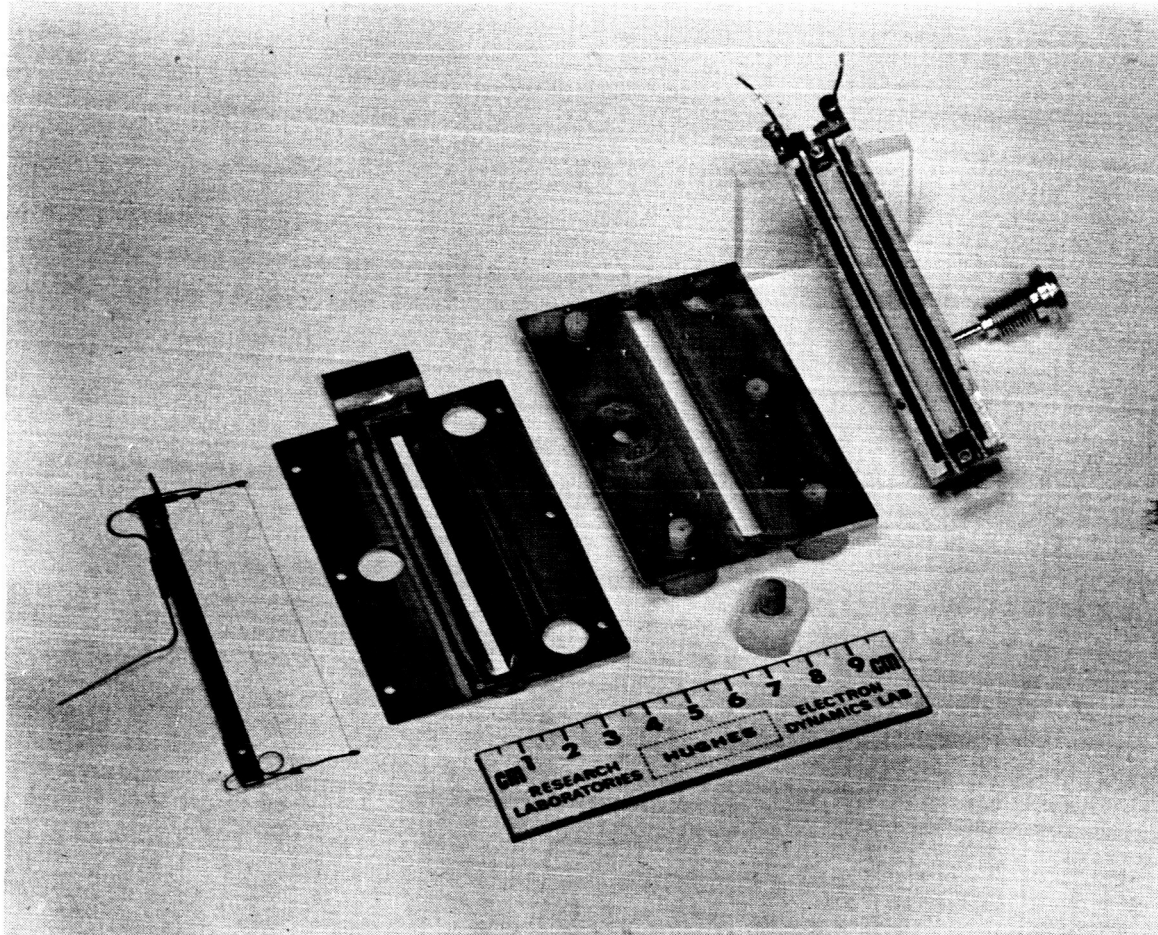


Fig. VI-18. Major subassemblies of thruster LB-7 after 2000 hour life test.

M 4162

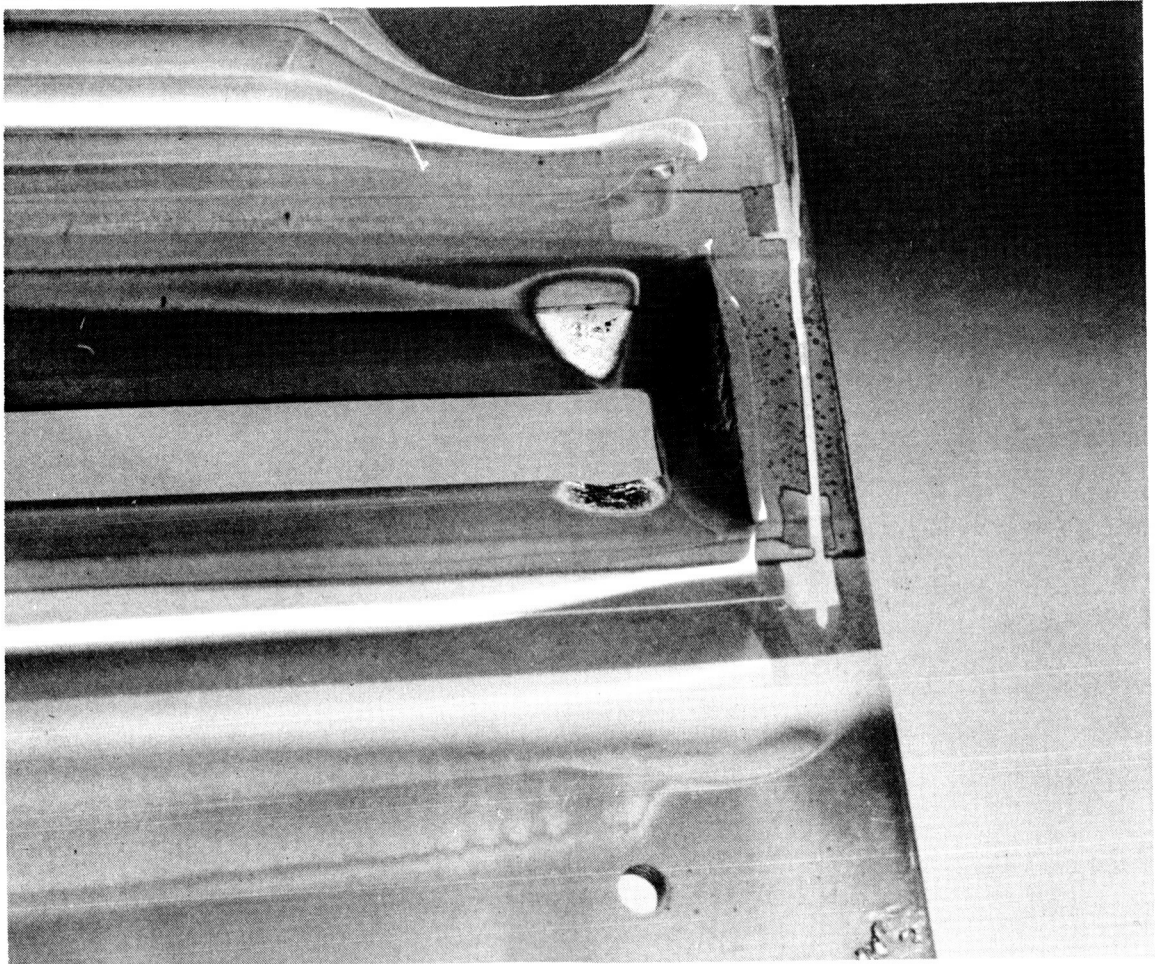


Fig. VI-19. Closeup photograph of pitted areas on downstream side of accel electrode after 2000 hour steady-state life test.

density of neutral particles, it is evident that the charge exchange collision frequency near the ends of the strip is higher than that in the central regions. If the distribution of these charge exchange ions is identical to that in the central region, then the ion bombardment rate, and hence the erosion of the accel electrode at the end, is approximately 16 times higher than that in the central regions. This would then explain the observance of pit-type erosions on the accel electrode only at the ends of the downstream side of the slit.

In summary, the hypothesis put forward to explain the four eroded regions of the accel electrode is that this erosion is due to ion bombardment from charge exchange ions. This erosion is greatly enhanced at the ends of the accel electrode because of peaking of the ion beam current density due to end effect corrections included in the ion optical system. Assuming that the electrode in Fig. VI-17 was fabricated from stainless steel, and that the erosion rate remains linear with time, anticipated lifetime of the accel electrode at its most heavily eroded region would be about three years.

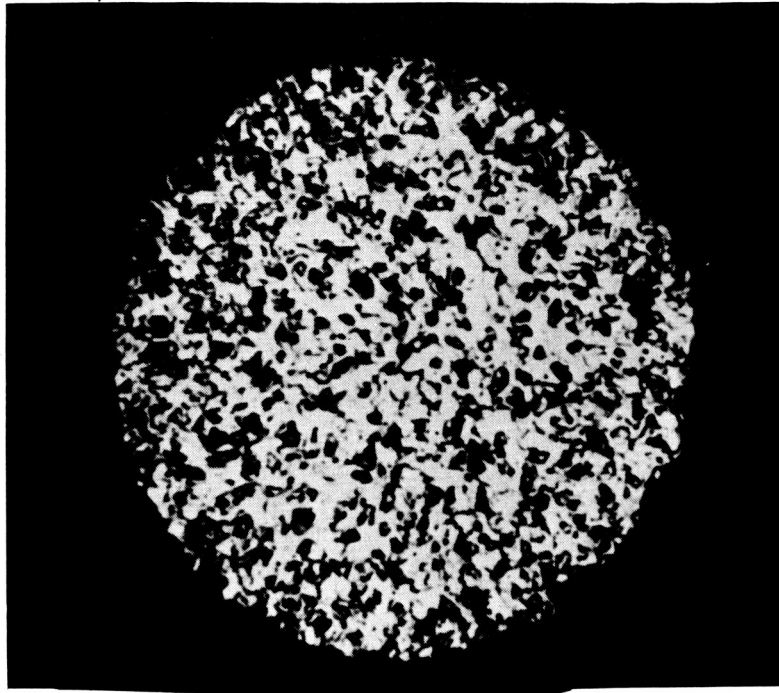
b. Neutralizer Filaments

Cross sections of the LB-7 neutralizer filament and a dummy filament wire that provided a ground potential on the opposite side of the accel aperture are presented in Fig. VI-20. The neutralizer filament shows no discernible wear. The other filament may be slightly worn or simply manufactured with a non-circular cross section. Accurate predictions of neutralizer lifetimes are not possible from these photographs, but 10,000 hours or more appears feasible.

c. Ionizer and Focus Electrodes

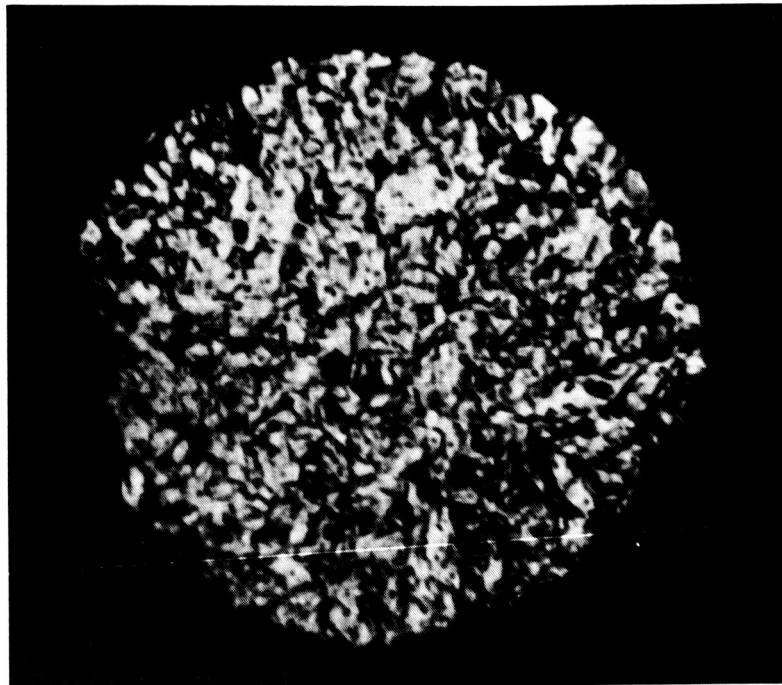
Microscopic examination of discolored areas on the ionizer and focus electrode of LB-7 reveals surface erosion in these regions. Roughening of the surface produces the darker appearance seen in Fig. VI-21. Spectrographic analysis of the deposit on the ionizer side of the accel shows a significant percentage of tungsten, supporting the ionizer erosion observations.

M 1692



(a)

M 1694



(b)

Fig. VI-20. Photomicrographs of (a) the neutralizer filament (0.002 in diameter) and (b) the dummy filament after 2000 hours of the cesium environment of thruster LB-7.

1683

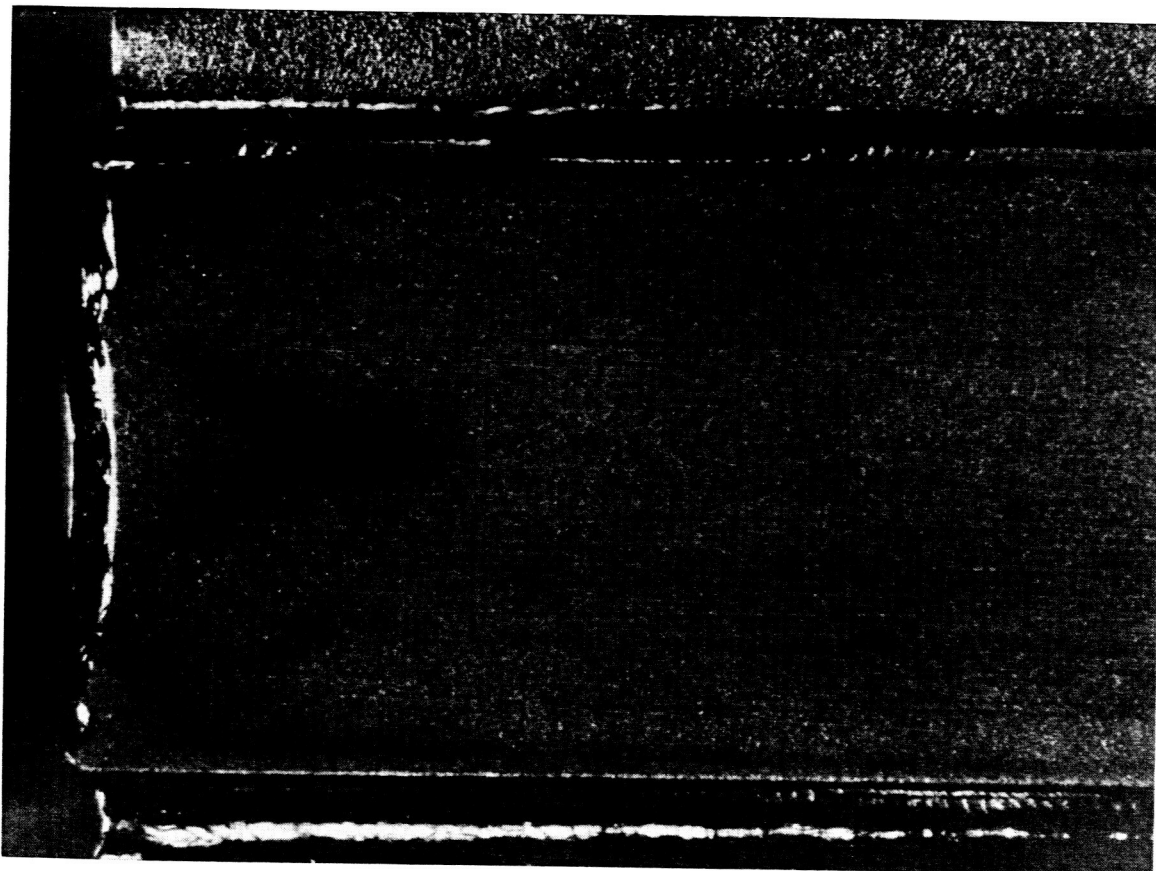


Fig. VI-21. Photograph of portion of ionizer surface from thruster LB-7. The dark areas are due to shadowing caused by surface erosion.

Typically, the erosion pattern consists of two grooves along each side of the ionizer strip, terminating in a rounded area near the end of the strip. These are visible in Fig. VI-21. The rounded area is a shallow crater.

Ionizer erosion requires high energy particles. Since the ionizer is at the most positive potential in the system, the eroding particles are assumed to be negative ions. The negative ions are created within the gun, otherwise they could not penetrate the negative potential barrier formed by the accel electrode. Ionization of residual gas within the gun by some interaction with the positive ion beam is considered not significant because the ionizer erosion pattern produced by a "steady rain" of gas ions would be much more uniform and might tend to be more pronounced along the center line of the strip. The erosion pattern on the ionizer strongly suggests the accel electrode as the ion source, especially at the ends where the pattern curves inward, as does the accel electrode. Heavier erosion at the ends can be attributed to ions from a relatively large area of accel being focused into a relatively small area of ionizer, as well as to the fact previously mentioned that charge exchange erosion is higher at the ends of the accel than at the center. Trajectory studies of the Model 70 optics show that if negative ions are created they would follow approximately the paths shown in Fig. VI-22.

The mechanism of negative ion production is suspected to be cesium ions bombarding the accel electrode and creating negative copper ions. Concerning the production of negative ions on metal surfaces, Massey⁴ states, "For impact of fast-moving atoms and ions, ejection of a negative ion from a (impure) metal surface by a positive ion of a different species is probably the most effective." Massey⁵ also indicates that negative ion production rises with positive ion energy. Krohn⁶ reports that a 50°C copper target bombarded by 1.1 keV cesium ions yields about 2% Cu^- and about 1.6% Cu_2^- ions/incident

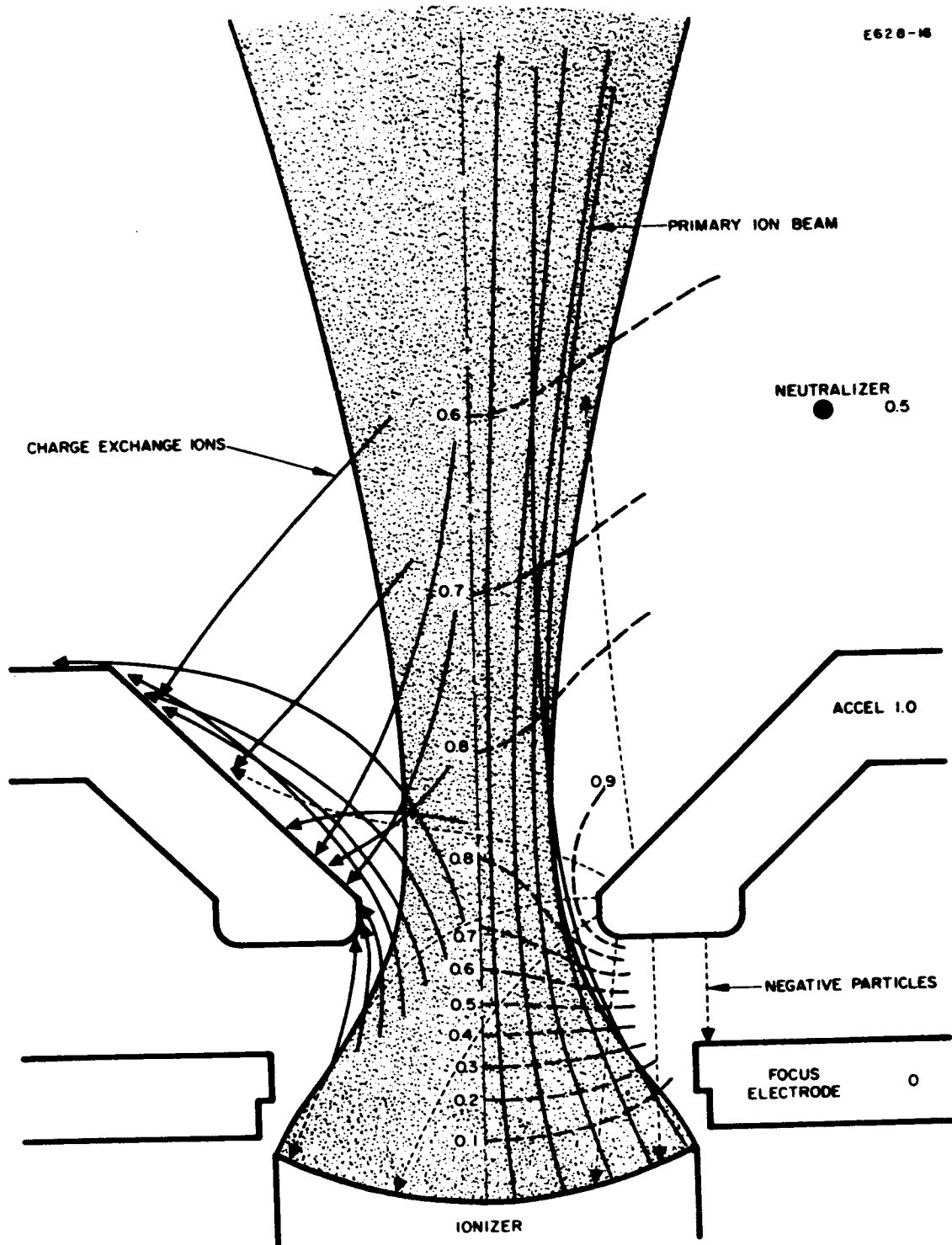


Fig. VI-22. Positive and negative charged particle trajectories in the Model 70 accelerator system for $3/4$ of full space charge.

ion. The sputtering yield for Cs on Cu at 1 kV is 3.4 (Ref. 7) so that the yields of Cu^- and Cu_2^- per sputtered particle are 0.6% and 0.5%, respectively. When the target was coated with cesium, the yields rose, especially that of Cu^- which attained 20% per incident ion.

In Fig. VI-23 a photomicrograph of the groove near the center section of the ionizer strip is shown. Assuming a total yield of negative copper ions of 1%, a 74% dense ionizer, an accel erosion area 0.124 in. long (45° deg ramp plus edge), uniform erosion over this area, a $\text{Cs}^+ \rightarrow \text{Cu}$ sputter yield of 3.4 and $\text{Cu}^- \rightarrow \text{W}$ yield of 1 to 5, the depth of charge exchange erosion on the accel necessary to produce this ionizer groove is 0.0021 to 0.00042 in. This is within the volume of copper that was sputtered although the distribution was probably different.

The above phenomenon depends on the accel sputtering yield, the percentage of negative ions emitted, thruster ion optics, and neutral fraction. The sputtering yield and negative ion yield may be altered by changing accel material. The single-strip thruster optics has the advantage of being able to focus some of the negative ions downstream. As with many thruster phenomena, reducing the neutral fraction would improve performance. The grooving of the ionizer did not pose any problem in beam generation and focusing during the 2000 hour test of LB-7 and a groove of larger dimensions probably could be tolerated before ion optical performance deteriorated.

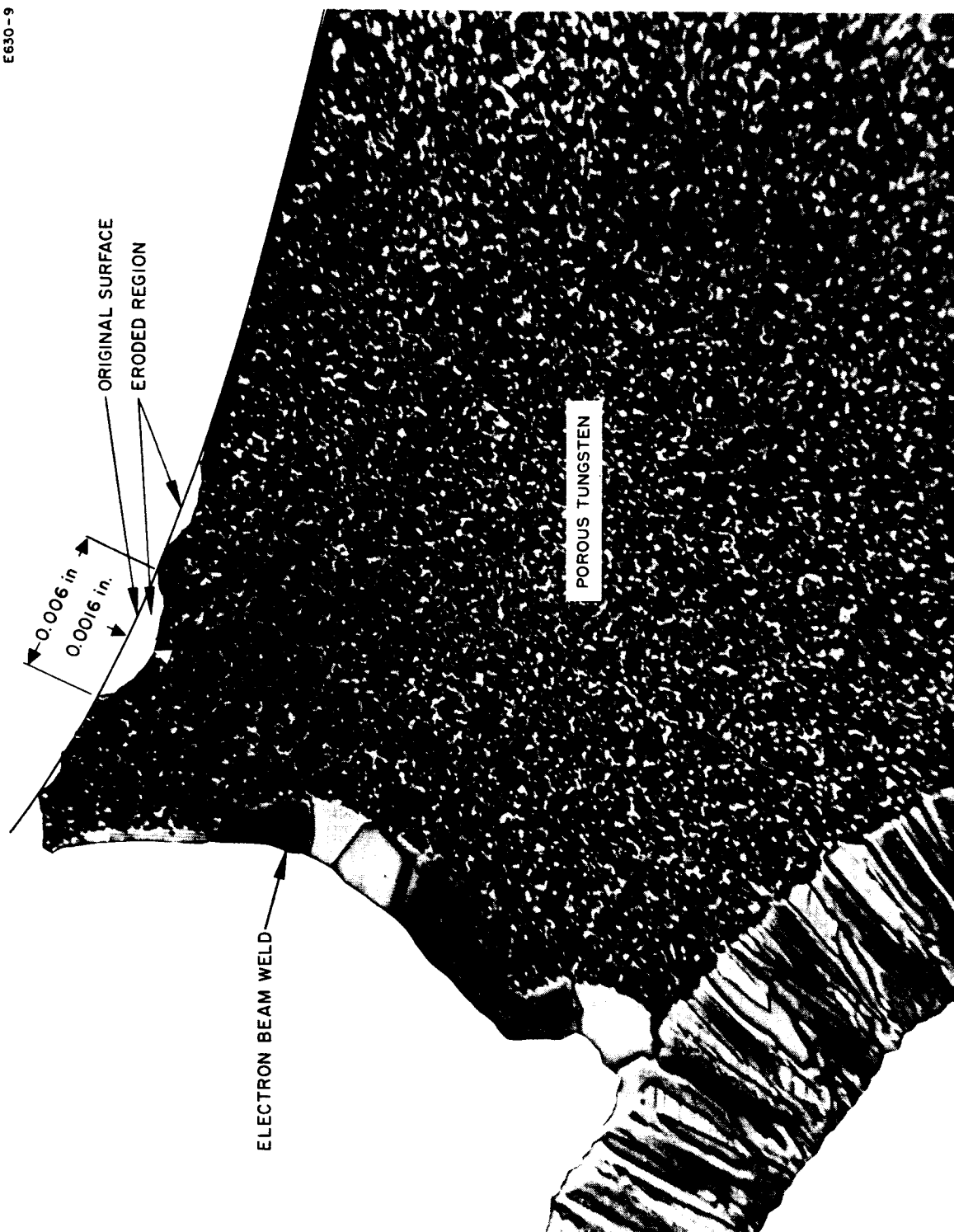


Fig. VI-23. Photomicrograph of LB-7 ionizer section showing shallow erosion groove along ion emitting surface.

d. Collector

Copper sputtered from the collector and intercepting baffles inside the vacuum chamber during the first 1000 hours of the LB-7 life test was estimated at 3.5 lb. Previous calculations of the copper expected to be sputtered during 1000 hours of normal ion beam incidence resulted in a value of about 1 lb. Since most of the ion beam bombarded copper surfaces at angles other than normal incidence, the weight of copper actually eroded indicates an enhancement by a factor of 3.5 over that of normal incidence. Thus, a rough value of the sputtering yield is 20 atoms/ion. This yield is in approximate agreement with recent experiments which included bombardment of polycrystalline copper by xenon ions for incidence angles ranging from 2 deg to 90 deg (normal).⁸

Back sputtering of copper from collector surfaces which are bombarded by the ion beam can be a serious problem in attaining very long life tests of ion thrusters. A photograph of the inside of the chamber after 1000 hours of beam-on time is shown in Fig. VI-24. Notice the eroded portion of the upper part of the first baffle inside the cryowall. This sputtered region is relatively close to the thruster and was the source of the major portion of copper that was back sputtered onto the thruster. The artificial environment of sputtered target material inside a vacuum chamber during steady state life tests of ion thrusters can degrade the performance whereas operation in a true space environment would not result in any change in the thruster characteristics. Consequently, life tests in a ground based chamber will be pessimistic unless the arrival rate of sputtered target material is reduced to an extremely low level or eliminated completely.

2. Thruster LD-2

Findings during post-test analysis of thruster LD-2 were predictable because of the previous analysis of LB-7. No indication of an ultimate failure was uncovered. All data confirm the conclusion that useful life of the thruster would have been many times longer than the 610 hour test period.

M 4006

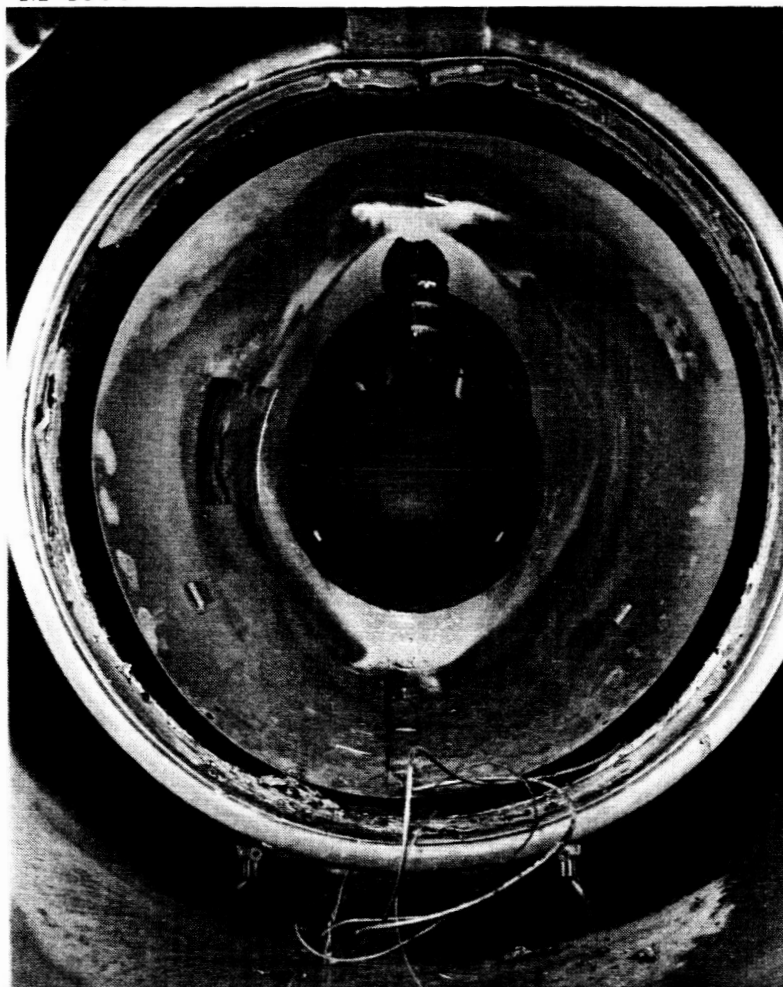


Fig. VI-24. Interior of vacuum test chamber after 1000 hour period of LB-7 life test.

Figure VI-25a is a photograph of the downstream side of the accel electrode. It is coated with backsputtered copper over most of the surface. The bright region around the accel aperture has resulted from sputter cleaning due to bombardment by charge exchange ions. Polished areas near the aperture ends are similar to those observed in LB-7. Figure VI-25b is a photograph of the upstream side of the accel electrode. The dark black area is composed of a thin coating of copper and tungsten. Spectrographic analysis of this deposit indicated a tungsten concentration of 47% at the ends and 22% at the center of the slit. This variation is consistent with light sputtering of the ionizer by negative copper ions.

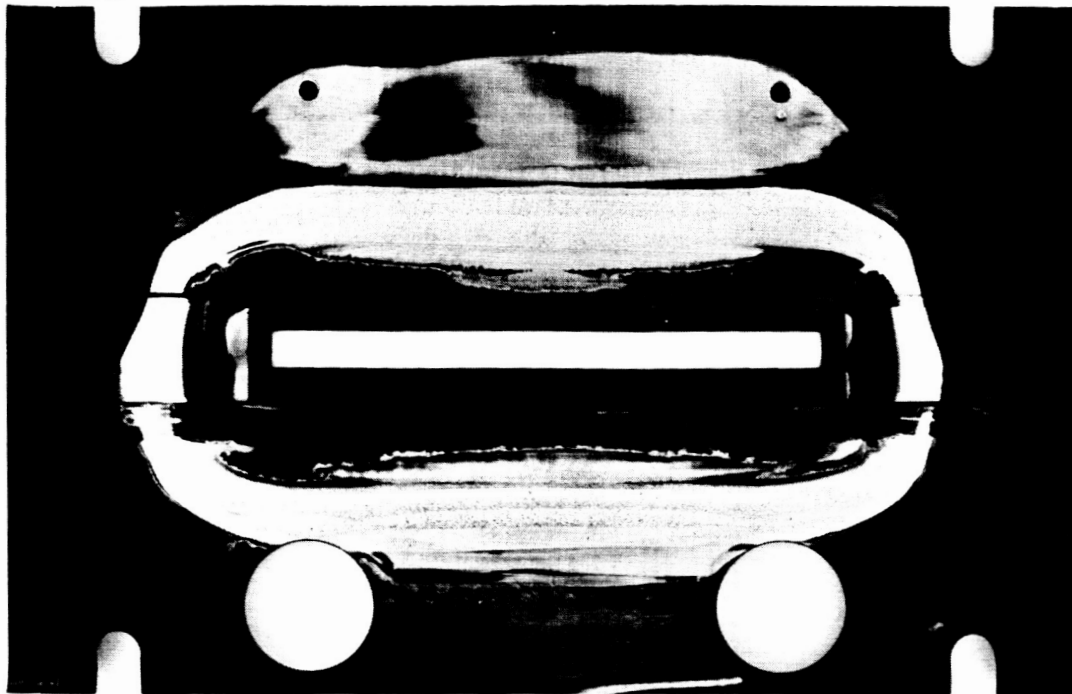
Cross sections of the electrode reveal little erosion during the 610 hour test. Figure VI-26a is a cross section adjacent to the accel aperture. Any erosion was so slight that it could not be measured. The critical optical surfaces are well defined. Similar results were obtained on center sections. Figure VI-26b is a section through the most heavily eroded part of the accel electrode. The deepest erosion is about 0.0025 in. and presents no serious problem to attainment of very long thruster life.

Slight erosion of the ionizer surface was observed, similar to that for LB-7. The bubble test pattern from the ionizer (see Fig. VI-27) showed that the ionizer ends were slightly more permeable than the central area.

3. Cesium Feed System

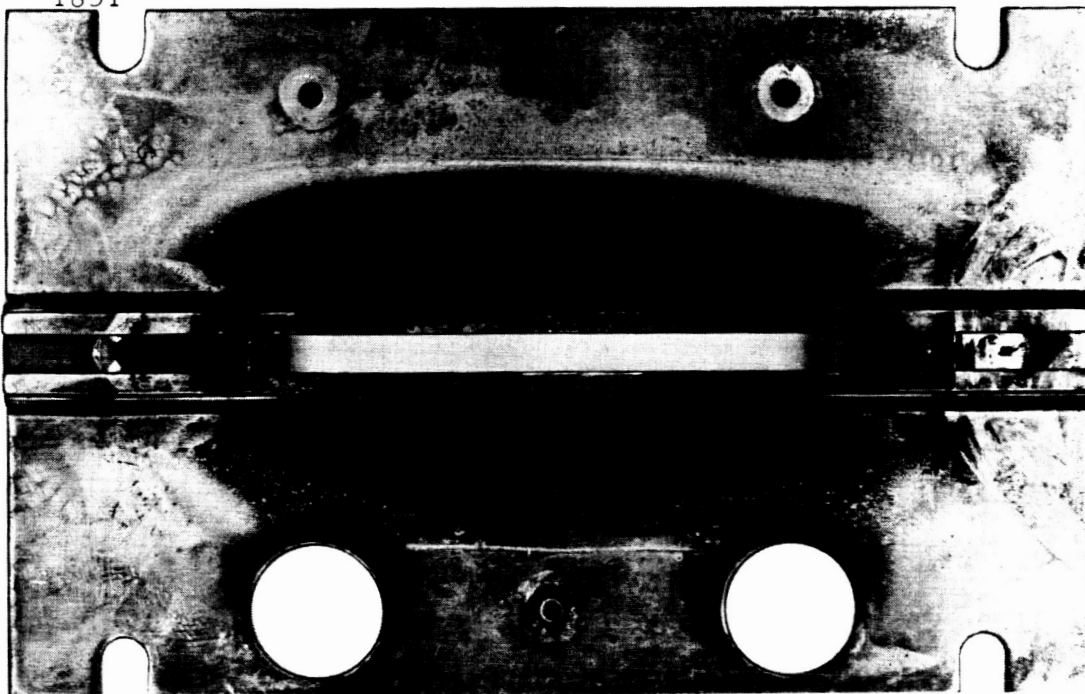
Following completion of the 2000 hour life test of thruster LB-7, the cesium feed system (Serial No. 006) was examined to determine the effect of long duration operation. This feed system, the new 250 g capacity unit designed for this thruster test program, showed no significant deterioration as a function of test time except for the solenoid-operated feed valve. During the course of this test, the feed system was cleaned and refilled with cesium twice, after 137 hours of

1852



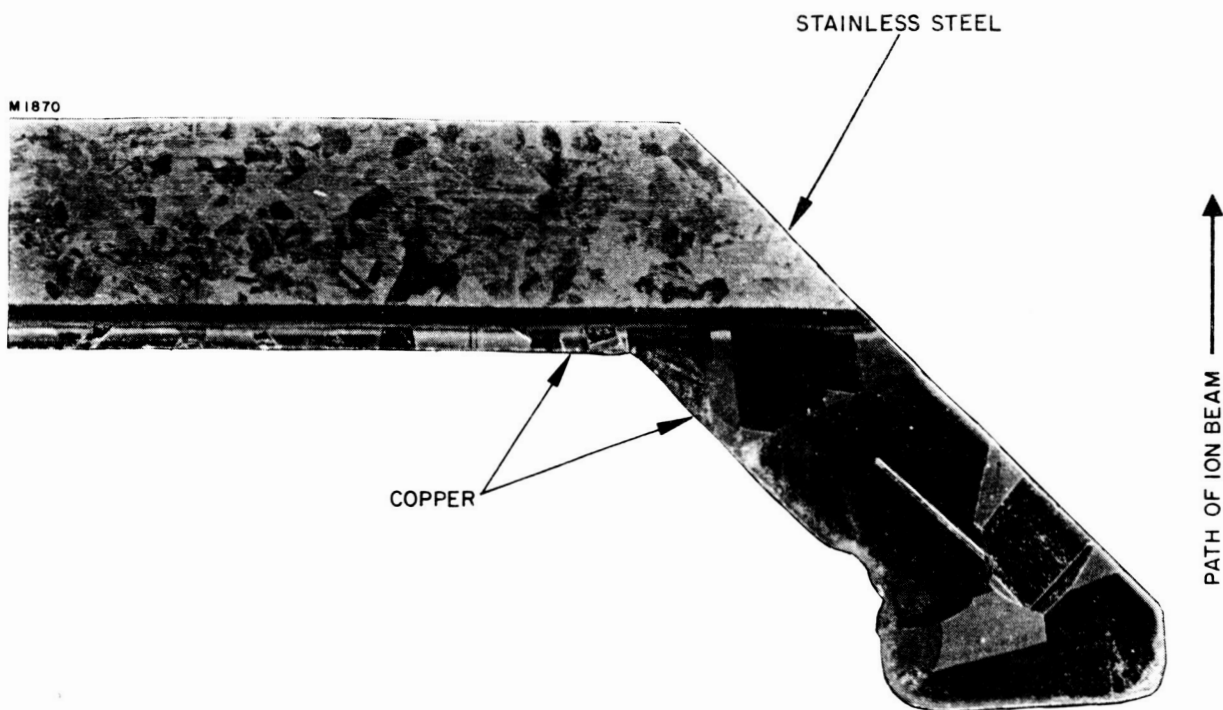
(a) Photograph of downstream side of the accel electrode from thruster LD-2.

1851



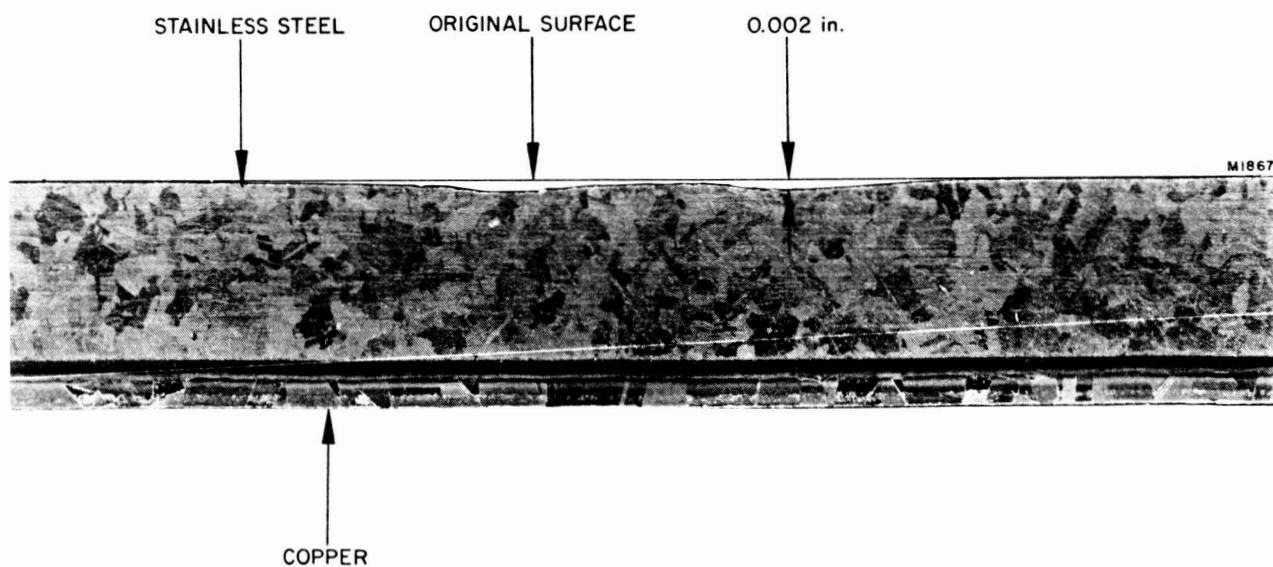
(b) Photograph of upstream side of the accel electrode from thruster LD-2.

Fig. VI-25.



(a) Photograph of cross section adjacent to the accel aperture of thruster LD-2.

E646-5



(b) Photograph of cross section in most eroded region of accel of thruster LD-2.

M4462

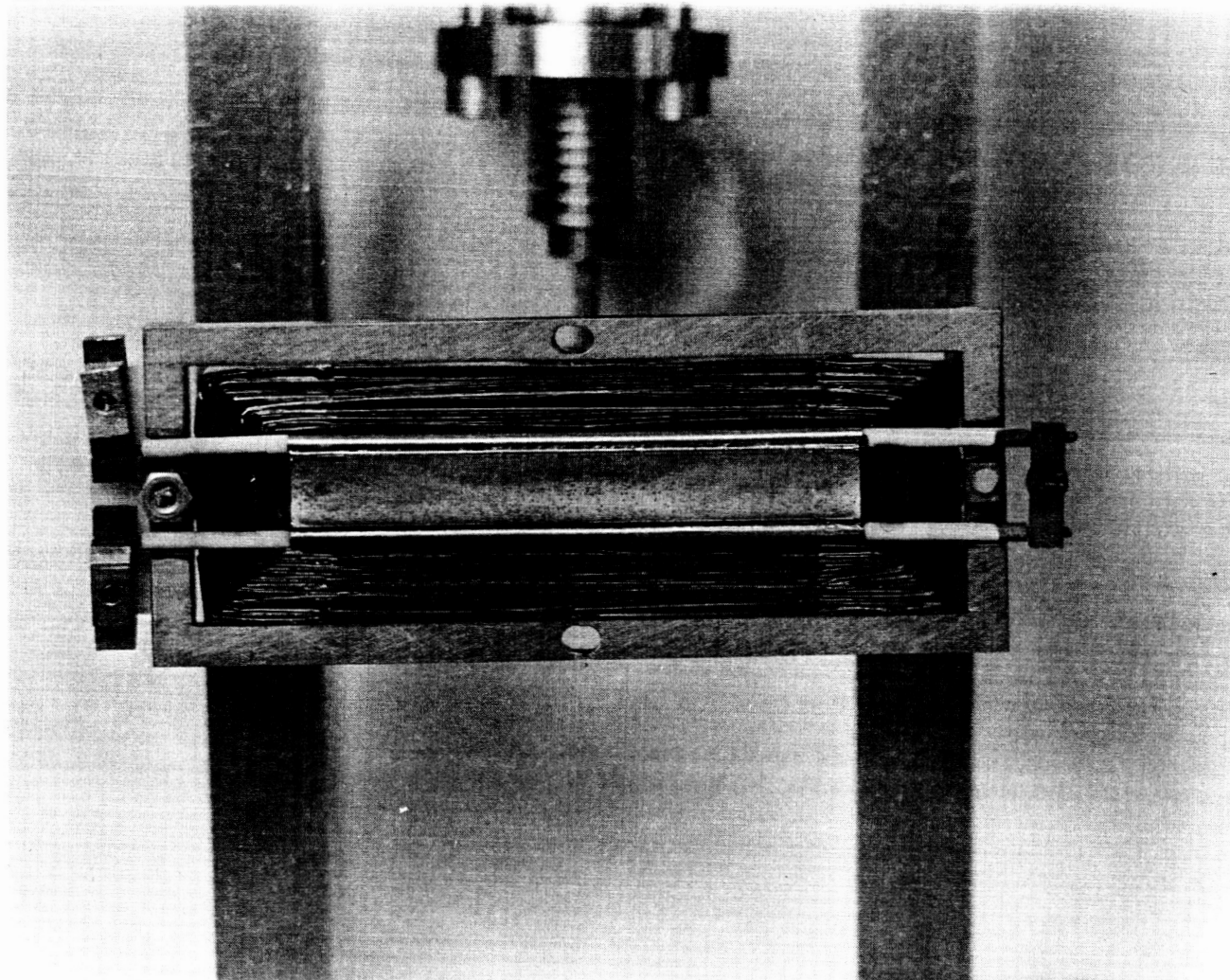


Fig. VI-27. Bubble test pattern from the ionizer of thruster LD-2 after life test.

beam-on test time following a solenoid coil failure and after 1001 hours of beam-on time when the thruster system was removed from the test chamber. Cleaning was limited to mechanical cleaning of the external parts of the feed system and was accompanied by replacement of the reservoir hermetic seal, replacement of the solenoid feed valve, and rearming of the piercing mechanism.

Total reservoir time accumulated at 280°C was 2166 hours during the 2000 hours of beam-on time. At the completion of the life test, the reservoir was examined and no significant change in appearance was detected other than surface discoloration. The piercing mechanism and the reservoir hermetic seal housing were equally unaffected. After being emptied, the reservoir weighed 1.5 g more than it had before being filled. This weight gain is attributed to residual cesium that could not be removed from the inside without cutting the reservoir apart. Samples of the cesium removed from the reservoir after completion of the test were analyzed and found to be of good purity. Table VI-3 shows the results of this analysis and includes the analysis of the original cesium supply for comparison. Reservoir heater resistance was essentially unchanged (9.4 Ω before test and 9.5 Ω after test) as was the manifold heater (1.9 Ω before test and 2.0 Ω after test).

The solenoid feed valve used during the final 1000 hours of the thruster life test was examined and subjected to electrical performance tests. No significant change in performance occurred although one solenoid coil lead shorted to the coil housing because of an insulation breakdown. This fault was caused by a combination of faulty magnet wire and winding technique and cannot be considered a time dependent failure. Table VI-4 shows the operating characteristics of the solenoid valve before and after the final 1000 hours of the thruster life test.

Following performance testing, the valve was disassembled and examined for deterioration. It is noted that, during the thruster life test the valve was cycled 984 times and was maintained at 380°C for

TABLE VI-3
CESIUM PURITY AFTER 2000 HOUR TEST

Element	Sample 1 (Submitted in Cu Tube), %	Sample 2 (Submitted in Glass Tube), %	Original Analysis, %
Al	<0.0002	0.0002	0.0003
Ba	<0.0008	<0.0008	<0.0008
B	<0.0016	<0.0016	<0.0016
Ca	0.0011	0.0005	0.0018
Cu	0.0006	<0.0002	0.0003
Cr	<0.0002	<0.0002	0.0003
Fe	<0.0003	0.0008	0.0024
Mg	<0.0002	<0.0002	0.0005
Mn	<0.0002	<0.0002	0.0014
Ni	<0.0002	0.0002	0.0006
Pb	<0.0002	<0.0002	<0.0002
Si	<0.0003	<0.0003	0.0019
Sn	<0.0008	<0.0008	<0.0008
Sr	<0.0002	<0.0002	<0.0002
Li	<0.0016	<0.0016	<0.0016
Ti	<0.0002	<0.0002	<0.0002
Tl	<0.0002	<0.0002	<0.0002
Na	0.0013	0.0018	0.0019
K	<0.0008	<0.0008	0.0003
Rb	0.0044	0.0039	0.0042

TABLE VI-4

VALVE OPERATING PARAMETERS BEFORE AND AFTER
LAST HALF OF 2000 HR THRUSTOR TEST

Parameter	Before	After
Solenoid Coil Resistance	34.8 Ω	35.0 Ω
Coil Insulation Resistance	∞	35.0 Ω (lead A) 0.1 Ω (lead B)
Minimum Operating Voltage	12.0 V dc	14.3 V dc
Minimum Operating Current	0.35 A	0.40 A
Minimum Holding Voltage	2.7 V dc	3.0 V dc
Minimum Holding Current	0.075 A	0.075 A
Internal Leakage (at $\Delta P = 15$ psi of N ₂)	33.6 cc/hr	0
Spring Preload	7.0 lb	6.8 lb

M4520

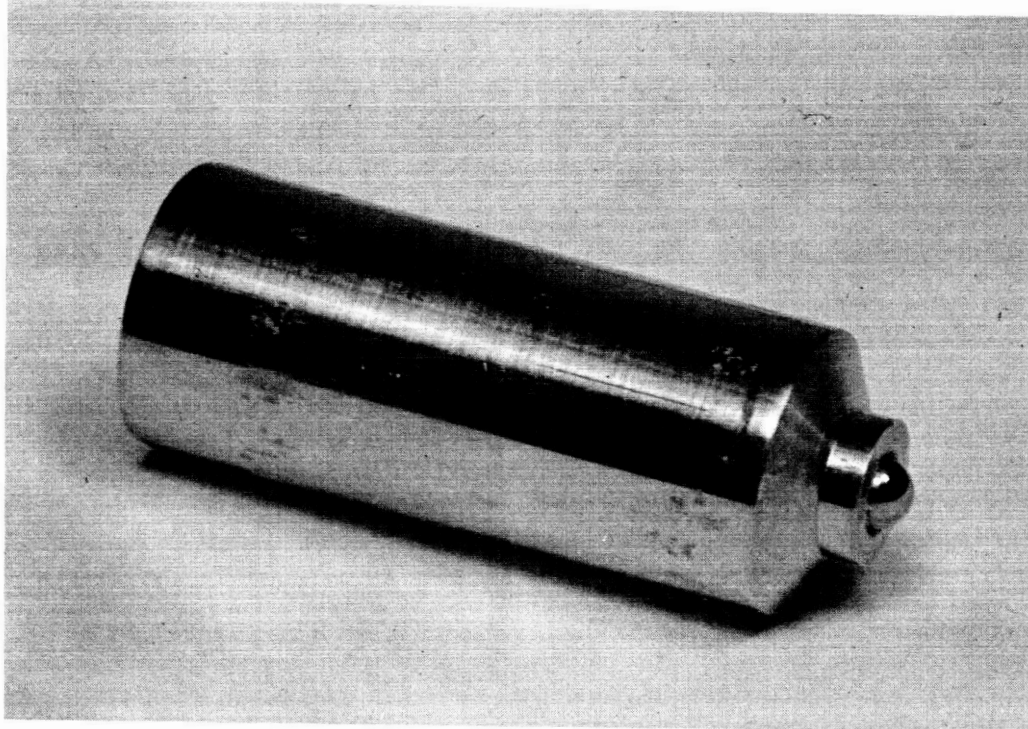


Fig. VI-28. Solenoid valve plunger after 984 cycles and 1000 hours in cesium at 380°C .

M4521

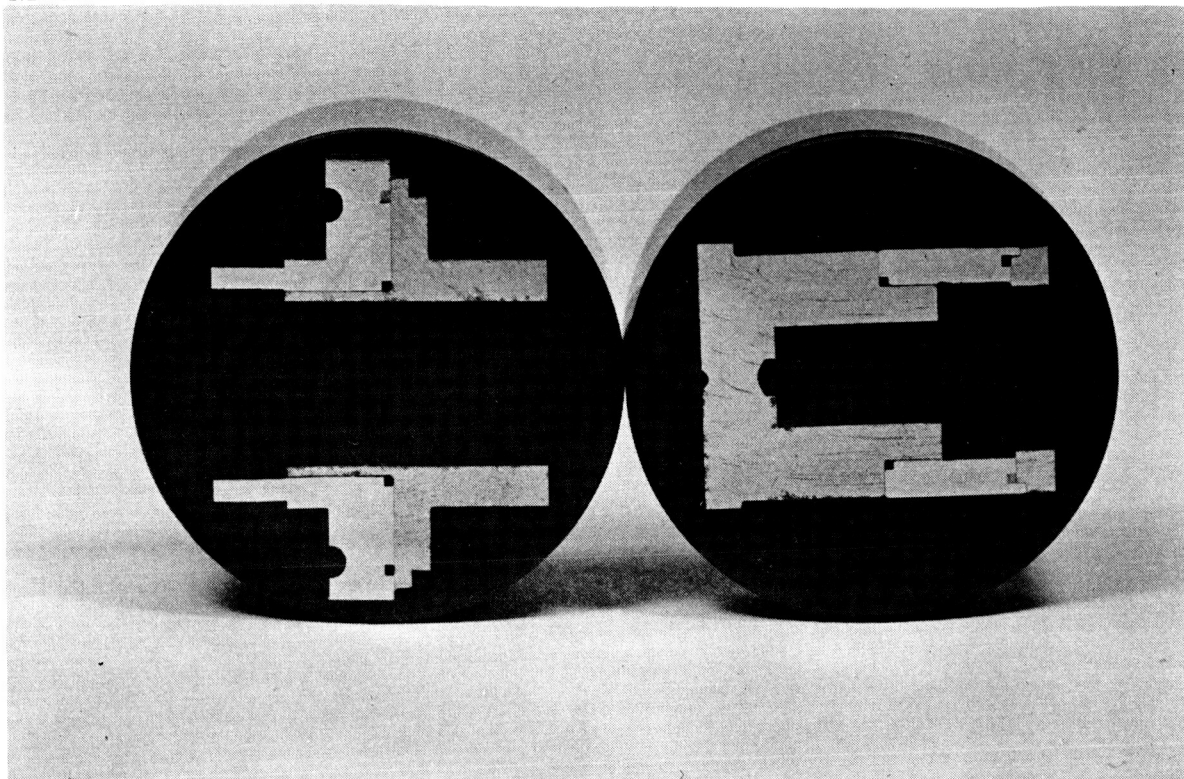
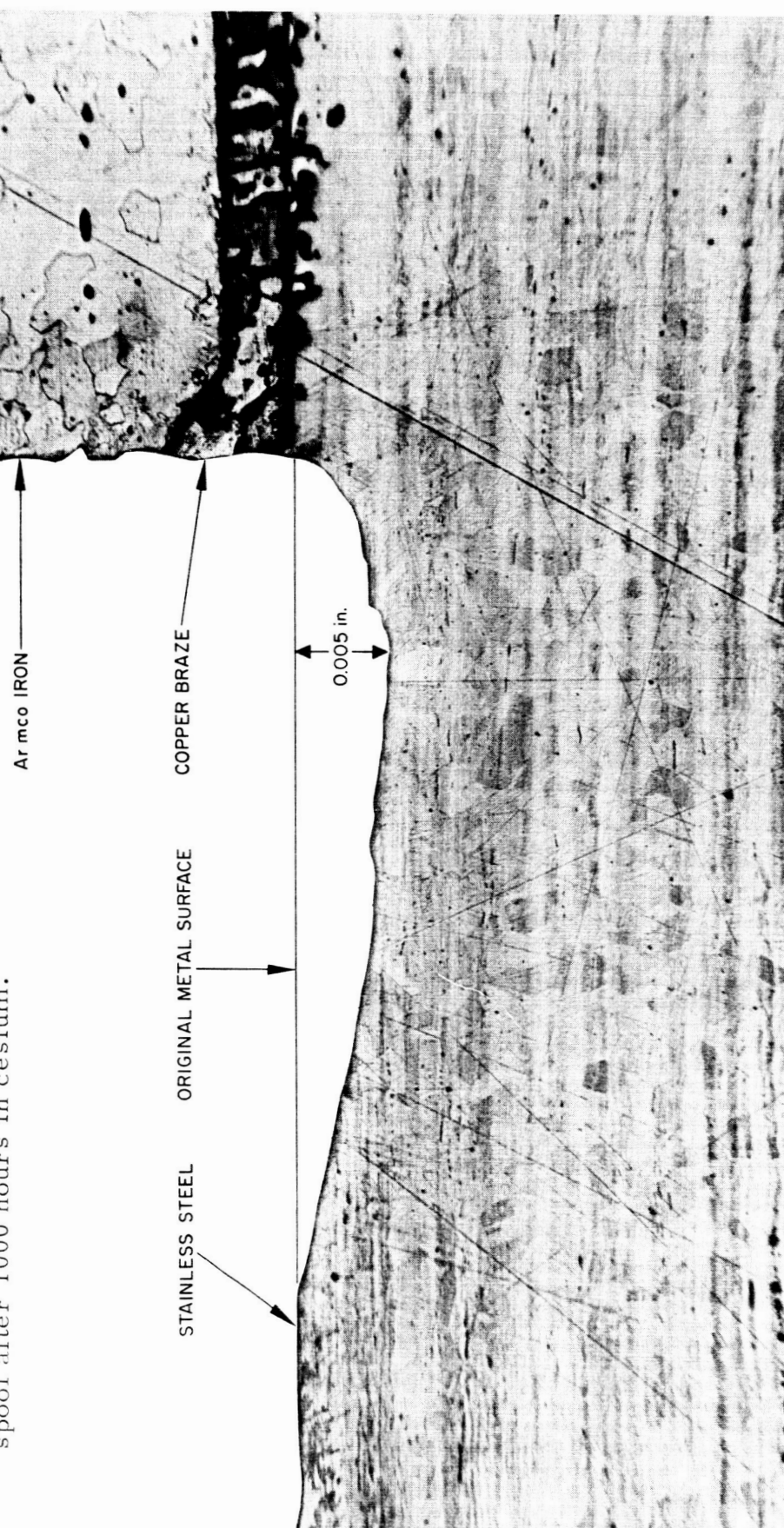


Fig. VI-29. Metallurgical sections of valve spool after 1000 hours in cesium.

Fig. VI-30.
Photomicrograph of light erosion in valve
spool after 1000 hours in cesium.



1032 hours. The plunger, shown in Fig. VI-28, had evidence of light galling and the carbide ball that is the valvular element was loose in its socket. Both of these conditions are dependent on the number of times the valve has been cycled.

The valve spool was sectioned and examined metallurgically. Figure VI-29 shows the two metallurgical samples. The only deterioration found was a slight erosion of the stainless steel spacer used in the valve spool at the point where it was copper brazed to the armco iron spool end. Figure VI-30 shows this erosion. At the point where the erosion occurred, the valve spool was continually exposed to cesium and was subjected to a mechanical scrubbing action due to plunger movement whenever the valve was operated. (When the valve was actuated, the end of the plunger moved from a point 0.020 in. away from the spool end to a point 0.003 in. from the spool end.)

This feed system was designed as a laboratory test system for use in thruster life tests. It also served as a test bed to assist in development and application of high temperature solenoid coil potting materials and techniques.

E. Summary

The major accomplishments of this life test program are itemized below:

1. A steady-state thruster life test of 2000 hours was completed. This represents a significant step in extending cesium-contact ion thruster lifetime. There appears to be no fundamental barrier to attainment of operating life in excess of 10,000 hours.
2. Erosion on the ionizer side of the accel electrode by cesium ions produced on the focus electrode was not detected in any of the life tests.

3. Critical temperatures at (or very near) the theoretical value for clean porous tungsten were regularly observed and remained stable after an initial period of up to 200 hours.
4. A power-to-thrust ratio of less than 200 W/mlb (extrapolated to free-space operation) was achieved with the 4.6 cm thruster at a specific impulse of 5000 sec.
5. No change in thruster perveance was observed during any life tests and the electrode surfaces responsible for establishing the proper electric field distribution remained intact and dimensionally stable.
6. Accel electrode temperatures low enough to restrict accel drain current to less than 1% are inherent in the thruster design. Copper coating of the oxidized stainless steel radiating surface was responsible for deviations in accel electrode temperature which resulted in higher drain currents at minimum ionizer temperatures.
7. The thoriated tungsten neutralizer filament remained intact after 2000 hours and appeared capable of operating much longer. Specific electron emission after this long life test was 50 mA/W at 1900°K.
8. Examination of the solenoid valve used in the cesium feed system indicated that its cyclic life would have been limited to several thousand cycles.
9. Post-test analysis of the entire laboratory feed system showed that for steady-state operation, this design is potentially capable of cesium operation for periods far in excess of the accumulated test time of 2166 hours.

VII. AUTOMATIC LIFE TEST CONSOLE

An automatic life test console was designed to operate an ion thruster, of the linear-strip type, continuously for a period of time in excess of 1000 hours. The console was built in two separate units: (1) Primary Power Supply Unit and (2) Power Conditioning and Control Unit.

A. The Primary Power Supply Unit

This power supply furnished regulated 50 V dc at 15 A and regulated 28 V dc at 10 A to the Power Conditioning and Control Unit. Batteries were chosen because of their inherent regulation and were continuously charged by two charging supplies. These supplies were controlled by voltage-sensing switching regulators, which supplied current to the batteries, as required, to maintain a constant voltage.

B. Power Conditioning and Control Unit

This unit (Fig. VII-1) contained the following power supplies with output characteristics as indicated:

1. Main Drive Supply:

Voltage	+ 5 kV dc
Current	60 mA
Regulation	5% line and load, 0-60 mA
Ripple	$\pm 1\%$
Adjustment Range	0 - 5 kV dc

2. Accel Supply:

Voltage	-5 kV dc
Current	30 mA
Regulation	5% line and load, 0-30 mA
Ripple	$\pm 1\%$
Adjustment Range	0 - 5 kV dc

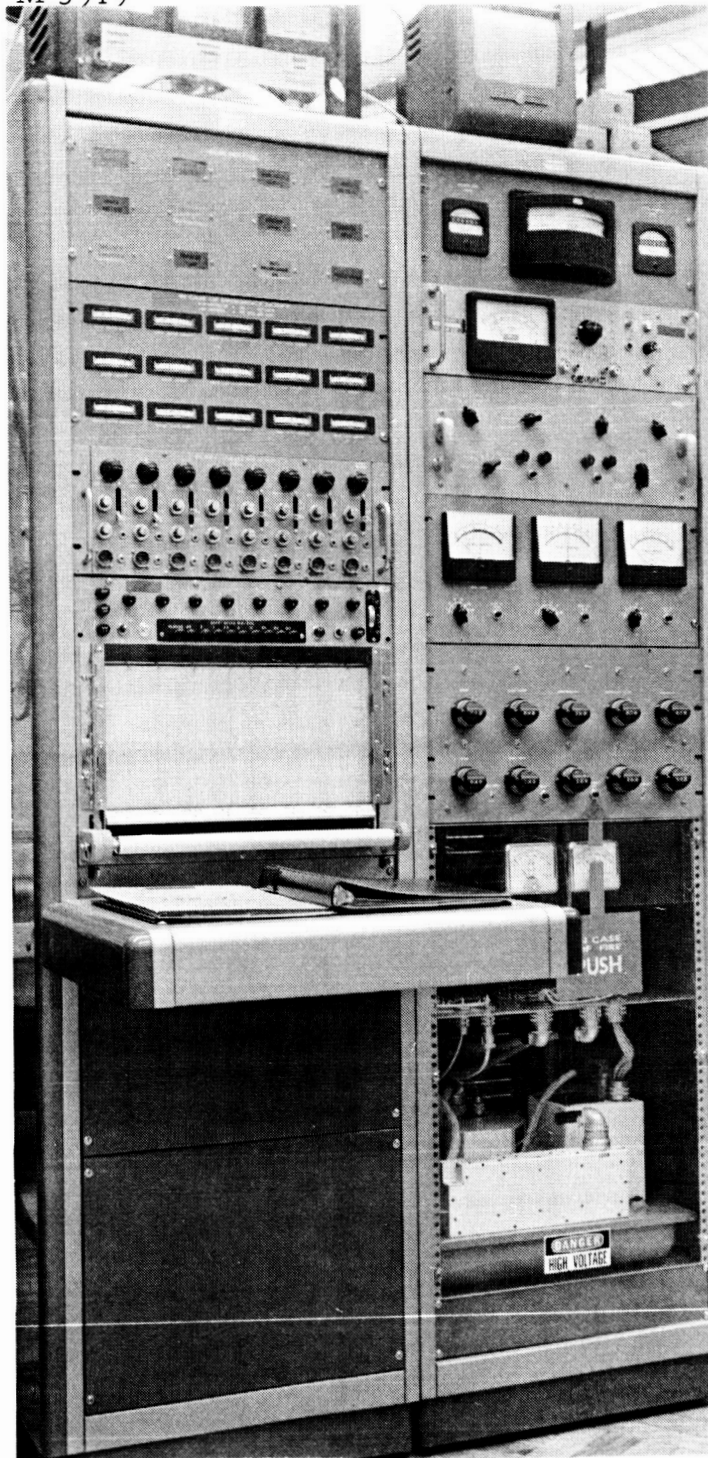


Fig. VII-1.

Photograph of the Automatic Life Test Console. The white boxes in the lower right hand portion are elements of ion thruster power conditioning developed by Hughes for the NASA SERT-I program.

3. Ionizer Heater Supply:

Voltage	35 V ac
Current	10 A
Temperature Regulation	$\pm 1\%$
Adjustment Range	15 to 35 V ac

4. Boiler Heater Supply:

Voltage	35 V ac
Current	1 A
Regulation	1%
Adjustment Range	0 - 35 V ac

5. Super Heater Supply:

Voltage	35 V ac
Current	7.5 A
Temperature Regulation	$\pm 1\%$
Adjustment Range	0 - 30 V ac

6. Feed Valve Supply:

No load voltages	80 V dc
30 Ω load voltage	30 V dc
Current	1 A
Regulation	None
Adjustment Range:	
No load voltage	40 - 80 V dc
Full load voltage	0 - 30 V dc

7. Neutralizer Heater Supply:

Voltage	20 V ac
Current	0.5 A
Regulation	$\pm 1\%$
Adjustment Range	0 - 20 V ac

Power conditioning equipment developed for the SERT-I Program was utilized to fulfill the requirements mentioned above. Only slight modification to the original equipment was necessary to meet these requirements. Five SERT-I power conditioning units were used in the life test console: 2 ac power supply units, 1 dc power supply unit, and 2 inverters. The individual supplies within these units were utilized as shown in Table VII-1. In order to accomplish the requirement for continuous duty operation, all the SERT-I modules were mounted on a water-cooled heat sink and operated at less than half of their design current requirements to insure maximum life.

The control unit (Fig. VII-2) contained all the level controls for the power conditioning modules, the logic circuits for unmanned operation of the life test console, and circuits for protection of the power conditioning modules in case of major thruster arcs, vacuum loss, or primary power failure.

The principal requirements were to maintain a constant beam current, optimum temperature of the ionizer heater and to protect the power conditioning against sustained thruster arcs. In order to achieve a constant beam current, an amplified control loop sensing beam current and controlling the boiler temperature was used. A similar control loop was used to control ionizer heater temperature by sensing accel electrode current.

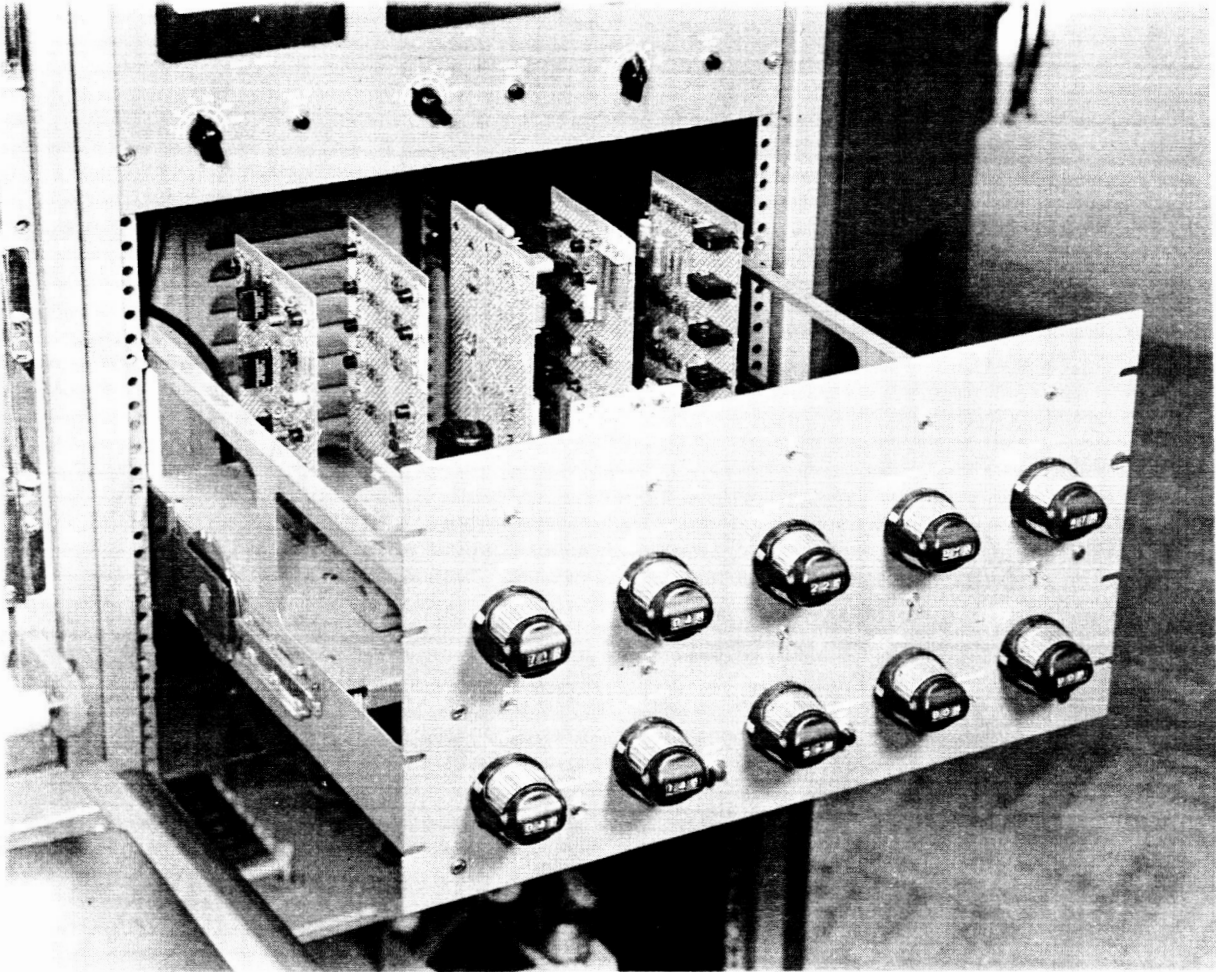


Fig. VII-2. Photograph of the control unit portion of the Automatic Life Test Console.

TABLE VII-1

SERT-I POWER SUPPLY FUNCTIONS IN LIFE TEST CONSOLE

SERT-I Description	Life Test Console Function
AC Supply (No. 1)	
Ionizer Heater Supply	Ionizer Heater Supply
Boiler Heater Supply	Boiler Heater Supply
Main Drive Supply	Main Drive Supply
Feed Valve Supply	Not Used
Stinger Supply	Not Used
AC Supply (No. 2)	
Ionizer Heater Supply	Super Heater Supply
Boiler Heater Supply	Feed Valve Supply
Main Drive Supply	Not Used
Feed Valve Supply	Not Used
Stinger Supply	Not Used
DC Supply	
Accel Supply	Accel Supply
Neutralizer Heater Supply	Neutralizer Heater Supply
Neutralizer Bias Supply	Not Used
Neutralizer Voltage Supply	Not Used
Inverter (No. 1)	
Bridge No. 1	2 kc power for Boiler, Feed Valve, Ionizer Heater, Neutralizer Heater and Super Heater supplies
Bridge No. 2	Not Used
Inverter (No. 2)	
Bridge No. 1	2 kc for Main Drive Supply
Bridge No. 2	2 kc for Accel Supply

Overloads caused by thruster arcs were sensed in the SERT-I inverter. Either a peak or average current overload could deactivate the inverter and terminate the voltage supplied to the overloaded power conditioning module. The inverters recycled at 1 sec intervals and if the overload was not present, normal operation was resumed.

The inverter trip was sensed in the system control unit and the following sequence resulted:

1. Close the feed valve
2. Disconnect the control loops
3. Advance an electronic arc counter one count
4. Activate the high voltage slow turn-on circuits
5. Disconnect the power to the beam-elapsed time indicator
6. Start the recorder, and turn on the appropriate failure indicator light.

If the arc was not repetitive, the high voltages were slowly increased to their normal operating level by the slow turn-on circuits, and after a 25 sec delay the feed valve was opened and normal system operation was resumed. The recorder continued to operate for approximately 2 min after an arc occurred. However, if the arc was repetitive, each additional inverter trip advanced the electronic arc counter. When ten arcs were counted, an Auto-Programmer was activated. The Auto-Programmer then:

1. Turned off the feed valve for the duration of the Auto-Programmer cycle.
2. Turned off both accel and main drive voltages for a period of 1 min, allowing the various heaters to evaporate any excess cesium remaining in the thruster.

After 1 min, the Auto-Programmer returned the high voltages to approximately one-half their normal operating level for 1 min, thus discharging any remaining cesium from the thruster. The Auto-Program was then terminated, returning the system to normal operation after the 25 sec feed valve delay.

When the Auto-Program was terminated, a pulse was fed to an electronic Auto-Programmer counter, advancing this counter one count. If an additional thruster arc recycled the Auto-Programmer before the feed valve opened, this counter continued to count until four Auto-Program cycles were counted. At this time the high voltages were turned off (the feed valve remained closed) and the Programmer light was activated on the failure-indicator panel. This condition existed until the console was manually reset by the operator.

If at any time during the above sequence, normal operation was resumed and the feed valve was opened, both the arc counter and the Auto-Programmer counter were returned to zero automatically.

VIII. RELIABILITY AND QUALITY ASSURANCE

The reliability and quality assurance effort on this program was designed to establish and maintain high standards of quality as well as careful documentation of critical hardware characteristics without burdening the program with requirements that do not enhance the total project effectiveness. In order to implement this effort a "Reliability and Quality Assurance Operating Plan," was issued to define specific activities and responsibilities. This plan was adhered to throughout the program and is presented on the following pages.

R & QA OPERATING PLAN
THRUSTOR DEVELOPMENT FOR ATTITUDE CONTROL
(Contract NAS 3-4117)

1.0 Purpose

This operating plan establishes reliability and quality assurance requirements for the Thrustor Development for Attitude Control program. and is effective as of this date. Prompt revision of the plan will be made as necessary to maintain it complete and current at all times.

2.0 Hardware Requirements

The following units are required by the contract:

- one Thrustor for thermal design verification
- one Thrustor for electrical design verification
- five Thrustors for thermal cycling tests
- three Thrustors for steady-state operation life tests
- one Thrustor for delivery to the customer

3.0 R&QA Requirements

3.1 Applicability of Requirements

Established Research Laboratory R&QA procedures, instructions and bulletins and special requirements of this contract are applicable as shown in the following table. Requirements and responsibilities set forth in the established R&QA requirements are applicable without exception unless noted otherwise in this operating plan.

RQR No.	Applicability of other requirements of this plan	Description	Thermal and Electrical Design Verification Thrustors (Quant: 2)	All Other Units Listed in Paragraph 2 (Quant: 11)
2.1.2	3.2.1	Drawing Control		x
2.1.3		Classification of Characteristics		x
2.1.4	3.2.1	Specification of Material		x
2.1.6		Initiation of Controlled Hardware Procedure		x
2.2.1		Procurement of Supplies		x
2.3.1		Receiving Inspection		x
2.3.2		Stock Room and Raw Material Control		x
2.3.3		Fabricated Parts Control and Inspection		x
2.3.6	3.2.2	Control of Nonconforming Supplies		x
2.4.1		Control of Data Acquisition Equipment	x	x
2.4.2	3.2.3	Failure Reporting, Analysis and Corrective Action		x
2.4.3	3.2.4	Equipment Logs		x
4.2-1		Project Bulletin - Equipment Logs		x

3.2 Additions and Modifications to Basic Requirements

The following additions and modifications to basic HRL R&QA requirements are applicable as noted in the table of paragraph 3.1. Where requirements of the basic procedures conflict with requirements listed below, the requirements listed below shall take precedence.

3.2.1 Drawings

The drawings used for fabrication shall contain materials and process requirements as set forth below.

a. General

Materials, process, test and inspection specifications as generated for Contract NAS 3-4108 (SERT-I) shall be utilized whenever they are applicable to the requirements of this Contract.

b. Processes

Process details, which if not complied with could degrade performance of the unit with respect to the technical objectives of the program, shall be included on the drawings.

c. Material Specifications

Material specifications shall appear on the drawings with the order of priority being Federal, Military, Contractor and Commercial. Where such specifications are inadequate or not applicable, those properties pertinent to the application shall be specified on the drawing.

3.2.2 Control of Nonconforming Supplies

The design engineer has authority to make all material review decisions in compliance with R&QA procedure 2.3.6 (no project R&QA representation required).

3.2.3 Failure Reporting, Analysis and Corrective Action

Three copies each of the initial and completed failure reports shall be submitted to NASA within one week of failure occurrence and upon completion of the analysis respectively. This requirement applies only to the tests specified in the Contract. The project engineer shall review all failure reports prior to submittal.

3.2.4 Equipment Logs

Deviations from critical dimensions or other critical characteristics contained on the drawing or specification shall be recorded in the applicable equipment log.

4.0 Other Requirements and Information

4.1 Intent of R&QA Program Requirements

It is not the intent of this R&QA program to force rigid adherence to requirements which do not enhance the total project effectiveness. Instead, this program plan is intended to invoke procedures which will require each departure from good R&QA practices to be deliberate, well thought out, and documented. Consistent with this objective cognizant engineers have been assigned full material review authority (per paragraph 3.2.2 above). The overriding R&QA requirement of this program is to maintain

documented records at all times of known critical or potentially significant design configuration parameters including dimensions, processes, constituent materials, etc.

4.2 Project Personnel Designations

For purposes of implementing the applicable R&QA procedures on this program, the following designations shall apply:

G. A. Work	Program Manager
J. R. Anderson	Project Engineer

The design engineers shall also act in the capacity of project R&QA representatives for units under their cognizance.

IX. RECOMMENDATIONS AND CONCLUSIONS

The Hughes Linear Ion Thrustor, with some 3000 hours of test history, is believed to have a potential lifetime on the order of 16,000 hours ($J = 7 \text{ mA/cm}^2$). However, this lifetime figure is extremely difficult to establish with any degree of precision for two principal reasons. First, the proper criteria for end of life is not known. Although contemporary knowledge points to erosion of the accel electrode by charge exchange ion bombardment as being the fundamental life limiting mechanism, how this is translated into a practical criterion for thrustor failure is purely intuitive at the present state of the art. Second, no life test yet conducted on any ion thrustor has yielded definitive data on the time dependency of erosion. Does erosion of the accelerator structure have a linear, logarithmic, or some other functional dependence with time? The answer to this question is of vital importance if we are to establish, with any reasonable assurance, the real lifetime capability of ion thrustors. Here then are two unsolved aspects of ion thrustors which are beckoning for fruitful investigation.

Interpretation of the Linear Ion Thrustor performance during long life tests with regard to power losses (particularly accel drain) was clouded because of the presence of an artificial sputtering environment within the vacuum test chamber. Some of the target material sputtered by the impinging ion beam redeposited on the ion thrustor itself, with consequent alteration of the thermal balance between the accelerator electrode and ionizer. In particular, it was observed that the emittance of the downstream surface of the accel electrode decreased with time so that the accelerator temperature gradually rose during the early portion of the life tests. This resulted in an increase of thermionic electron emission from the cesiated surfaces of the accelerator to the positive high voltage electrodes. Since such an environment of back sputtered target material does not in any way simulate the real space environment, it is believed that the thrustor was forced to operate under conditions

which were less favorable than would be experienced in space. It is because of the above phenomenon that accel drains and consequent power losses were relatively high during the major portions of several steady-state life tests. Because cesiated surfaces can exhibit very low work functions, an increase of electrode temperature, due to back sputtered target material, has significantly greater influence on the performance of ion thrusters using cesium as opposed to other propellants. It is well known that if the arrival flux of sputtered target material on a tungsten ionizer is sufficiently high the ionizer work function can be altered so that the surface ionization characteristics and over-all thruster performance are changed to the point where they do not correspond to free-space performance. Consequently, either a readily evaporated material, such as copper, is generally used for ion beam collectors, or the collector is removed at a far distance from the ionizer to decrease the flux of returning particles. However these measures are insufficient when one is attempting to maintain a given isothermal surface over a very long period of time, particularly if the electrode is designed for cooling principally by thermal radiation. We recommend that further study be given to this space simulation problem.

The results reported herein demonstrate long-life capability of the Linear Ion Thruster. However, the degree of reliability of the thruster is conjectural depending upon the point of view. It is believed by the authors to be relatively high, but this point cannot be proven with the available data. Many more steady-state life tests will be needed to establish the unit reliability of this thruster. Since this point is of such vital concern to possible systems application, it is recommended strongly that additional life tests under identical operating conditions be conducted in the near future.

The ionizer heater problem that was present at the beginning of this contract has now been solved and statistical evidence is available to demonstrate the very good reliability of the heater design that evolved during this program. We are now ready to embark upon long-duration cyclic tests with cesium. Such cyclic tests are necessary to verify that the Linear Ion Thrustor is satisfactory for applications requiring intermittent-thrust operation. Completion of cyclic life tests with cesium is one of the major performance milestones expected to be attained during the follow-on contract (NAS 3-7927) period.

Although it was possible to obtain a power-to-thrust ratio of less than 200 W/mlbf during testing of the LD thrustor, continuous operation at this higher efficiency level was found to be marginal. This was because thermal heating losses have not yet been reduced to as low levels as practical and also because the high voltage insulators arced over more frequently at the higher electric fields. A number of methods for improving and overcoming these limitations are known and are available. Further advanced development, including extended thrustor tests where called for, is desirable for realizing the full potential of the Linear Ion Thrustor. In particular, application of sound engineering principles should be capable of reducing the power-to-thrust level to 165 W/mlbf at 4500 sec. It is believed that such performance can be attained repeatedly and maintained for long periods of time if additional technical effort is devoted to such thrustor improvements.

Performance of the Linear Ion Thrustor has been demonstrated to a degree that one can and should consider the initiation of complete system integration testing. By this we mean, that the time is appropriate for mating of the Linear Ion Thrustor with a flight type feed system, power conditioning and controls. Before any firm decisions can be made with regard to application of ion thrustors in spacecraft, a basic module of an ion propulsion system must be put together and thoroughly evaluated in the laboratory. Of necessity this evaluation should include vacuum qualification and life testing of the entire system.

The Automatic Test Console that was utilized to operate the thruster during the 2000 hour steady-state life test resulted in a considerable manpower and dollar savings. Furthermore, the use of test equipment which was specifically designed to operate into an ion thruster load is believed to have contributed favorably to the successful thruster operation.

Finally, we wish to say that the support of the NASA personnel involved in this program has been most gratifying. The course of action chosen by NASA in supporting development of a cesium-contact action ion thruster covering the thrust range from 0.1 to 1.0 millipound has been most fruitful. We believe that this effort should continue to be supported strongly in the next few years in order to complete the development of an ion propulsion system built around the Linear Ion Thruster.

X. CONTRIBUTORS

The work reported above was accomplished by a small but dedicated group of scientists, engineers, and technicians. These people have been working together as a closely coordinated team for the past several years. Such a project organization has resulted in rapid reduction to practice of design ideas and principals. In the list below an attempt has been made to give credit to each staff member and to indicate his area of greatest contribution to the program. Certainly the work reported herein could not have been accomplished without the untiring efforts and close cooperation of all of the following persons plus the skilled technicians who were also members of the project.

J. Robert Anderson	Project Engineer
Robert Kuberek	Responsible for cesium feed systems, mechanical engineering, R&QA.
Walter E. Perkins	Supervisor in charge of thruster assembly; contributed strongly to key aspect of thruster design.
Joe M. Simpkins	Supervisor in charge of electronic test equipment.
Stephen A. Thompson	Thruster life test and evaluation.
Vert Upshaw	Responsible for ionizer heater development and test.
George A. Work	HRL Program Manager.

REFERENCES

1. "Development of an Ion Rocket Engine System for Attitude Control and Station Keeping." Final Report, Contract NAS 3-2510, Hughes Research Laboratories, Malibu, California, 1 February 1965.
2. "CS-1200 Ceramic Coil System," Publication No. EB-39, Anaconda Wire and Cable Co., 1963.
3. O. K. Husmann, D. M. Jamba, and D. R. Denison, "The influence of the residual gas atmosphere in space chambers on the neutral efflux and critical temperature of tungsten ionizers," AIAA J., 4, 273-282 (1966).
4. H. W. Massey, Negative Ions p. 83 (Cambridge Univ. Press, 1950).
5. Ibid., pp. 80-81.
6. Victor E. Krohn, Jr., "Emission of negative ions from metal surfaces bombarded by positive cesium ions," J. Appl. Phys. 33, 3523-3525, (1962).
7. G. D. Magnuson, "Sputtering Mechanism Under Ion Propulsion Conditions," Sixth Quarterly Progress Report, Contract NAS 8-1592, General Dynamics/Astronautics, Nov. 1962.
8. K. B. Cheney and E. T. Pitkin, "Sputtering at acute incidence," J. Appl. Phys. 36, 3542-3544 (1965).

LIST OF ABBREVIATIONS

W	watt
W-hr	watt-hour
mlbf	millipound force
LB	single strip thruster with 8 cm long ionizer
LC	single strip thruster with 5 cm long ionizer
LD	single strip thruster with 4.6 cm long ionizer
g	gram
mA	milliampere
lb	pound
zero-g	zero gravity
OFHC	oxygen-free high conductivity
TIG	tungsten-inert-gas
SERT	Space Electric Rocket Test
cc	cubic centimeter
hr	hour
HRL	Hughes Research Laboratories
LMI	low mass ionizer
cm	centimeter
μ	micron
in.	inch
ml	milliliter
min.	minute
A	ampere
V	volt
eV	electron-volt
J	current density
T	temperature

ϵ_{λ}	spectral emittance
kc	kilocycle
η_e	thruster efficiency (ion beam power divided by input power to the thruster)
I_s	specific impulse
P	power
msec	millisecond
tpi	turns per inch

DISTRIBUTION LIST FOR SUMMARY REPORT

CONTRACT NAS 3-4117

<u>Recipient</u>	<u>Address</u>
NASA Headquarters RNT/James Lazar (1)	NASA Headquarters FOB-10B 600 Independence Ave. N W Washington, D. C. 20546
NASA-Lewis Spacecraft Technology Proc. Section (M.S. 54-2) (1)	NASA-Lewis Research Center 21000 Brookpark Road Cleveland, Ohio 44135
NASA-Lewis Technology Utilization Office (M.S. 3-19) (1)	NASA-Lewis Research Center 21000 Brookpark Road Cleveland, Ohio 44135
NASA-Lewis Technical Information Division (M.S. 5-5) (1)	NASA-Lewis Research Center 21000 Brookpark Road Cleveland, Ohio 44135
NASA-Lewis Library (M.S. 3-7) (2)	NASA-Lewis Research Center 21000 Brookpark Road Cleveland, Ohio 44135
NASA-Lewis Spacecraft Technology Division (M.S. 54-1) C. C. Conger (1)	NASA-Lewis Research Center 21000 Brookpark Road Cleveland, Ohio 44135
NASA-Lewis Spacecraft Technology Division (M.S. 54-1) D. L. Lockwood (1)	NASA-Lewis Research Center 21000 Brookpark Road Cleveland, Ohio 44135
NASA-Lewis Spacecraft Technology Division (M.S. 54-1) D. M. Shellhammer (4)	NASA-Lewis Research Center 21000 Brookpark Road Cleveland, Ohio 44135
NASA-Lewis Electric Propulsion Laboratory (M.S. 30101) W. Moeckel (1)	NASA-Lewis Research Center 21000 Brookpark Road Cleveland, Ohio 44135

<u>Recipient</u>	<u>Address</u>
NASA-Lewis Electric Propulsion Laboratory (M.S. 30101) H. R. Kaufman (1)	NASA-Lewis Research Center 21000 Brookpark Road Cleveland, Ohio 44135
NASA-Lewis Electric Propulsion Laboratory (M. S. 30101) E. A. Richley (1)	NASA-Lewis Research Center 21000 Brookpark Road Cleveland, Ohio 44135
NASA-Lewis Report Control Office (M. S. 5-5) (1)	NASA-Lewis Research Center 21000 Brookpark Road Cleveland, Ohio 44135
NASA Scientific and Technical Information Facility (6)	NASA Scientific and Technical Information Facility Box 5700 Bethesda 14, Maryland
NASA-Marshall Space Flight Center Ernst Stuhlinger (M-RP-DIR)(1)	NASA-Marshall Space Flight Center Huntsville, Alabama 35812
Research and Technology Division AFAPL (APIE-2)/R. F. Cooper (1)	Research and Technology Division Wright-Patterson AFB, Ohio 45433
AFWL WLPC/Capt. C. F. Ellis (1)	AFWL Kirtland AFB, New Mexico
Aerospace Corporation Library/Technical Documents Group (1)	Aerospace Corporation P. O. Box 95085 Los Angeles, California 90045
Jet Propulsion Laboratory Jack Stearns (1)	Jet Propulsion Laboratory 4800 Oak Grove Drive Pasadena, California 91103
Electro-Optical Systems, Inc. A. T. Forrester (1)	Electro-Optical Systems, Inc. 300 North Halstead Pasadena, California 91107
TRW Space Technology Laboratories D. B. Langmuir (1)	TRW Space Technology Laboratories Thompson Ramo Wooldridge, Inc. One Space Park Redondo Beach, California

<u>Recipient</u>	<u>Address</u>
Westinghouse Astronuclear Laboratories Electric Propulsion Laboratory H. W. Szymanowski (1)	Westinghouse Astronuclear Laboratories Electric Propulsion Laboratory Pittsburgh, Pennsylvania 15234
University of California Space Science Laboratory H. P. Smith (1)	University of California Space Science Laboratory Berkeley 4, California
NASA-Langley Research Center Langley Field Station Technical Library (1)	NASA-Langley Research Center Langley Field Station Hampton, Virginia 23365
AVCO Corporation Research and Advanced Development Division R. R. John (1)	AVCO Corporation Research and Advanced Development Division 201 Lowell Street Wilmington, Massachusetts
AVCO Corporation Research and Advanced Development Division R. J. Cybulski (1)	AVCO Corporation Research and Advanced Development Division 201 Lowell Street Wilmington, Massachusetts
The Marquardt Corporation Russell Page (1)	The Marquardt Corporation 16555 Saticoy Street Van Nuys, California
Western Operations Office Patent Counsel (1)	Western Operations Office 150 Pico Boulevard Santa Monica, California
Air Force Plant Representative RWRAAC-2 (1)	Air Force Plant Representative Hughes Aircraft Company Culver City, California
Air Force Plant Representative RWRAPS-9 (1)	Air Force Plant Representative Hughes Aircraft Company Culver City, California
NASA-Goddard Space Flight Center William Isley - Code 623 (1)	NASA-Goddard Space Flight Center Greenbelt, Maryland